HIGH RESOLUTION NUCLEAR MAGNETIC RESONANCE SPECTROSCOPIC STUDIES OF SOME ASPECTS OF MOLECULAR INTERACTION IN SOLUTION.

A thesis
presented to the University of Aston in
Birmingham for the degree of Doctor of
Philosophy.

by

Peter James Huck B.Sc., A.R.I.C.

The Chemistry Department, October, 1968.
The University of Aston in Birmingham

SUMMARY

The investigations described herein concern the proton magnetic resonance studies of complexes transiently formed by nitroform and the haloforms with benzene and its methyl homologues.

The association constant for each of the complex equilibria in cyclohexane, and the difference between the solute proton screening in free and fully complexed situations are determined at a number of temperatures from the solute proton shift dependence on solution composition.

The chemical shift difference is used to estimate the average position of the proton in each complex which is found to be in contact with the aromatic ring on its six-fold symmetry axis. The distance between the solute proton and the aromatic ring for most of the complexes is found to be slightly less than expected from the sums of the proton and aromatic ring Van der Waals radii. Parallel compression of the π-system is independently indicated.

The nature of the associative bond between solute and aromatic molecules is found to be consistent with a dipole-induced dipole interaction. Two models for describing the nature of the complex are suggested but that favoured has the solute proton fixed in the position mentioned above with the remainder of the solute "wobbling" relative to the aromatic.

ΔG^o, ΔH^o, and ΔS^o for complex formation are deduced. The enthalpy changes are found to be independent of temperature within the range investigated and indicate the exothermic nature of the formation of each complex. The entropy changes indicate in each case the expected increased order on complex formation. The free energy changes are correlated with calculated interaction energies for the favoured model.

Published dipole moment data are used to determine the solute-aromatic inter-dipole distances. From these and the complex geometries, the location of the solute equivalent point dipole is deduced.

ACKNOWLEDGEMENTS

I would like to place on record my deep appreciation of the assistance offered to me throughout these investigations by my supervisor Dr. J. Homer. In particular, for the many helpful and stimulating suggestions offered in the interpretation of the experimental data. I am also grateful to my colleagues D. Callaghan, M. C. Cooke, and C. J. Jackson for helpful discussion and to Mrs. Poole, A. Clark, and E. J. Hartland who drew the illustrations for this thesis.

My appreciation is also due to the Department of Chemistry for providing the facilities for the research, and to the City of Birmingham for making available a Research Assistantship.

CONTENTS

Page

CHAPTER 1

An Introduction to Nuclear Magnetic Resonance Spectroscopy

CHAPTER 2

Practical Considerations

CHAPTER 3

The Determination of the Structures of Some Complexes and the Stability Constants for their Formation

CHAPTER 4

Investigation of Complex Formation at Different Temperatures

CHAPTER 5

The Determination of the Effective Dipolar Centres of Some of the Solutes Studied

APPENDICES

ILLUSTRATIONS

CHAPTER 1

An Introduction to Nuclear Magnetic Resonance Spectroscopy

1:1 Historical

For nuclear magnetic resonance (N.M.R.) to occur an interaction must take place between a nucleus and externally applied magnetic fields. This implies that the nucleus possesses magnetic properties i.e. a magnetic moment. Recalling the fact that all nuclei possess a positive charge it is reasonable to imagine that the magnetic moment arises from the rotation of the nucleus with a certain spin angular momentum, about the magnetic moment vector axis.

The first indications that some nuclei possessed angular momenta and magnetic moments were given by Pauli in 1924 (1). He postulated that the so-called satellites of bands observed in atomic spectra were caused by coupling of electron and nuclear angular momenta. In 1939, experiments were carried out by Rabi (2) along the lines of the classic experiment of Stern and Gerlach (3) in 1921. A molecular beam was passed successively through two oppositely inclined magnetic fields of similar gradients. Molecules which were influenced by the first field causing the beam to become diffuse were brought to focus again by the second field onto a detector. The situation was then changed so that when travelling between these two fields the molecules passed through a third uniform magnetic field, and a coil energised by a radio-frequency (R.F.) signal. The coil was so placed that the oscillating magnetic component of the R.F. signal was perpendicular to the main magnetic field. Those nuclei which possessed magnetic moments precessed at their Larmor frequency in the central steady field, and when the applied R.F. signal corresponded to this, nuclear transitions occurred altering the individual nett moments of the molecules passing through and thus diminishing the intensity of these at the detector.

N.M.R. effects in bulk matter, as known today, were first detected in 1945 by Purcell, Torrey and Pound (4) in paraffin wax and by Bloch, Hansen and Packard in water (5).

1:2 Nuclei in a Magnetic Field

Not all nuclei are found to possess magnetic moments, but for those that do, the magnetic moment and angular momentum behave as parallel vectors related by (see fig. 1 - 1)

$$\mu = \gamma I \hbar \qquad 1 : 1$$

where γ is an empirical constant, known as the magnetogyric ratio, characteristic of each nuclear species, $\hbar$ is the reduced Planck's Constant $h/2\pi$, and I is the nuclear spin quantum number. Nuclear angular momentum is quantised, and the maximum measureable component of angular momentum in a particular direction, is always on integral or half integral multiple of $\hbar$ governed by the value of I. In fact, the angular momentum is more strictly represented by $(I\,[I+1]\,)^{\frac{1}{2}}\hbar$. The number of allowable energy or spin states is limited and 2I+1 levels are possible with spin values from +I to -I.

If I = 0, then $\mu = 0$, and no magnetic effects are observed, but if I is non-zero, μ has a finite value and is parallel to $I\hbar$. The quantisation of the values of I necessarily places the same restriction on μ which thus possesses only discrete components, corresponding to different orientations of μ to the reference axis. This axis is invariably taken as the direction of the applied magnetic field H_o i.e. the z direction. For a particular orientation of μ to the H_o

direction, characterised by an angle θ (see figure 1 - 1), the energy of the nucleus is given by

$$E = E_o - E_z \tag{1 : 2}$$

where E_o is the energy in the absence of a field and $E_z = \mu_z H_o$. The change in energy when H_o is imposed is thus

$$E_z = - \ \ \mathrm{Cos}\ \theta .\ H_o \tag{1 : 3}$$

The values of μ_z, the component of μ in the z direction are governed by the allowed values of I which can be described by m, the nuclear magnetic quantum number which is allowed the values

$$m = I,\ I-1,\ \ldots\ \ \ldots .\ -I+1.\ -I \tag{1 : 4}$$

It follows, therefore that Cos θ = m/I and consequently

$$\mu_z = \frac{m\mu}{I} \tag{1 : 5}$$

and $$E_z = \frac{-m\mu}{I}.H_o \tag{1 : 6}$$

In the absence of a magnetic field, therefore, the different levels are degenerate, but the application of H_o causes separation in a manner analogous to the Zeemann Splitting of electronic levels. The energies of each level, characterised by their values of m, are

$$-\mu H_o,\quad \frac{-(I-1)}{I}\mu H_o,\ \ldots\ldots\quad \ldots\ldots\frac{(I-1)}{I}.\mu H_o,\ \mu H_o$$

and the energy between any two adjacent levels is

$$\Delta E = \frac{\mu H_o}{I} \tag{1 : 7}$$

For the simplest case when $I = \frac{1}{2}$, as for example for the proton, the splitting may be represented thus:

$$\Delta E = \frac{\mu H_o}{I} = 2\mu H_o$$

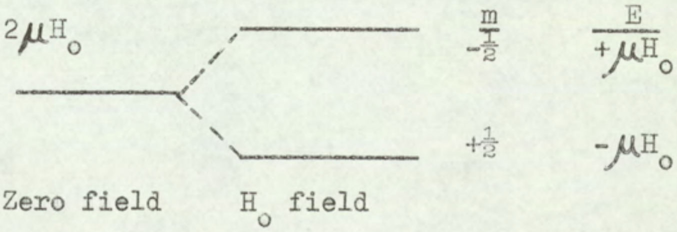

The basis of the N.M.R. method is to induce transitions of the nuclei between the lower and higher energy levels and to detect the nett change in energy. The frequency which corresponds to energy absorption is determined by the Bohr frequency condition $\Delta E = h\nu$. Transitions are only permissible for $\Delta m = \pm 1$, (6) thus a given nucleus, however many energy levels it may have access to, has only one characteristic resonance frequency in a given field, whose value is

$$\nu = \frac{\Delta E}{h} = \frac{\mu_o}{Ih} H_o \qquad 1 : 8$$

A particular nuclear species has constant values of μ and I and hence ν is directly dependant on H_o.

For protons, two typical conditions are

H_o = 14,092 gauss ; ν = 60.000 MHz

H_o = 23,490 gauss ; ν = 100.00 MHz

Other nuclei have different values of γ, and at the above field strengths, have different characteristic frequencies.

1:3 Classical Concept of Nuclear Resonance

An understanding of the mechanism of resonance absorption can be obtained by a classical treatment of the nuclear dipole. The effect of H_o on the dipole is to alter the value of θ, but because the nucleus is spinning, it precesses instead about the H_o direction at its Larmor Precessional Frequency, ν_o, with angular velocity ω_o. This motion is described by the vectorial equation

$$\frac{d\mu}{dt} = \omega_o . \mu \qquad 1 : 9$$

The vectorial equation describing the simultaneous orienting effect of the H_o field is

$$\frac{d\mu}{dt} = \gamma . \mu . H_o \qquad 1 : 10$$

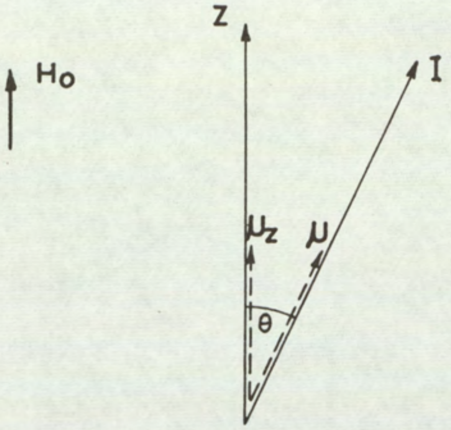

FIG. 1-1 THE RELATIONSHIP BETWEEN THE MAGNETIC MOMENT μ AND THE SPIN ANGULAR MOMENTUM I

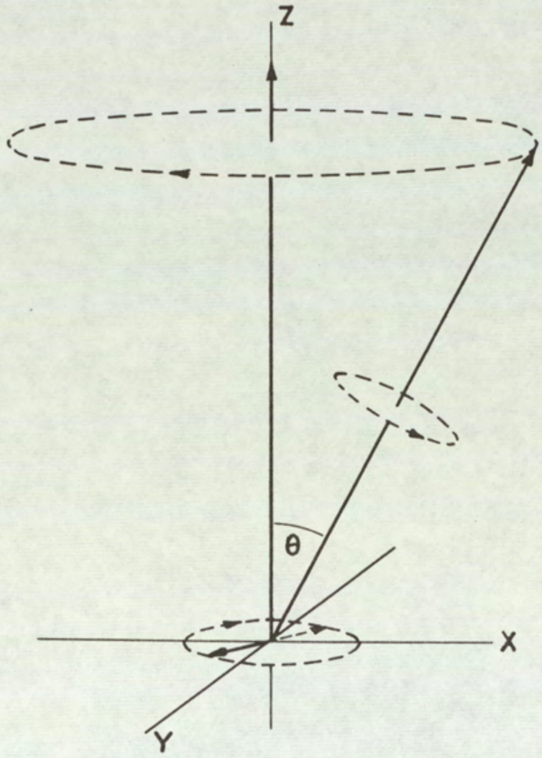

FIG. 1-2 VECTORIAL REPRESENTATION OF THE CLASSICAL LARMOR PRECESSION

Hence it can be shown that

$$\omega_o = -\gamma . H_o \qquad 1 : 11$$

The precessional angular velocity and thus the frequency is therefore governed solely by the value of the imposed static field.

From equation 1 : 3 it is evident that the energy of the nucleus is dependant on θ and any energy change of the nucleus will involve a change in θ. This can be achieved by applying a field H_1 perpendicularly to H_o which will exert a torque on μ. In order to have any appreciable effect, H_1 must rotate at a frequency close to ν_o, and to have the optimum effect must rotate at ν_o and be in phase with the rotating nuclear vector. When these conditions are fulfilled, μ is tilted towards the XY plane (see fig 1 - 2) and transitions between different orientations are possible.

The rotating field H_1 is obtained by applying an R.F. voltage to a coil surrounding the sample so arranged that the oscillating magnetic component of the R.F. field produced is perpendicular to the H_o direction in the manner required for resonance. This sinusoidally varying linear field can be regarded as consisting of two superimposed contra-rotating magnetic fields each having half the amplitude of the unresolved field. One field will be rotating in the opposite sense to the nucleus and will therefore have little effect on it, whereas the other component can be used to perturb its precessional motion. The resonance condition can be obtained either by varying the precessional frequency (by varying H_o) while maintaining the irradiating frequency constant or vice versa. The choice is usually made on technical grounds.

1:4 Nuclear Energy Level Distribution

When a group of nuclei is at the resonance condition, the probabilities of transitions occurring by absorption or emission of energy are identical and the factor which governs the nett effect is the distribution of nuclei between the various energy levels. In the absence of the radiofrequency field H_1, there is a thermal Boltzmann Distribution between the various allowed energetically different nuclear levels. Thus the number, n_i, of nuclei in a particular level with energy E_i and at thermal equilibrium at a temperature T is given by

$$\frac{n_i}{n} = \frac{e^{-\frac{E_i}{kT}}}{\sum_i e^{\frac{-E_i}{kT}}} \qquad 1 : 12$$

In the general case of 2I+1 levels, the probability of a given nucleus occupying a particular level, of magnetic quantum number m, is

$$\frac{1}{2I+1}\left[e^{\frac{m}{I} \cdot \frac{\mu H_o}{kT}} \right] \qquad 1 : 13$$

Since $\mu H_o/kT$ is small under normal operating conditions, this approximates to

$$\frac{1}{2I+1}\left[1 + \left(\frac{m}{I} \cdot \frac{\mu H_o}{kT}\right) \right] \qquad 1 : 14$$

There is thus an excess of nuclei in the lower states. In the case of the proton, the excess in the lower of the two allowed states is of the order of 1 in 100,000 for a field strength of 10 K Gauss.

1:5 Relaxation Phenomena

If the numbers of nuclei present in the upper and lower states are n_H and n_L respectively, and the probability of an absorption or an emission is P, the nett change at resonance is (7)

$$P.n_L - P.n_H = P.n_{excess} \qquad 1 : 15$$

which corresponds to an overall absorption of energy.

During resonance $n_{excess} \longrightarrow 0$ and the phenomenon known as saturation of the system occurs (section 1:8). After the resonance condition is passed, however, n_{excess} increases once again to its thermal equilibrium value. This is brought about by interaction of the system of nuclei with the lattice (18) during which radiationless transitions occur which have higher probabilities for emission than absorption. These natural relaxation processes occur continuously and during resonance compete with the stimulated absorption and, furthermore, are responsible for the establishment of the Boltzmann Distribution in the first instance.

Spin lattice relaxation, as it is called, occurs because neighbouring nuclear magnetic moments are in continuous motion by virtue of their thermal energy. The magnetic field produced by this fluctuating environment has components at the resonant frequency and causes transitions in the same manner as H_1.

A mechanism for spin-spin relaxation (8,9,10,11) also occurs when adjacent nuclei interact. Each precessing nucleus produces a field at adjacent nuclei which has both static and rotating components. If the precessing component has the same frequency as that for a nearby nucleus of the same type an exchange of spins can occur. This relaxation takes the form of a loss of any phase relationship of a precessing nucleus with its neighbours.

1:6 Equilibration of Population Levels

When a sample is inserted into a magnetic field the approach to the thermal equilibrium distribution of nuclei between the various levels can be expected to occur over a finite time. For two adjacent levels it will be governed by the probabilities for the two relaxation transitions $P_{HIGHER \rightarrow LOWER}$ and $P_{LOWER \rightarrow HIGHER}$ which are non-equivalent, together with the number of nuclei initially present in both levels. At equilibrium

$$n_H . P_{H \rightarrow L} . \quad = \quad n_L . P_{L \rightarrow H} \qquad 1 : 17$$

Rearranging, and using equation 1 : 13 for the ratio of n_H to n_L the following expression is derived:

$$\frac{P_{H \rightarrow L}}{P_{L \rightarrow H}} \quad = \quad \frac{n_L}{n_H} \quad = \quad \frac{e^{\left(\frac{m+1}{I}\right) \cdot \frac{\mu H_o}{kT}}}{e^{\frac{m}{I} \cdot \frac{\mu H_o}{kT}}} \qquad 1 : 18$$

$$= \quad e^{\left(\frac{\mu H_o}{IkT}\right)}$$

$$\simeq \quad 1 \; + \; \frac{\mu H_o}{IkT} \qquad 1 : 19$$

If P is taken as the average value of $P_{L \rightarrow H}$ and $P_{H \rightarrow L}$ it is possible to derive the expressions

$$P_{H \rightarrow L} \quad = \quad P\left(1 + \frac{\mu H_o}{2IkT}\right) \quad \text{and} \quad P_{L \rightarrow H} \quad = \quad P\left(1 - \frac{\mu H_o}{2IkT}\right) \qquad 1 : 20$$

The movement of a nucleus to the upper state will decrease the excess population in the lower state by two and hence the differential equation describing the rate of increase of the number of nuclei (n) in the upper state is

$$\frac{dn}{dt} \quad = \quad 2n_L . P_{L \rightarrow H} \; - 2n_H . P_{H \rightarrow L} \qquad 1 : 21$$

Substituting from equation 1 : 20

$$\frac{dn}{dt} \quad = \quad -2P.(n_{eq} \; - \; n) \qquad 1 : 22$$

where n_{eq} is the equilibrium value of the excess number of n given by

$$n_{eq} \quad = \frac{\mu H_o}{2IkT} \quad . \quad (n_H \; + \; n_L) \qquad 1 : 23$$

Integration of 1 : 22 leads to

$$n - n_{eq} = (n_i - n_{eq})e^{-2.P.t} \qquad 1 : 24$$

where n_i is the initial value of n. The characteristic time for equilibration, which is the spin lattice relaxation time T_1 is seen to be

$$T_1 = \frac{1}{2P} \qquad 1 : 25$$

and gives the time for a 65% return to equilibrium conditions.

1:7 N.M.R. in Macro Samples

Approaching N.M.R. from a macroscopic viewpoint, Bloch (12,13,14) was able to describe the bulk magnetisation of a sample using a series of phenomenological equations. In a static field H_o, it is possible to define a susceptibility χ_o

$$M_o = \chi_o . H_o \qquad 1 : 26$$

where M_o is the bulk magnetisation in the direction of the static field. When an oscillating magnetic field, H_1, is applied in a manner suitable to cause resonance the total magnetisation of the sample, M, becomes time dependent and by analogy with the equation of motion of a single precessing nucleus (equation 1 : 10)

$$\frac{dM}{dt} = \gamma.M.H \qquad 1 : 27$$

where H is the vector sum of H_o and H_1, which may be resolved into its constituent parts along the co-ordinate axes.

$$H_z = H_o \qquad 1 : 28$$

$$H_x = H_1 . \cos \omega_1 t \qquad 1 : 29$$

$$H_y = -H_1 \sin \omega_1 t \qquad 1 : 30$$

where ω_1 is the angular velocity of H_1.

The components of the bulk magnetisation, M, vary according to:-

$$\frac{d\,M_x}{dt} = \gamma(M_y.H_o + M_z.H_1.\sin \omega_1 t) \qquad 1 : 31$$

$$\frac{d\,M_y}{dt} = \gamma\,(-M_x.H_o + M_z.H_1.\cos\omega_1 t) \qquad 1 : 32$$

$$\frac{d\,M_z}{dt} = \gamma\,(-M_x.H_1\ \sin\omega_1 t - M_y.H_1.\cos\omega_1 t) \qquad 1 : 33$$

Apart from the effects of the applied field, the relaxation mechanisms described above are present and are regarded as following an exponential law. Spin lattice relaxation, governing the distribution of nuclei in the parallel or anti-parallel orientations with respect to the z direction will clearly affect M_z alone and for this reason is called the longitudinal relaxation time defined by

$$\frac{d\,M_z}{dt} = \frac{-(M_z - M_o)}{T_1}. \qquad 1 : 34$$

The time dependance of M_x and M_y follows a similar relationship governed by T_2 which is called the transverse relaxation time because it governs relaxation in the XY plane. The equilibrium values of M_x and M_y are zero in the absence of the H_1 field and therefore:-

$$\frac{d\,M_x}{dt} = -\frac{M_x}{T_2} \qquad 1 : 35$$

$$\frac{d\,M_y}{dt} = -\frac{M_y}{T_2} \qquad 1 : 36$$

By combining equations 1 : 31 to 1 : 36 the final equations are obtained:-

$$\frac{d\,M_x}{dt} = \gamma(M_y.H_o + M_z.H_1.\sin\omega_1 t) - \frac{M_x}{T_2} \qquad 1 : 37$$

$$\frac{d\,M_y}{dt} = \gamma(M_z.H_1.\cos\omega_1 t - M_x.H_o) - \frac{M_y}{T_2} \qquad 1 : 38$$

$$\frac{d\,M_z}{dt} = \gamma(-M_x.H_1.\sin\omega_1 t - M_y.H_1.\cos\omega_1 t) - \frac{(M_z - M_o)}{T_1} \qquad 1 : 39$$

These are the Bloch Equations, and the solutions of these which are of importance in N.M.R. spectroscopy are those for which M_z is constant and for which transverse components of M in the XY plane rotate with H_1. It is found that M_x contains components which are in-phase and out-of-phase with H_x and this leads to the concept of a complex susceptibility, χ, which is a function of χ_0.

$$\chi = \chi' - i\chi'' \qquad 1 : 40$$

The expression for M_x is, in fact,

$$M_x = \chi' . 2H_1 \cos \omega_1 t + \chi'' . 2H_1 \sin \omega_1 t \qquad 1 : 41$$

The absorption signal shape is dependant upon the rate of absorption of energy per unit volume as $(\omega_1 - \omega_0)$ changes i.e. upon $H_x . dM_x/dt$ and from equation 1 : 41 only upon χ'', the component of χ out-of-phase with the rotating field. χ' and χ'' are both plotted as a function of $(\omega_1 - \omega_0)$ in fig. 1 - 3. The out-of-phase component (the V-mode) represents the absorption line shape and the in-phase component χ' represents the dispersion mode (the U-mode), both of which can be detected.

The area under an absorption curve can be obtained by the integration of the corresponding susceptibility term (χ'') over all values of $\omega_1 - \omega_0$. The result is directly proportional to χ_0 the susceptibility in the z direction, which is, in turn a direct function of the number of nuclei (N) per unit volume. The area under each resonance is therefore a direct indication of the number of nuclei of a particular type undergoing resonance, and this feature is of particular importance in the analysis of N.M.R. spectra. The area under an absorption signal is

$$A \propto \frac{(I+1)\, N \mu^2 . H_1 .}{3IkT(1 + \gamma^2 H_1{}^2 T_1 T_2)^{\frac{1}{2}}} \qquad 1 : 42$$

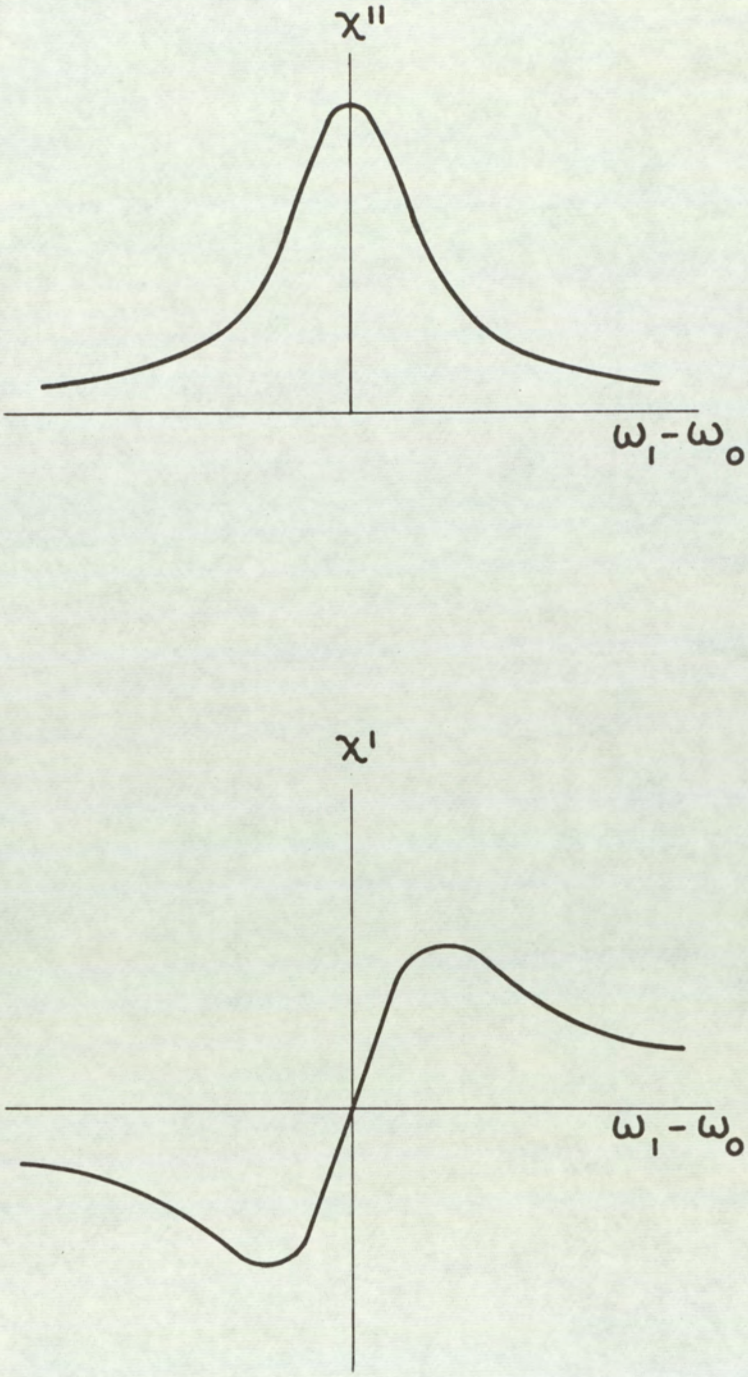

FIG. 1-3 THE ABSORPTION LINE SHAPE (THE V MODE)
AND THE DISPERSION LINE SHAPE (THE U MODE)
OF N.M.R. RESONANCE

1:8 Factors Affecting Line Widths

Because of the less complex shape of the V-mode this is almost invariably used in N.M.R. spectroscopy and will be considered exclusively hereafter. An important characteristic of any resonance line is its width and this is often defined as the width at half height and is expressed either in terms of applied field or frequency. Half height line widths vary from 10^{-2} milligauss in some liquids to several gauss in solids. The shape usually found in liquids for single lines under high resolution is Lorentzian (15). The broadness of the lines are determined by various factors but are primarily influenced by T_1 and T_2. These will now be considered.

Spin Lattice Relaxation

As explained earlier, the fluctuating magnetic field produced by the environment of a nucleus can cause transitions of that nucleus and this places some uncertainty on the lifetime of a nucleus in a particular energy state and hence in the transition energy. The uncertainty principle requires that

$$\Delta E . \ \Delta T \simeq h/2\pi \qquad 1 : 43$$

Since $\Delta E = h\Delta\nu$ 1 : 44

the uncertainty in the absorption frequency $\Delta\nu$ is $(1/2\pi . \Delta T)$ which is $P/2\pi$, and since P is equal to $(1/2T_1)$

$$\Delta\nu \simeq \frac{1}{4\pi T_1} \qquad 1 : 45$$

where T_1 is the spin lattice relaxation time. Small values of T_1 will therefore lead to line broadening.

Spin Spin Relaxation

N.M.R. line widths in solids are almost invariably very broad and of the order of gauss. These in principal arise from magnetic dipole-dipole interactions. The static field produced by a dipole is

$$H = \frac{\mu}{R^3}(3 \cos^2 \theta - 1) \qquad 1 : 46$$

at a point, distance R from the dipole, and lying on a line inclined to the dipolar axis at an angle θ. In the solid state, adjacent nuclei maintain approximately the same orientation with respect to each other and over the whole sample, if amorphous, all values of θ between 0 and 2π are allowed. Consequently, the effective field $(H_o + H)$ is spread out by this effect and resonance occurs over a range of frequencies. If a single crystal is examined the total field at atoms of a particular chemical type will depend on the orientation of the crystal to the applied field and so more than one absorption line may be observed (16).

The precessional motion of individual nuclei will produce oscillating fields at adjacent nuclei and this affords a mechanism of spin exchange and equilibration. Any phase coherence of the precessing nuclei is lost in a time T_2. For spin exchange to occur, the energy change of each nucleus must be identical and it is therefore clear that only essentially equivalent nuclei can be involved in this. Because the nuclei will frequently be precessing at identical frequencies this form of relaxation is very efficient and hence T_2 is much shorter than T_1 and line widths are correspondingly larger. As the temperature of a sample rises and thermal motion increases, the averaging of the local oscillating fields by molecular motion makes the mechanism of phase loss of the precessing nuclei less efficient. T_2 therefore diminishes (17) until in the liquid state it is of the same order of magnitude as T_1 and the observed lines are very narrow. Typical values of T_1 and T_2 for protons in liquids lie between 0.1 and 10 seconds.

Spontaneous Emission

A possible factor contributing to line width could arise from spontaneous downward transitions reducing the lifetime of the upper state. This was investigated by Bloembergen, Purcell and Pound (18) and found to be negligible.

Electric Quadrupole Effects

Nuclei having values of $I \geqslant 1$ possess electric quadrupole moments. If the environment of an atom, possessing such a nucleus undergoing resonance, produced an electric field gradient across the nucleus, the interaction of its asymmetric charge distribution with the electric field facilitates pseudo spin lattice relaxation (17) which increases the resonance line width. A large splitting of the energy levels also occurs which leads to very broad lines.

Saturation

If the applied R.F. field is large in amplitude, (i.e. several milligauss) the excess number of nuclei in the lower energy state will be removed before the resonance line has been traversed, the effect of the various relaxation mechanisms being inadequate to maintain a ground state excess. The absorption of R.F. energy will decrease as the excess in the lower energy level diminishes until an equilibrium situation is achieved and saturation occurs which is characterised by the so-called saturation factor

$$Z_o = (1 + \gamma^2 H_1{}^2 T_1 T_2)^{-1} \qquad 1 : 47$$

This expression is the maximum saturation value applying at the centre of the absorption band. At the edge of the band, saturation is much less and hence line broadening is observed. If sufficient R.F. power is applied the signal may disappear entirely. Values of T_1 and T_2 may vary for different nuclei within one molecule giving rise to differing saturation effects for different lines in the same spectrum (19).

Magnetic Field Inhomogeneity

This is a technical factor causing apparent line broadening. If the magnetic field is non-uniform over the volume of the sample used the observed line is a super-imposition of the true lines produced by resonance of magnetically identical nuclei in different parts of the sample. Modern instruments have reduced this contribution to negligible proportions except in unusual cases.

1:9 The Chemical Shift

The nuclei of a molecule rarely experience the true value of the externally applied magnetic field, because this is always modified by structural features within the molecules themselves (20) and to a lesser extent by effects arising from the surrounding medium. The effects have their origin in the various diamagnetic circulations of electrons in the molecule, together with those associated with individual atoms. The local field is altered by a factor σ, the screening constant, so that the actual field experienced by a nucleus is given by

$$H_{local} = H_o (1 - \sigma) \qquad 1 : 48$$

σ is dimensionless and most commonly positive. The reduction in H_o reduces the Zeemann splittings and for the specific case of $I = \frac{1}{2}$ this is illustrated below (21).

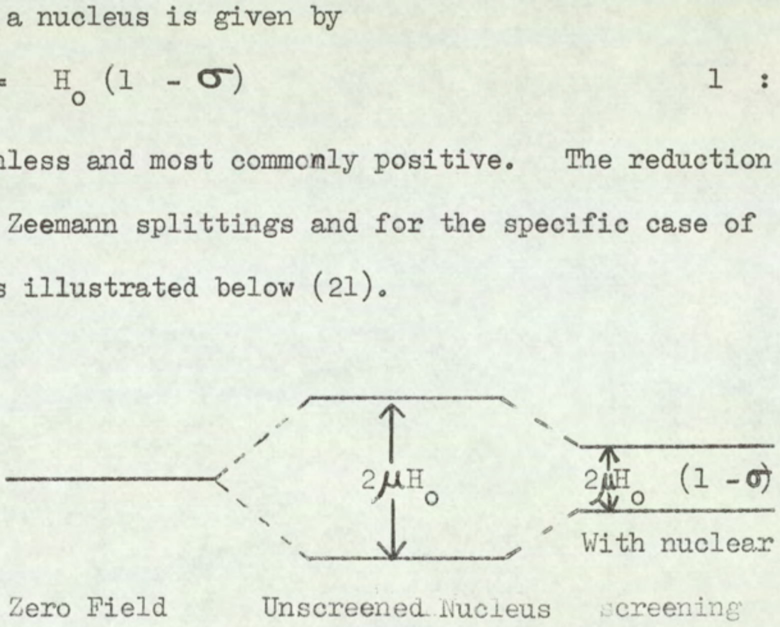

The reduction in the effective value of H_o means that a high external field must be applied to secure resonance at a particular frequency. The differences in the screening of nuclei are known as 'chemical shifts'.

It is extremely difficult to measure the resonance condition of a nuclear species absolutely in terms of field strength (or frequency) to the accuracy required for narrow line N.M.R. To remedy this, reference compounds are used which give single sharp lines, and chemical shifts (δ) are measured from these in terms of a fraction of the field (or frequency), the units used being parts per million (p.p.m.).

$$\delta = \frac{H - H_R}{H_R} \times 10^6 \text{ p.p.m.} \qquad 1 : 49$$

The normal method of calibration of spectra is described in Chapter 2 and involves measurement of frequency differences. These are, of course, directly proportional to magnetic field measurements and δ may be redefined as:

$$\delta = \frac{\nu - \nu_R}{\nu_R} \times 10^6 \text{ p.p.m.} \qquad 1 : 50$$

These two definitions of δ lead to the convention that nuclei which are less shielded than the reference have negative chemical shifts. The commonly accepted reference for proton studies is tetramethylsilane (T.M.S.) (22), whose resonance is a clear sharp line occurring to high field of most resonances of interest which have, as a result, negative values of δ. To remedy this inconvenience, the 'τ-scale' has been defined (22) such that the τ value of a resonance is equal to (δ + 10) p.p.m. Because of the possibility of solvent effects the scale is defined only for infinite dilution in carbon tetrachloride and τ values are only strictly obtainable by extrapolation to this condition. A recent publication (135) investigates the errors introduced by the use of other solvents and provides a list of corrections enabling an accurate τ value to be ascertained.

1:10 The Origins of the Chemical Shift

Intra-Molecular Screening Effects

The factors which determine the magnitude of nuclear screening and hence of the chemical shift within molecules can be resolved into a number of terms (23), which are usually conceived to rationalise the details of rigorous theoretical treatments (24,25,26) of chemical shifts in terms of acceptable classical concepts. The terms are defined to provide reasonable estimates of the contribution to shielding arising from electrons localised in atoms and in chemical bonds. For a resonant nucleus A in the neighbourhood of another equivalent or non-equivalent, nucleus B, the screening of A may be written as (27):-

$$\sigma_{A} = \sigma_{AA}^{dia} + \sigma_{AA}^{para} + \sum_{B\neq A} \sigma_{AB} + \sigma_{A}^{deloc} \qquad 1 : 51$$

The various terms in this will now be discussed briefly.

Diamagnetic Electron Shielding (σ_{AA}^{dia})

This arises from induced diamagnetic currents on A and its magnitude depends on the electron density around A.

Paramagnetic Contribution to Shielding (σ_{AA}^{para})

This term is regarded as arising from the mixing of ground and electronically excited states (28,29) which is induced by the applied field H_o. The precise evaluation (30,31) of this is difficult since this requires a knowledge of the energies and wavefunctions of both the ground and excited states for the molecule.

Inter Atomic Shielding (σ_{AB})

This term, arising from induced currents in adjacent magnetically anisotropic electron groups, may be diamagnetic or paramagnetic in character (23). The electron groups may be considered to be those in the individual atoms but for convenience are often taken as isolated bonds (32).

Delocalised Electron Shielding (σ_{A}^{deloc})

This arises from electron circulation induced by H_o in fully conjugated orbitals such as exist in the benzene molecule (33). If the orbital consists of a closed loop, diamagnetic currents circulate, and the accompanying magnetic field contributes to the screening of adjacent nuclei. Those nuclei in atoms situated in the vicinity of the symmetry axis of the loop experience a decrease in H_o while those lying in the plane experience the reverse effect (21). The very large diamagnetic anisotropy of hexamethylbenzene crystals was attributed to this effect by Pauling (34).

Differences in any of the terms referred to above for two resonant nuclei contribute to the observed shift between them and the various contributing terms are thought to have different magnitudes for different nuclear species (35,36). For example, in the case of fluorine chemical shifts the electric fields produced by the polar bonds are thought (32) to be the most significant, thus altering σ^{dia} and σ^{para}. In the case of proton shieldings, however, electric field effects are commonly supposed to be negligible, and observed chemical shift differences have been attributed to bond anisotropies (37,38) and therefore, to variations in σ_{AB}. More recently, it has been shown (39) that proton shifts can be rationalised in terms of apparent bond anisotropies which are thought to accommodate variations in nuclear screening arising from electronegativity, electric field and real anisotropy effects.

Inter-Molecular Screening Effects

As in the case of the intra-molecular screening effects, the influence of the medium is conveniently resolved into a number of components resulting from various types of inter-molecular interaction and may be given by (40)

$$\sigma_M = \sigma_B + \sigma_A + \sigma_E + \sigma_W \qquad 1 : 52$$

As in the case of intra-molecular effects, differences between any of the terms for different nuclei contribute to the shift between them which, as indicated earlier, are measured relative to some convenient reference nucleus. So far as medium effects are concerned both the solute and reference will be subject to these terms and if they are affected differently a correction to the recorded chemical shift is necessary in order to provide an accurate shift value free of medium complications. The reference compound may be dissolved in the liquid under examination or, if this is not possible, may be contained in a small capillary tube within the main sample tube. The medium effects on the measured shifts can be different for two reference situations and in the light of this the various effects will be outlined here and a more detailed investigation given in Chapter 3.

Bulk Magnetic Susceptibility (σ_B)

When an external reference is used, the difference in the volume susceptibilities of the solute and reference liquids leads to difference shieldings of the solute and standard. The effective field at a molecule in a medium of volume susceptibility χ is (40)

$$H = H_o \left[1 + \left(\frac{4\pi}{3} - a\right)\chi \right] \qquad 1 : 53$$

where a is a shape factor for the sample container; this is equal to 2π for a cylinder with its length large compared to its diameter. Because sample tubes with accurately known dimensions (which are most commonly cylindrical) are difficult to make, it is the practice, whenever possible chemically, to employ an internal reference compound which will experience the same susceptibility effect as the solute under investigation so that $\Delta\sigma_B = 0$.

Solvent Anisotropy Effect (σ_A)

In the case of solvent molecules which exhibit anisotropy in their magnetic susceptibility this may become significant in affecting the field experienced within the sample by individual molecules. This term will arise particularly when a solute molecule adopts a preferential orientation with respect to the solvent molecules, perhaps by reason of steric or other specific interactions (40). If an external reference is used, considerably difficulties in providing a correction arise because the precise nature of any screening contribution has proved difficult to predict. An internal reference compound can be expected to reduce this term considerably and in the absence of any evidence to the contrary the effect is often neglected.

Electric Field or Reaction Field Screening (σ_E)

When a solvent molecule experiences the electric field of a polar solute molecule an electric dipole is induced in it. The electric field of this induced dipole modifies the electron distribution (41) of the solute molecule causing a change in the screening of the nuclei within it.

Van der Waals or Dispersion Screening (σ_W)

This effect is similar mechanistically to σ_E, and arises from Van der Waals or dispersion interaction forces which act when any molecular species come together. When two molecules approach each other the time varying electric dipoles in each polarise the other molecule and this polarisation, in turn, modifies the electron distribution in the original molecule (42,43). This modification to the free movement of electrons is, like the reaction field effect, effectively paramagnetic.

1:11 Spin-Spin Coupling

High resolution experiments on samples whose molecules contain two or more chemically shifted resonances frequently reveal that a band assigned to one type of nucleus is split into two or more peaks (44,45). This is attributed to intramolecular interaction between the nuclear magnetic moments and is called spin-spin coupling which is characterised by a line splitting of J(Hz).

Characteristics of Spin-Spin Coupling

Spin coupling interactions exhibit several important features (45) which help to distinguish them from chemical shift effects.

(a) Coupling constants are independant of field strength and also of temperature.

(b) Spin coupling effects are mutual i.e. the splitting observed in one band is identical to the splitting in the band of the interacting nuclei.

(c) Coupling is not observed between nuclei in a magnetically equivalent group. Nuclei are described as magnetically equivalent when they have the same chemical shift individually, and have the same coupling constants to all other nuclei in the molecule.

(d) Coupling can occur between nuclei of different types.

(e) The magnitude of J values generally decreases as the distance between the interacting nuclei increases.

(f) J values increase with the atomic weight of the nuclei concerned.

Spin-spin coupling occurs because the basic energy of a nucleus is modified by interaction with other nuclei to allow resonance at different conditions. This modification arises from the perturbations caused by the energy states of other nuclei. An assembly of identical nuclei can have different total energies because of the different possible ways in which individual nuclear spins are orientated with respect to the applied field. In the case of protons where $I = \frac{1}{2}$, a single nucleus has, of course, two energy levels and the resonance line of an adjacent nucleus would be observed as a doublet, each line having equal intensity. Two identical nuclei have 3 possible total energies and give 3 lines of equal spacing for adjacent nuclei. In general, n equivalent nuclei with spin I can cause adjacent nuclei to show $2nI+1$ lines having intensities that follow a binomial distribution.

These rules of line intensity and spacing are only strictly applicable when the chemical shift between the interacting nuclei is large compared with the coupling constant. When this is not the case, second order spectra occur in which the simple intensity and spacing rules are no longer valid and additional lines appear in the spectrum. This situation has not been encountered in the work reported herein and will therefore not be considered further.

The Mechanism of Spin Coupling

The simplest generally accepted mechanism of spin-spin interaction involves the effect of electrons in the intervening bonds between nuclei. A physical interpretation (46) of the mechanism envisages magnetic interaction between each nucleus and the bonding electron spin of its own atom together with the exchange coupling of the electron spins with each other. Because the spins of electron bond pairs lie anti-parallel, the spin orientation and hence the energy state of a nucleus will be detected by an adjacent nucleus.

Ramsey (47,48) has given a general theoretical expression for spin-spin coupling which, however, cannot be evaluated accurately even in simple cases. Approximate calculations (49,50,51) show that the electron spin mechanism described above is the most important term although in general all magnetic interactions could play a part.

Description of Nuclear Systems

Because of the presence of spin coupling fine structure, it is convenient to distinguish between groups of interacting nuclei with large chemical shift separations which will exhibit first order effects and those with small shifts where second order effects can occur (21). Nuclei with small shift separation of the same order of magnitude as the coupling constants involved are designated by letters close together in the alphabet, e.g. A,B,C,D, and are called a basic group of nuclei. Other basic groups within a molecule separated from the A,B,C,D, group are designated by letters placed together in some other part of the alphabet, e.g. P,Q,R or X,Y,Z. Magnetically equivalent nuclei are designated by the same symbol and the number present is indicated by a suffix. Thus acetaldehyde, at 60MHz, is described as an AX_3 system (or A_3X). If the applied field strength were reduced in this case to a level where the chemical shift difference was of the same order of magnitude as the coupling constant the system would then be described as an AB_3 indicating that the spins were "strongly coupled" and that the spectrum was no longer first order.

1:12 The Effect of Chemical Exchange on N.M.R. Spectra

When an atom containing a resonant nucleus is involved in chemical exchange, the appearance of the spectrum may be modified depending on the rate of exchange (52,53). If this is very slow the N.M.R. spectrum will exhibit features characteristic of each allowed chemical environment. However, if for example the atom experiences two different chemical environments for time periods short in comparison with the reciprocal of the chemical shift difference (Hz) that it would have if fixed in both situations, a time average of the chemical shifts is observed. For similar reasons, if an atom is removed from an environment in a time short compared with the reciprocal of the spin coupling constant, spin coupling features are also affected (54,55).

If, therefore, two molecules in solution are in dynamic equilibrium between associated and non-associated states, the observed chemical shifts of nuclei in the molecules can result from time averaging as described above. A particular example where this occurs is that of chloroform and benzene in a solvent such as cyclohexane (56) where the non-bonded molecules are in equilibrium with a specific chloroform-benzene complex. In this case, the result of the two molecules bonding together is to enhance the effect especially for the chloroform, of the inter-molecular screening constants above because of the relatively close and long lasting contact between them. The main contribution arises from the anisotropic shielding by the aromatic ring arising from the electron circulation in the carbon π-orbitals. The form of the well authenicated chloroform and benzene complex is illustrated in fig. 3 - 1.

Dipole-induced dipole complexes of this type, formed between polar solutes and aromatic molecules, can be investigated by studying the dependance of the observed solute time averaged shift on sample composition. Investigations of this type form the basis of the work reported herein, which was directed to the determination of the stereochemistry and thermodynamic parameters of various complexes.

CHAPTER 2

Practical Considerations

2:1 The Requirements of an N.M.R. Spectrometer

In order to produce high-resolution spectra from which the maximum amount of information may be derived, all spectrometers must incorporate the following basic features.

(a) A high intensity magnetic field possessing high stability and homogeneity.

(b) A 'probe', which is essentially a sample holder supporting the irradiation and, if desired, detection coils, and having provision for sample spinning.

(c) Facilities for linearly sweeping either the magnetic field or the irradiation frequency.

(d) An R.F. source of high stability (of the order of 1 part in 10^9).

(e) An R.F. receiver and amplifier system designed to produce high gain with low noise.

(f) Presentation facilities utilising an oscilloscope and/or recorder.

2:2 The Magnet

Both electro-magnets and permanent magnets find use in N.M.R. spectrometry and their differing characteristics determine their usefulness in different applications.

The electro-magnet is often preferred because of its high degree of flexibility, and the field strength can typically be set at any value up to about 24,000 gauss or in the case of super-conducting magnets, 50,000 gauss. This facility permits the examination of all magnetic nuclei at more than one resonant frequency and is of great assistance when interpreting spectra containing multiplet bands of uncertain assignment. To this end, variation of field strength may assist in distinguishing features arising from chemical shift effects (proportional to H_o) from those due to spin-spin interaction (H_o independent). Other factors in favour of electro-magnets are the high resolution which can readily be attained and the generally more advanced state of electro-magnet technology. The principal disadvantages of the electro-magnet are its high cost and relatively short life-time. Furthermore, present day high performance electro-magnets do not always take advantage of the field variation feature but are designed to work at the highest feasible field strength, and different nuclei are examined at different frequencies.

The principal assets of the permanent magnet are its high field and resolution stability and negligible running cost. Because the field strength cannot be varied by more than a fraction of 1%, different nuclei require different operating frequencies. However, because of the present usage of electro-magnets this can no longer be considered a disadvantage.

Field homogeneities obtainable from the two types of magnet are comparable and are of the order of 3 parts in 10^9.

2:3 Optimising Magnet Performance

N.M.R. resonance line widths are frequently less than 0.01 p.p.m. and it is important that the performance of the magnet both in terms of field stability and resolving power should equal and preferably exceed this natural specification.

Resolution

In order to achieve high performance in this respect the pole pieces of the magnet must be optically flat (57) and strictly parallel. The ratio of pole piece diameter to pole gap found necessary is generally about 8:1 (58) for electromagnets but is considerably lower (4:1) for permanent magnets.

An effective sample volume of 0.1 c.c. is generally found to be the largest permissible if high resolution is to be achieved and the variation in field strength over such a sample is about 1 p.p.m. when placed in the most uniform part of the field. This is improved by the use of printed circuit current carrying shim coils (59,60) which can be manipulated to remove residual field gradients, in particular the barrelling effect of the field. By these means the observed line width may be reduced to the equivalent of a few hertz.

The final improvement to resolution is brought about by spinning the sample (61,62,63), in a precision drawn cylindrical glass tube about an axis parallel to the pole faces.

In this way, if the field varies by an amount ΔH over the sample, then a molecule during each time interval t will be exposed to ΔH. As the spinning becomes quicker and t smaller a given nucleus effectively sees a time averaged field which removes the inhomogeneity. This becomes effective when

$$t \simeq \frac{1}{\gamma \Delta H} \qquad 2 : 1$$

The observed line width after spinning can be as low as 0.005 p.p.m. or less and this compares favourably with line widths which commonly occur.

The smaller diameter pole pieces necessary on permanent magnets make shim design very critical and generally more shims are needed than with an electro-magnet. Resolution is more difficult to achieve but often lasts much longer for a magnet which has "settled in". The more rapid loss of resolution of electro-magnets is nowadays effectively removed by automatic shims which continuously optimise peak height.

Field Stabilisation

For accurate measurement of chemical shift differences it is essential that great attention be paid to the stability of the field.

Permanent magnets are readily stabilised by extensive lagging (64,65) which also ensures high stability of resolution. Even so, the sensitivity of the N.M.R. technique is such that careful ambient temperature control is also necessary if the use of pre-calibrated chart paper is intended. Ambient field disturbances are commonly minimised by mu-metal screening or by a field sensing device (66) which applies a correction at the pole gap by means of field compensation coils.

Electro-magnet stability is more difficult to control because it depends critically on the stability of the current passing through the coils and on the temperature of the cooling water (67). The commonest method of control of the gross current is to pass it through a small resistance and to compare the voltage drop with a stable reference voltage, and after amplification utilise the voltage difference for correction purposes. Instabilities of the order of 1 p.p.m. frequently occur within the reference cells used and this sets a limit to this method of stabilisation. A further complication arises from the use of the D.C. amplifier which is difficult to design with drift free characteristics.

Further correction of field drift is achieved by the use of a flux stabiliser (68). In principle, this often consists of detector coils, wound round the pole pieces, in which an induced voltage occurs as a result of flux changes across the pole gap. This voltage is amplified and integrated by a galvanometer amplifier and the resulting signal is used to apply a correction through a pair of compensating coils, with the result that the original error is removed. Flux stabilisers are not normally sensitive enough to compensate for slow steady magnet field drifts, but these can be minimised by reference to the change in the position of N.M.R. signals scanned repetitively. An artificial error signal is introduced to the flux stabiliser until the observed drift is removed.

The problem of field drift in electro-magnets has, more recently, been solved in a more satisfactory manner by the introduction of so-called field/frequency lock techniques. In the first applications (69,70,71) of this technique, a separate control sample containing water was situated in the vicinity of the test sample and irradiated by a frequency adjusted to cause resonance. The sharp signal was detected in the dispersion mode which has zero amplitude at exact resonance. Any variation of the field created an error signal (see Fig. 1 - 3) which was used to apply a correction either to the field or to the frequency used for spectral observation. The spectrum was observed by linearly varying the observing frequency. A present day refinement (72,73) of this technique uses a strong sharp peak in the sample under investigation for correction purposes. The signal from this is differentiated from the required normal spectrum by phase sensitive detection techniques.

2:4 The Probe Assembly

This is supported centrally in the air gap between the magnet pole pieces on a carriage which allows both vertical and horizontal adjustment in order that it may be placed in the most uniform part of the field. The R.F. coil is wound on a vertical glass former and usually consists of 3 or 4 turns of fine copper wire. The small number of turns is all that is necessary to enclose the volume over which high resolution can be obtained. Larger sample volumes and greater numbers of turns are used when nuclei of lower sensitivity are to be examined but, naturally, the resolution attainable is not the highest.

The sample, in its cylindrical glass tube (typically 5 mm.o.d) is inserted down the inside of the vertically placed glass former and is supported at the top and bottom by bearings to faciliate spinning for the purpose of improving resonance line width.

The probe assembly frequently incorporates other units closely associated with the function of the probe. These include the R.F. bridge, shim coils, sweep coils and preamplifiers.

2:5 Scanning the System

The difficulty of providing an R.F. signal which is both stable and capable of linear variation over large frequency ranges led early instrument manufacturers to use magnetic field sweep for spectral scanning in conjunction with a highly stable crystal controlled R.F. source for sample irradiation. The field sweep may be conveniently derived from the output of a saw-tooth generator which is amplified and fed to a pair of Helmholtz coils wound either on the pole pieces or mounted with the probe assembly. The spectrum can thus be swept repetitively and the sweep rate and sweep amplitude can be conveniently altered (74). If the saw-tooth generator governs the time base of an oscilloscope, simultaneous display of the signal is possible. The field sweep can also be derived from a motor driven potentiometer linked to a recorder to produce a permanent record of the spectrum.

The above methods can be used for both permanent magnets and electro-magnets. However, when it is necessary to apply permanent field shifts the two types of magnet require different methods. Permanent magnets need simply, additional pairs of coils which carry current to produce pre-calibrated field shifts. With an electromagnet this is not really possible with the field under high stability flux stabiliser control and instead the flux stabiliser is used to vary the field by the introduction of a false error signal in a manner similar to that described above. Calibration is carried out by a method described later (2:7). When a field/frequency lock device is used, manipulation of the frequency is all that is necessary and chemical shift measurements are made by direct read-off from calibrated charts or by measuring the beating of the irradiating frequency at resonance and the locking signal.

If an absorption line is traversed rapidly, the relaxing nuclei produce a signal which beats with the irradiating frequency. The shape and duration of this beat signal may be used as a good indication of field homogeneity. Having achieved resolution it is necessary, in order to obtain accurate line shapes and to distinguish very small chemical shifts, to sweep the spectrum slowly. Unfortunately, a slow sweep rate emphasises any field instabilities and may also lead to signal saturation and line broadening, so, in practice, a compromise is necessary. For wiggles to be absent the following condition must be satisfied (75):-

$$\frac{dH}{dt} \ll \gamma(\delta H_o)^2 \qquad 2 : 2$$

where δH_o is the line width expressed in field units.

2:6 The Facilities Used

For the investigations reported herein a Perkin-Elmer model R10 spectrometer was used. This utilises a permanent magnet having a field strength equivalent to 14,093 gauss. This permits proton resonance studies at 60.004 MHz.

The Magnet

The effective field is produced in an air gap between pole pieces, of approximately 5 inches diameter, separated by about 1 inch. Coarse adjustments of its strength are made by means of a mechanical shunt but field adjustments required when the machine is in use are made by pairs of Helmholtz coils in the manner described previously. There is a steady drift of the magnetic field of about 0.1 p.p.m. per hour arising principally from temperature changes of the environment. No rigorous attempt is made to correct for this, but rapid magnetic disturbances arising in the vicinity of the magnet are minimised, using a field compensator. This device incorporates a sensing head situated at a magnet field node outside its console which detects flux changes. A compensating field is applied at the pole pieces by means of a spare pair of Helmholtz coils. Disturbances originating more than 15 feet away can be accurately eliminated. An additional pair of coils allow computer controlled field shifts to be made when necessary.

The probe assembly is mounted on a bar, traversing the air gap, and carries the nine shim coils necessary to obtain good resolution.

The magnet assembly is totally enclosed and surrounded by thick layers of expanded polystyrene containing temperature sensing devices and heating elements. These enable the magnet to be thermostatted to an accuracy of $\pm$ 0.001°C at 33.4°C.

Detection and Presentation of the N.M.R. Signal

The overall schematic diagram of the spectrometer is shown in Fig. 2 - 1. The R.F. signal for proton resonance studies is derived from a crystal controlled oscillator operating at 5.000 MHz. with a high harmonic content. The second harmonic (15 MHz), is selected by

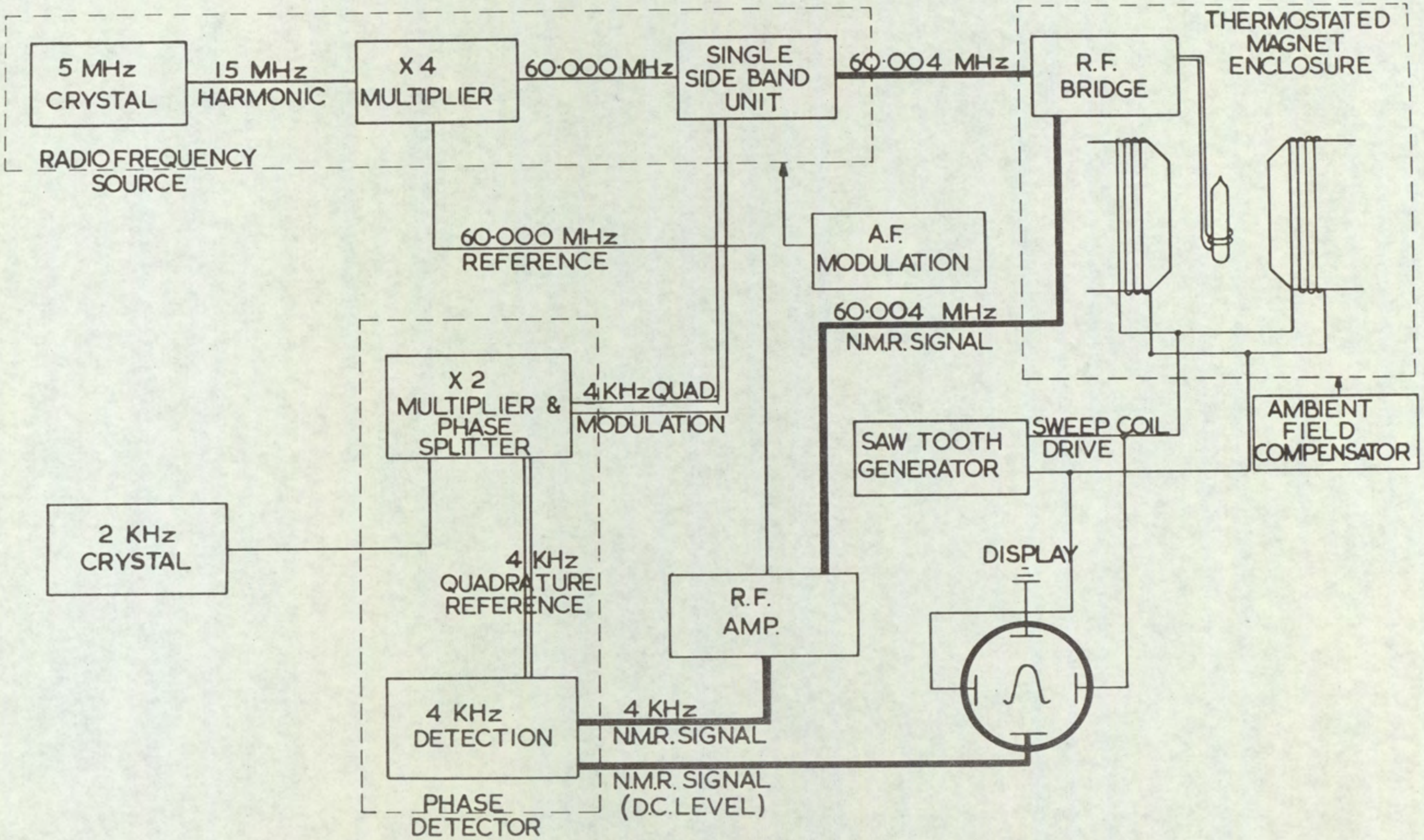

FIG. 2-1 SCHEMATIC DIAGRAM OF THE PERKIN-ELMER MODEL R.10 N.M.R. SPECTROMETER.

a tuned circuit and multiplied to 60.000 MHz. A separate crystal controlled oscillator (4 KHz) provides a signal used for modulating this R.F. signal in a single side-band unit which essentially displaces the R.F. signal by 4 KHz. while suppressing the original carrier and the unwanted side-band. After amplification and automatic gain control the supply passes via a variable attenuator to the bridge and probe. The overall stability of the frequency source is of the order of 1 part in 10^9. Detection is by means of the single coil method, the sample coil forming part of a twin-T type R.F. bridge circuit. After a sample has been inserted into the probe the bridge is balanced to an exact null using phase and amplitude controls, care being taken at that time to avoid the resonance condition of any nucleus.

At resonance the inductance of the sample coil changes and the bridge circuit is no longer balanced. The N.M.R. signal (at 60.004 MHz), with phase and amplitude characteristics is passed to the R.F. amplifier in the main operating console. After preamplification it is mixed with a 60.000 MHz. homodyne reference derived directly from the R.F. source. After three further stages of amplification the mixed signals pass through a diode detector whose output is the beating signal at 4 KHz.

After further amplification the signal passes to a phase sensitive detector (76) where its phase is compared with part of the original 4 KHz acting as a reference signal, of variable phase. The reference phase is adjusted manually to obtain the desired mode of presentation. The output of the phase detector which is now a D.C. level can be supplied to the oscilloscope or recorder.

To assist in improving the quality of the final spectrum, a series of condensers in an RC circuit can be selected which cut down the response time of the circuit and improve the apparent spectral signal-to-noise ratio.

By passing the signal through a circuit containing a D.C. amplifier connected across a condenser, an integral of the absorption spectrum can be obtained. Because the amplitude of an N.M.R. signal is directly proportional to the number of nuclei involved (section 1:7) an integral provides valuable information about the relative numbers of hydrogen atoms (or other atoms) present in the different groups in the molecule.

The N.M.R. spectrum is scanned by a linear variation of the field derived from an oscilloscope time-base or a recorder driven potentiometer as described earlier.

2:7 Accurate Chemical Shift Measurement

The calibrated charts and field shift controls of the R10 allow quite accurate chemical shift measurements to be made routinely, but for work of the highest accuracy some improvements are possible and indeed necessary in this work.

If the irradiating frequency (60.004 MHz) is modulated at (say) a few hundred hertz, each resonance line will be accompanied by two sidebands, because each frequency will require a separate value of H_o for resonance. The frequency separation of the lines is identical with the modulation frequency, and so the spectra may be readily calibrated. In the systems under examination the calibration sidebands of a strong reference peak were used to encompass the peak of interest by varying the modulation frequency in set increments as the latter peak was traversed. The advantage of this method, where each spectrum is independently calibrated, is that minute by minute changes in field (or frequency) drift are accounted for. Provision is made on the R10 for this method to be used and the audio-frequency (A.F.) signal necessary was obtained from a Muirhead-Wigan D-890-A oscillator and the frequency of this ascertained using a Venner 3336 counter.

2:8 The Accessory for Variable Temperature Studies

The normal probe described above works at the temperature of the magnet enclosure and precautions are taken to ensure that as little thermal disturbance as possible occurs in the region of the probe assembly. It is however, very useful and, in the work to be reported, necessary to study the effect of temperature changes on N.M.R. spectra.

The facilities available for the R10 allow any temperatures from -100°C to +200°C to be readily attained. One of the most important parts of the accessory is the small dewar flask which is positioned in the magnet gap, replacing the standard assembly, and effectively insulating the magnet from the environment of the sample tube. This, in turn, is surrounded by a water jacket at 33.4°C which completes the thermal isolation of the magnet from the sample. To raise the temperature of the sample, air is drawn in through a large copper block and heated electrically before passing to the probe. This minimises any temperature gradients in the hot air stream. To reach temperatures below that of the magnet a supply of liquid nitrogen droplets and gas, boiled from the liquid, is mixed with dry air, and the mixture is heated as above to obtain the desired temperature. Within 0.5 cm. of the R.F. coil is a platinum resistance thermometer which monitors the sample temperature in order that automatic correction to the pre-set temperature can be made.

Very steady temperatures can be achieved repetitively with the device and this feature makes it particularly useful in the determination of thermodynamic data. In order to determine the temperature to 0.1°C an independant copper constantan thermocouple is incorporated in the probe and the e.m.f. it produces can be monitored by means of a potentiometer (fig. 2 - 2) and reference to an e.m.f. - temperature table.

2:9 A Device for Improving the Signal-to-Noise Ratio

For reasons which will become apparent in subsequent chapters it was desirable to use the solutes under investigation at as low a concentration as was practical. Because of the very small excess number of hydrogen nuclei in the lower energy levels at 14,093 gauss, resonance lines arising from proton concentrations less than 1% molar cannot readily be observed using the R10 spectrometer. In an attempt to overcome this problem, several methods of improving the signal-to-noise ratio (S/N) were examined. The method adopted by commercially available equipment is the spectrum accummulation technique (77) in which a computer digitises each spectral run and adds them together. Over a period of time the random noise tends to zero while the signals continually add, even though on a single scan they are not observable. The improvement after N accummulations is proportional to $\sqrt{N}$. Although this method is the most suitable it appeared prohibitively expensive and a number of cheaper alternatives were considered.

One method (78) which has been used is to cut down the response time of the presentation circuit by the use of a large condenser in the RC circuit but the disadvantages of this method lie in its susceptibility to saturation distortion. A better method, based on an idea of Crutchfield (79) involves the use of the integration circuit. If the spectral scan is halted on a resonance line while

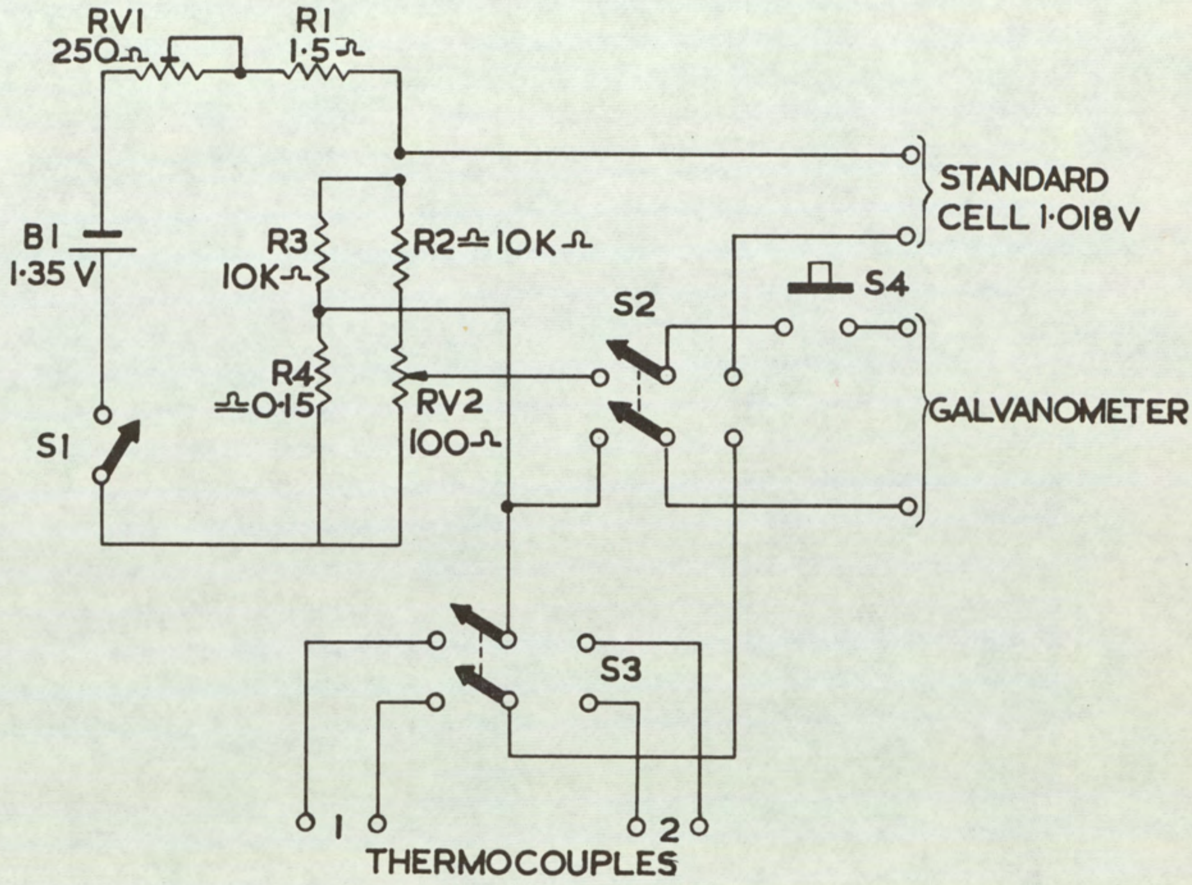

Switch Functions

S1 ON/OFF

S2 MEASURE/STANDARD

S3 +/− Thermocouple Polarity

S4 GALVO ON

FIG. 2-2 POTENTIOMETER CIRCUIT FOR VARIABLE TEMPERATURE EQUIPMENT the integration circuit is in use, the integral of the N.M.R. signal accumulates while the noise oscillates about a mean value. There is thus an improvement in S/N over a period of time and this can be displayed as a vertical deflection of the pen on the chart paper. After the integral has been cancelled the pen returns to the base line, the spectral sweep is resumed for a short interval then stopped, and the cycle is repeated. Gradually, the spectrum appears as the scanning continues. Because of the way most integrals are presented the spectrum will appear upside down but with the R10 this is easily remedied by inversion of the reference voltage.

The apparatus which was devised (known as a MOUSE) performed the above cycles repetitively by means of a closed loop of timers which operated a series of relays opening and closing the necessary circuits. A full description of the details of operation of the MOUSE including its schematic diagram are to be found in the Appendix of this thesis.

It was found that a S/N improvement was possible using this device but because of the rate of field drift an unacceptable degree of error in the calibration of each spectrum was anticipated and it was decided ultimately to accept a concentration of 1% molar as the lowest practical concentration for study and to reduce random errors in the calibration by running the same spectrum a number of times.

CHAPTER 3

The Determination of the Structures of Some Complexes and The Stability Constants for their Formation

3:1 Introduction

The work described in this and subsequent chapters is based on examinations of the collision complexes formed by interactions of the haloforms and nitroform (hereinafter referred to as the solutes) with benzene and with some methylbenzenes. The systems studied are listed below:-

Nitroform and:-
- Benzene
- Toluene
- O-Xylene
- M-Xylene
- P-Xylene
- 1,3,5-Trimethylbenzene (Mesitylene)
- 1,2,4,5-Tetramethylbenzene (Durene)
- Pentamethylbenzene (P.M.B.)
- Hexamethylbenzene (H.M.B.)

Chloroform and:-
- Benzene
- P-Xylene

Bromoform and:-
- Benzene
- P-Xylene

Iodoform and:-
- Benzene
- P-Xylene

Fluoroform and:-
- Benzene
- P-Xylene

The ability of the N.M.R. method to critically study this type of complex stems from the freedom of the π-electrons of the aromatic molecule to circulate and provide unique shielding characteristics, as explained in section 10 of Chapter 1. It has been well-known for many years (80,81,82) that when chloroform is dissolved in benzene a pronounced upfield shift of the chloroform proton resonance occurs, relative to its position in most other solvents, because of specific interactions with the benzene (81,83, 84,85,87). Bearing in mind the direction of the induced magnetic lines of force around the aromatic molecule in an applied field (87,88) it is readily apparent that the chloroform proton lies on or near the six-fold symmetry axis of the benzene ring. That this hydrogen atom is intimately concerned in the interaction of chloroform and benzene is indicated by infra-red studies (89,90,91) which show that the C-H bond (or C-D) (90) stretching band of the chloroform increases in intensity many times due to the presence of the benzene. Copious other evidence of the interaction of chloroform and benzene is available from other techniques (92,93,94,95,96,97,98, 99) which also substantiate the existance of a 1:1 molecular complex.

It was anticipated that the other haloforms and nitroform would complex with benzene and it homologues in a similar manner to chloroform and evidence is available that this is so (100).

The objective of this study was to determine as accurately as possible, the structure of the complexes formed, the thermodynamic parameters relating to the formation of the complexes, and also the effective point of action of the electric dipole in the various dipolar solutes studied.

By measuring the overall chemical shift change of the solute proton in passing from the free to the complex state it is possible, by reference to tables (102) or by calculation (101), to determine the effective position of the proton in relation to the aromatic ring.

From the dependance of solute proton shift on aromatic concentration the stability constant for complex formation may be deduced and thus the thermodynamic parameters, enthalpy and entropy, may be derived by determination of the stability constants at a number of temperatures.

The results of the N.M.R. studies can be compared with those of dielectric investigations, carried out in this department and elsewhere (103), which afforded determinations of the apparent dipole moment of the haloforms when dissolved in various aromatic solvents. The results of the latter investigations clearly show that a small dipole is induced in the aromatic molecule because the apparent dipole moment of the solute is invariably larger than its value in a non-complexing solvent such as cyclohexane (104). From theoretical considerations developed by Frank (105) it is possible to deduce the distance (R2) between the centre of the induced dipole and the effective point of action of the inducing dipole. Comparison of this value (R2) with the distance of the proton (R1) from the ring deduced from the N.M.R. studies, together with a knowledge of the structure of the complex, enables the effective dipolar centre of the solute to be located.

3:2 The Nature of the Complex

Because N.M.R. chemical shifts depends partly on the disposition of electric charges within and around molecules, which may be disturbed when chemical action occurs, it is important, when interpreting shift variations caused by complex formation, to consider possible contributions to these by the formation of bonds and the general re-distribution of electric charge in the system when the complex forms. However, little information is available concerning the nature of the intermolecular bond in species of this type. Of the various possible explanations of the bond type, two are most probable. The first of these would require charge transfer between the aromatic and the solute and the second, purely electrostatic attraction between the participant species. In order to resolve which of these postulates might be valid, the system p-xylene/

nitroform/cyclohexane was examined by U.V. spectroscopy. Using the equilibrium constant for this system (derived from N.M.R. chemical shift data as described later), a sample was made up containing 1% molar free p-xylene and 1% molar free nitroform plus complex dissolved in cyclohexane. This was inserted into the observation arm of a U.V. spectrometer. On the reference side were placed at the same time separate cells containing 1% molar p-xylene and 1% molar nitroform dissolved in cyclohexane. An absorption peak was observed at 350 mμ, with an absorbance of 1.5. This was attributed to the complex and indicated an extinction coefficient of about 50. This is of the order expected for normal intra-molecular perturbations (106), since genuine charge transfer complexes produce extinction coefficients of the order of 10,000 (107). It is evident from these results that charge transfer can be considered insignificant in the type of complex formation as studied herein.

This lack of evidence for migration of charge from the vicinity of the aromatic ring is very important because such migration would drastically alter the screening effect arising from the π-electrons in the vicinity of the ring. The observed shielding change of the solute on complex formation, which can be readily calculated on the basis of undisturbed π-electrons circulation, could not then be confidently related to the observed shielding effect. Any minor re-distribution of electric charge occurring wholly within the aromatic molecule can be readily interpreted as a movement of the π-system as a whole. That some re-distribution of charge does occur is evident from the apparent increase in the dipole moment of the solutes when measured in aromatic solvents e.g. μ_e of nitroform in cyclohexane is 2.52 Debye (104) whilst in benzene it is 2.61 Debye (108). This increase is attributed to a dipole moment induced in the aromatic molecule when complexed and must arise from electronic re-distribution within the aromatic molecule. This is most likely to occur in the π-system because of the geometry of the complex. The concept of a dipole induced dipole bond of purely electrostatic origins is therefore tentatively adopted.

To provide a basis for subsequent discussion it is proposed that on complex formation the solute approaches the aromatic ring along its six-fold axis and that the permanent electric dipole moment of the former molecule induces an electric moment in the polarisable aromatic molecule to form the basis for electrostatic bonding between the molecules. A further assumption is that the solute dipolar axis and aromatic six-fold axis are coincident (see fig. 3 - 1).

In greater detail, it is envisaged that the electric field of the dipolar molecular has a large gradient in the vicinity of the hydrogen atom (109) and that this field polarises the π-electron system of the aromatic ring. The fact that association occurs with aromatic systems and not to any obvious extent with inert solutions can be attributed to the presence of vacant low-lying anti-bonding p- π^* orbitals of the aromatic nucleus which will hybridise readily with the occupied bonding orbitals of the aromatic in the presence of the electric field of the solute. No hybrid orbitals extending over both participating molecules are anticipated because none are available on the H atom or C-H bond of the solute with energies low enough for interaction to occur. Thus charge transfer of the type occurring in metal-ligand complexes can reasonably be regarded as absent in the type of complex studied here. Charge transfer complexes involving aromatic rings do occur (110,111) but generally only with other

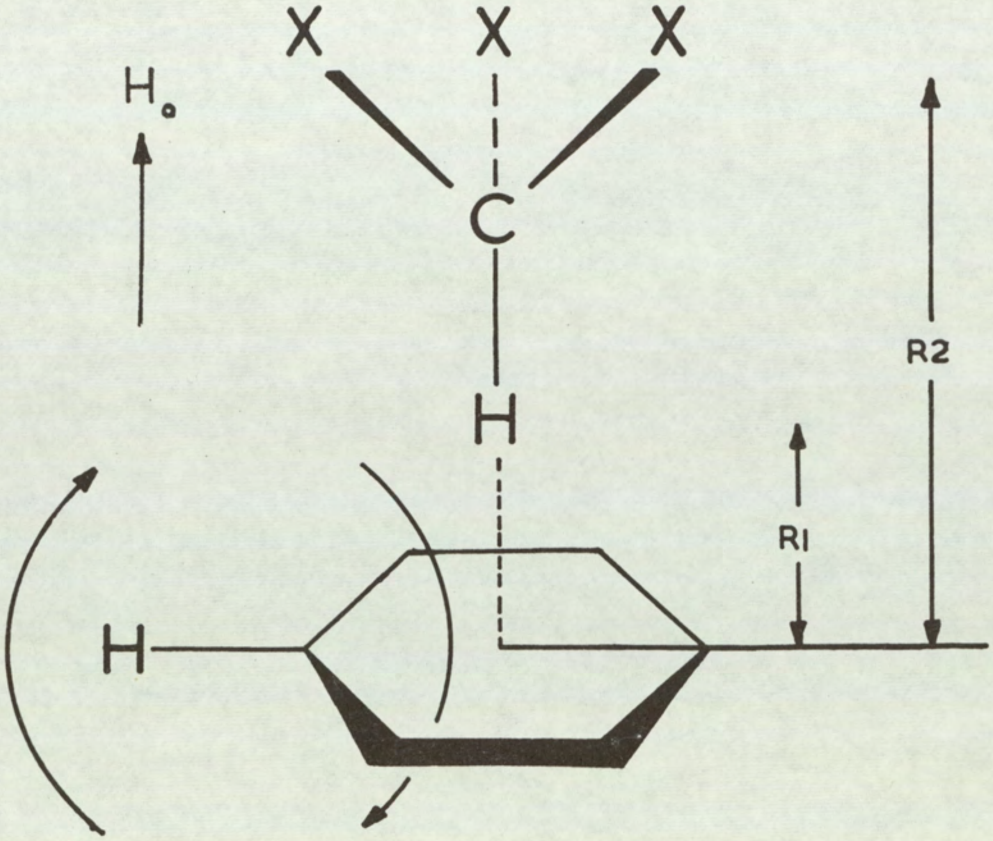

FIG 3-1 THE POSTULATED ARRANGEMENT OF THE COMPLEX, THE DEFINITIONS OF THE DISTANCES R1 AND R2, AND THE DIRECTION OF THE INDUCED MAGNETIC FIELD IN THE VICINITY OF THE AROMATIC RING.

π- delocalised systems.

A further factor which must be considered, is whether substituents around the aromatic ring are likely to modify the basic π-electron density. For this reason investigations herein are restricted to the methyl homologues of benzene in order to minimise any such disturbances. Previous investigations (112,113,114) of the shielding effects of substituents have been largely confined to groupings where large interaction with the π-system can be anticipated e.g. to the groups $-NO_2$, $-CHO$, $-OCH_3$, $-NH_2$. Spiesecke and Schneider (115) have investigated such systems and interpreted the shifts of the o-, m-, and p- hydrogens in terms of inductance and resonance effects, the latter of which implies interaction with the π-system. It was, however, also necessary to invoke bond anisotropy considerations to obtain full agreement. In the case of methyl substituents it is anticipated that this effect is the predominant one and this is supported by the small value of the shift (about 0.15 p.p.m. in the case of one methyl group) and by its similarity in magnitude to the effect produced by methyl substitution on the resonance position of the ring hydrogens of cyclohexane ($\triangleq$0.1 p.p.m.). Therefore it is assumed that the presence of methyl groups does not appreciably influence the magnitude or disposition of the π-system.

3:3 Theoretical Approaches to Shielding Around the Aromatic Ring

It is evident that in attempting to determine the precise magnitude of the induced magnetic field in the vicinity of the aromatic ring arising from the π-electron motion, it is essential to develop a model which is demonstrably accurate and at the same time convenient to use. A rigorous treatment involving consideration of the shape of the π-orbitals would necessarily be extremely complicated and a number of simpler models have been conceived and had varying degrees of success in use.

Pople (33), following Pauling (87), considered the π-electrons to move in the carbon plane and to produce a ring current, magnitude I, given by

$$I = \frac{ne^2 H_o \text{ Cos } \theta}{4 \pi mc} \qquad 3 : 1$$

where n is the number of circulating π-electrons, m is the mass of the electrons, c is the velocity of light, and Cos θ is a term allowing for the time averaged orientation of the ring with respect to the H_o (z) direction. The current can be considered to produce a point magnetic dipole ($\bar{m}$) acting at the ring centre, which has magnitude

$$\bar{m} = \frac{ne^2 a^2 H_o \text{ Cos } \theta}{4mc^2} \qquad 3 : 2$$

where a is the aromatic ring radius. This causes a magnetic field at the aromatic proton, distance R from the centre of the ring of (expressed as a screening)

$$\sigma_{HOR} = \frac{-ne^2 a^2 \text{ Cos}^2 \theta}{4mc^2 R^3} \qquad 3 : 3$$

Using $n = 6$, $a = 1.395$ Å, $\text{Cos}^2 \theta = 1/3$, and $R = 2.465$ Å. σ_{HOR} is calculated to be -1.83 p.p.m. which may be compared with the experimental value of -1.48 p.p.m. (101). (For details of the other data used see Table 3 - 1). This latter value is the observed chemical shift difference, in an inert solvent, between the proton resonance of benzene and the olefinic proton resonance of 1,3-cyclohexadiene, which is not a molecule possessing a delocalised π-system capable of allowing the free flow of electrons as occurs in the benzene molecule, but is similar to it in other respects. The difference of -1.48 p.p.m. is, therefore taken as the screening contribution arising from the motion of the π-electrons alone.

TABLE 3 - 1

The Values of Some Constants Used in Calculations

Avogadro's Number	6.023×10^{-23} molecules per Gm - molecule
Mass of the Electron	9.107×10^{-28} gms.
Charge of the Electron	4.8029×10^{-10} e.s.u.
Velocity of Light	2.998×10^{-10} cm sec.$^{-1}$
Planck's Constant	6.62×10^{-27} erg - sec.
Radius of the Benzene Ring	1.395 Å
Length of the C-H bond	1.07 Å

It was considered worthwhile to extend Pople's treatment to a two point dipole model, which is a closer representation of the accepted aromatic structure, characterised by two regions of high π-electron density above and below the carbon plane. By resolving the magnetic contributions, by the two dipoles, at the ring protons in directions parallel and perpendicular to the H_o field it can be shown that

$$\sigma_{HOR} = \frac{ne^2 a^2 \operatorname{Cos}^2 \theta}{4m\, c^2(R^2+d^2)^{3/2}} \left[\frac{3d^2}{R^2+d^2} - 1 \right] \qquad 3 : 4$$

where 2d is the separation of the two point dipoles which are equidistant from the plane of the ring and situated on its six-fold axis. Equation 3 : 4 can be seen to reduce to equation 3 : 3 when $d = 0$. For a value of $d = 0.64$Å (which arises from subsequent considerations) equation 3 : 4 gives a value for $\sigma_{HOR} = -1.35$ p.p.m. which is much nearer to the experimental value than that predicted by the single dipole model.

Shortly after Pople's work, Waugh and Fessenden (120) produced a more rigorous approach and deduced an expression, using elliptic integrals, for determining the magnetic field at the ring protons by considering the current to circulate in a loop of radius equal to that of the aromatic ring. Their first attempt still considered the π-electron circulation to take place in the plane of the ring and in this way they obtained the poor result of -2.7 p.p.m. for σ_{HOR}. However, by considering three π-electrons to be circulating in each of two loops in a manner analogous to that for the two point dipole model described above, they obtained good agreement when a loop separation of 1.2Å was used. More recently, Johnson and Bovey (101), in similar calculations, have shown that by taking the separation of the two conducting loops representing the regions of maximum π-electron density as 0.918 ring radii i.e. (1.28Å), the calculated shifts for a wide range of aromatics (including poly-nuclear compounds) are in excellent agreement with the observed values. This clearly indicates that a two loop model of electron circulations can be considered reliable when estimating π-electron shielding effects in the plane of the ring. It is reasonable, therefore, to extend the use of this model for the calculation of shielding in the direction of the six-fold symmetry axis of the ring. By use of simple electromagnetic theory, equation 3 : 5 can be derived to give the shielding effect of the two loops along the six-fold axis, and at a distance R1 from the plane of the aromatic ring.

$$\sigma_{vert} = \frac{ne^2 a^2 \cos^2 \theta}{4 mc^2} \cdot \left[\frac{1}{\left[(R1-d)^2 + a^2\right]^{3/2}} + \frac{1}{\left[(R1+d)^2 + a^2\right]^{3/2}} \right] \qquad 3 : 5$$

Whilst tables have been published (102), based on Johnson and Bovey's work, giving shielding values at various positions around the aromatic ring, the use of the above formula allows of more precise determinations between observed shifts and complex structure and also enables an assessment of the effects on the shielding, along the six-fold axis, of varying the value of d.

The value σ_{vert} can be determined experimentally as the difference between the solute proton shift in the complex (δ_{comp}) and unassociated (δ_{free}) situations. Because measurements in the gas phase were not practicable, solution shifts had to be used and suitable corrections for medium screening effects made. δ_{free} can be taken reliably (subject to medium screening effects) as the observed shift in a non-bonding solvent such as cyclohexane. However, the observed shift of nitroform in the presence of aromatic solvent is not usually δ_{comp} because of incomplete association. The next section sets out a method which takes these facts into consideration.

3:4 The N.M.R. Method for Investigating Complex Formation

In 1962 Creswell and Allred (56) proposed a procedure for determining equilibrium constants and total shift due to complex formation, for systems similar to those considered here, in which the interactions were examined in solution in cyclohexane.

They described the association

$$CX_3H + B \rightleftharpoons CX_3H \ldots\ldots B \qquad 3:6$$

between a dipolar molecule CX_3H (or generally, A,) and an aromatic molecule, B, by an equilibrium constant, K, expressed in terms of mole fractions (m.f):

$$K = \frac{[CX_3H \ldots\ldots\ldots B]}{[CX_3H][B]} \qquad 3:7$$

$$= [C]_j \frac{\{[S]_j + [A]_j + [B]_j - [C]_j\}}{\{[A]_j - [C]_j\}\ \{[B]_j - [C]_j\}} \qquad 3 : 8$$

where for a sample j, $[A]_j$, $[B]_j$, and $[S]_j$ are the initial numbers of moles of solute, aromatic and solvent respectively and $[C]_j$ is the number of moles of the complex present at equilibrium. This assumes that only 1:1 molecular complexes are formed and this can be substantiated for chloroform by reference to the work of Reeves and Schneider (81) among others (121,122).

Although the solute proton will experience the effect of two distinct environments in the liquid system these are for the reasons given in section 1:12 of Chapter 1 essentially time averaged and only one line attributable to it is observed. The resulting chemical shift observed is, therefore, the weighted average of the shieldings experienced between the two extreme values and is conveniently expressed in terms of these values by an equation whose form was first given by Gutowsky and Saika (123). The relevant form of this expression is:-

$$\delta_{\text{obs } j} = \frac{[C]_j}{[A]_j} \cdot \delta_{\text{comp}} + \frac{[A]_j - [C]_j}{[A]_j} \delta_{\text{free}} \qquad 3 : 9$$

which can be modified to

$$\delta_{\text{obs } j} = \frac{[C]_j}{[A]_j} \left\{ \delta_{\text{comp}} - \delta_{\text{free}} \right\} + \delta_{\text{free}} \qquad 3 : 10$$

From these equations it is clear that for a series of samples with a range of concentrations of reactants, a plot of $\delta_{\text{obs } j}$ versus $[C]_j / [A]_j$ will be linear and of gradient ($\delta_{\text{comp}} - \delta_{\text{free}}$), tentatively identified with σ_{vert}. $[C]_j$ cannot be determined explicitly and trial values of K must be chosen to evalue $[C]_j / [A]_j$ for each sample. Calculated values of $[C]_j / [A]_j$ which lie between 0 and 1 can then be plotted with the corresponding values of $\delta_{\text{obs } j}$

and only when the correct value of K is chosen will the plot be linear and represent equation 3 : 10. σ_{vert} can then be obtained and after various corrections inserted into equation 3 : 5 to obtain R1. The accuracy of the stability constant obtained by the above means may be subject to error because of the unproven assumption that the activity coefficients of the various species in solution are unity or cancel each other out. This assumption will be held for all of the work subsequently reported herein.

Examination of the interaction in a non-bonding solvent such as cyclohexane has several important advantages. Firstly, studies can be carried out on solid dipolar and solid aromatic materials. Secondly, it allows the concentration of the polar solute to be maintained at a low and constant value so that the effects of possible self association of the solute can be minimised. Thirdly, cyclohexane is particularly suited to the investigations because it possesses a single relatively sharp resonance well clear of the peaks of interest, which can be used conveniently for internal reference measurements and which remains narrow down to the freezing point. The solute resonance lines also are found not to suffer from viscous broadening at low temperatures.

In order to be able to rely on the shifts measured relative to cyclohexane it is of course necessary that this molecule does not take part in any chemical interactions that can appreciably modify its shift. To verify this, the spectra were obtained for two four-component systems containing low concentrations of tetramethylsilane (which is most unlikely to be involved in specific interactions with other components of the medium) and chloroform with different benzene/cyclohexane contents. From these it was evident that only $\delta_{\text{T.M.S.} - \text{CHCL}_3}$ varied between samples and, more importantly

$\delta_{T.M.S. - C_6H_{12}}$ remained constant.

3:5 Factors Which Influenced the Choice of Sample Composition

In making up the samples it is necessary to avoid conditions where interactions, other than that under investigation, as well as other possible complicating factors are likely to be present.

The sensitivity of the R10 spectrometer precluded the use of a mole fraction of the solute less than 1% and it was therefore, necessary to ascertain whether such dipolar molecules are appreciably self associated at this concentration. To study this Jumper, Emerson and Howard (124) measured the shift change of the chloroform resonance in increasing quantities of cyclohexane and attributed it to the formation of a chloroform dimer. They reported an equilibrium constant of 0.16 $m.f.^{-1}$ They were in some doubt as to whether the observed shift was due to the reaction field effect between the chloroform and the medium affecting its resonance position but calculations* have now shown that the shift change due to this would be an order of magnitude smaller, so the association affect may be genuine. The self association constant is, however, still an order of magnitude lower than the values found in these studies and is therefore unlikely to be significant when the chloroform (or the bromoform or iodoform) is only present to 1% mole fraction.

The solutes fluoroform and nitroform could conceivably be exceptional because of their larger dipole moments and consequential greater tendency to self associate. The N.M.R. shifts of nitroform were examined for any indications of self association, in various dilutions in cyclohexane with mole fractions between 0.05 and 0.005. No change in chemical shift outside experimental error was detected

* See Table 3-9.

and therefore self association was considered to be negligible at this concentration level. Fluoroform is normally a gas liquifying at -82°C and appreciable self association is unlikely.

The behaviour of benzene itself has been studied by Bothner-By and Glick (114) who observed that when it was progressively diluted in carbon tetrachloride the single absorption line moved progressively to lower field (measured against an external water reference). They suggested that this was due to the breakdown of weak intermolecular forces between the aromatic rings. If this is indeed that case, the interaction must be very weak because the observed shift, as the mole fraction of benzene decreases, deviates only slightly from the strict linearity characteristic of non-interaction.

Probably more important than these considerations of self association of the solution components is the question of 'ideality' of the mixtures studied. Because of the interactions being studied, the mixtures cannot be regarded as perfect. However, because little or no information is available concerning the Raoult activity coefficients of components in three components mixtures in general, and certainly not for the system studied here, it must be assumed that in equation 3 : 7 the various activity coefficients are mutually exclusive.

As a result of these foregoing considerations the samples for investigation were prepared using a constant mole fraction (0.01) of the solute with varying ratios of the aromatic and cyclohexane mole fractions.

3:6 Experimental

Preparation and Purification of Materials

Nitroform, the principal dipolar substance used, was prepared by a method reported by Young, Holt and Walker (104). It was stored in solution in petroleum spirit in a refrigerator and portions were removed as required and the nitroform precipitated by further cooling in an acetone carbon dioxide mixture.

Chloroform and iodoform were purified by the methods recommended by Vogel (125) and examined by G.L.C. and U.V. respectively.

A commercial sample of bromoform when examined by G.L.C. and N.M.R. was found to have no detectable impurities.

Fluoroform, stated to be 98% pure was taken directly from a commercial lecture bottle.

Cyclohexane, which was obtained commercially in a high state of purity was distilled from sodium and stored over the same metal. The G.L.C. trace indicated that no detectable impurities were then present in it.

All the aromatic compounds studied were "AnalaR" quality where obtainable and G.L.C. traces indicated the absence of any detectable impurities. Although only single G.L.C. peaks were observed for each of the three xylene samples it was recognised that there might be small amounts of the other xylenes present in samples of the individual isomers. This was not considered likely to be a serious source of error because it was anticipated that the three xylenes would have very similar complexing characteristics with the solutes and this was borne out by the results. Furthermore, the N.M.R. spectra of the separate materials did not reveal any detectable impurities to be present.

Sample Preparation

No estimates of the equilibrium constants to be encountered with nitroform were available so an arbitary system of sample preparation was used at first which was designed to allow variation of the ratio of aromatic and cyclohexane while keeping the solute constant at about 1% mole fraction.

The expression for the mole fraction of solute in each sample is:-

$$\frac{[A]_j}{[A]_j + [B]_j + [S]_j} = 0.01 \qquad 3 : 11$$

If

$$x = \frac{[S]_j}{[B]_j + [S]_j} \qquad 3 : 12$$

a series of samples can be made up by varying x from 0 to 1 and the molar quantities required can be derived from the proportionality

$$\left\{ [A]_j = \frac{0.01}{0.99x} \right\} : \left\{ [B]_j = \frac{1-x}{x} \right\} : \left\{ [S]_j = 1 \right\} \qquad 3 : 13$$

The quantities were multiplied by a common factor to give a final total volume of about 5 c.c. from which a sample was removed for N.M.R. investigation.

Nitrofrom Samples

Nitroform is slightly hygroscopic and ideally should be handled in a dry-box. Unfortunately, one of suitable dimensions was not available and sample preparation had to be carried out in the open air, although the nitroform for immediate use was kept at hand in a dessicator. Because of this, the procedure adopted was that now detailed.

A small conical flask was weighed and to this was added quickly, using a glass spatula, an appropriate amount of nitroform (about 0.08 gms). This was quickly weighed and the flask fitted immediately with a "Suba" seal and reweighed. Cyclohexane was then added by injection through the seal using a fine syringe until the correct quantity was delivered. The aromatic (if liquid) was added last in a similar manner. After careful agitation to ensure that the nitroform was completely dissolved and uniformly distributed throughout the liquid, the seal was removed and a portion of the liquid was transferred to an N.M.R. tube sufficient to fill it to a depth of about 60 mm. After prompt sealing the tube was stored in the freezer of a refrigerator. If the aromatic used was a solid, this was weighed in first and followed by the nitroform and cyclohexane as described above.

Two series of nitroform samples were, in fact, prepared during the course of the studies. The first series was used at 33.4°C and afterwards stored in the refrigerator to await the arrival of the variable temperature equipment. After some time these samples were checked and it was found that the nitroform peak had diminished in intensity and in some cases had completely disappeared. These samples were discarded and a new series were made up immediately prior to the variable temperature studies and were stored, when not in use, in solid carbon dioxide or liquid nitrogen.

Chloroform and Bromoform Samples

The procedure adopted for making up the samples was broadly similar to that used for the nitroform samples. Because of the relative volatility of the two haloforms they were added last to the mixture. In order to obtain shifts covering a wide range, samples containing large fractions of benzene had to be used.

Iodoform Samples

Iodoform is not soluble to the extent of 1% molar in cyclohexane and samples could only be made up in a narrow range where benzene was present in large proportions. Considerable trouble was experienced with discolouration of freshly made samples after sealing but this was obviated by preparing the samples in subdued light and taking care to keep the inside walls of the upper parts of the tubes uncontaminated.

Fluoroform Samples

Various attempts to secure a suitable mole fraction of fluoroform dissolved in cyclohexane, benzene and p-xylene were made by bubbling the gas through these solvents, and also by mixing in the gas phase and subsequent cooling, but none proved successful to the extent required.

It was therefore decided that, in order to prepare samples on a reliable quantitative basis, fluoroform would have to be dissolved under pressure in the required mixtures. To carry this out, weighed quantities of benzene (or p-xylene) and cyclohexane were placed directly into an N.M.R. sample tube. After attaching the tube to a vacuum line via an adaptor, it was immersed in liquid nitrogen and when the contents were solid, was immediately evacuated (to avoid accumulation of liquid oxygen). After isolation from the remainder of the vacuum line, fluoroform was introduced in sufficient quantity to provide a 0.01 molefraction solution (about 3 c.c. at atmospheric pressure). The fluoroform condensed on top of the solid mixture and with the bottom of the N.M.R. tube still immersed in liquid nitrogen, the top was sealed by an air-coal gas flame. The sealed tube was removed to a safe place and allowed to warm up. By this method it was found that several per-cent of fluoroform could be dissolved in cyclohexane, benzene or p-xylene.

Although an approximate idea of the amount of fluoroform in the sample tube could be obtained from a knowledge of the volume at normal pressure introduced to the sample tube, spectral integration was used to give a more accurate estimate of the amount of fluoroform actually in solution. The integrations were carried out on the high field peak of the intense central pair of the fluoroform quartet. This was well clear of any other resonances in the spectrum. The aromatic peak of the spectrum was chosen as integral reference for the fluoroform as it was almost invariably nearer in intensity, than the cyclohexane, to the fluoroform peak. The measurement of the reference peak was carried out on a lower instrument sensitivity than the fluoroform peak but comparison of integrals of the same peak at different sensitivities showed that deflections were proportional to the sensitivity ratio to within a few per-cent. To counteract any inaccuracies from integrator instability several integrals were taken for the fluoroform. Allowing for the fact that the benzene peak represented six protons (four in the case of p-xylene) and the fluoroform peak 0.375 of a proton, the numbers of moles of fluoroform present in each sample were estimated. The results are set out in Table 3-2.

Results and Data Processing

All N.M.R. shift measurements were carried out using the frequency modulation side-band technique described in Chapter 2. The solute shifts measured at 33.4°C are presented in Table 3-3 and 3-4, together with the corresponding numbers of moles of the different sample constituents and the final computed values of ($[C]_j$ / $[A]_j$), the fraction of the initially free solute complexed for each sample. The aromatic shifts for each sample were also measured to estimate changes in π-cloud distribution, mentioned in section 3;3 to allow of corrections which are dealt with later. These shifts are also included in the Tables referred to above. Because of the small changes between these shifts the

TABLE 3-2. The Data Used in the Estimation of Fluoroform Concentrations in the Aromatic/Cyclohexane Solutions

Sample	Integral Deflections (mm) (C_6H_6)	Sensitivity	≡ On Sens. 8	Integral Deflections (mm) (CHF_3)[c]	Nbr. Moles CHF_3 x 10	Moles % CHF_3 in Samples
0/ØH/F	103.2[a]	0.125	66,048	7.7	0.0375	3.75
A	99.4	2	398	4.3	0.4842	0.50
B	142.0	1	1,136	7.5	0.5657	0.56
C	146.7	0.5	2,347	22.3	2.376	2.3
D	98.3	0.25	3,144	13.5	1.628	1.6
E	85.5	0.25	2,736	17.5	3.215	2.8
F	127.7	0.25	4,085	19.4	4.658	4.0
G	139.3	0.25	4,458	19.0	2.693	2.8
H	160.1	0.25	5,122	29.0	4.871	5.4
J	165.6	0.25	5,300	38.2	9.036	7.9

TABLE 3-2 (contd)

A/PXy/F						6.6^b
B						1.2^b
C	147.8	1	1,183	22.4	2.063	2.1
D	121.1	0.5	1,938	25.6	1.872	2.6
E	144.4	0.5	2,310	22.2	1.666	2.4
F	162.8	0.5	2,605	20.0	1.477	2.1
G	149.5	0.5	2,392	36.8	3.888	4.2
H	112.7	0.25	1,803	21.2	3.179	2.9

a. Measured Relative to Cyclohexane. b. Due to breakage before integral measurements could be made these values have had to be estimated by comparison of peak height with samples of similar concentrations of fluoroform. c. Average of 12 Deflections on Sensitivity 8.

TABLE 3-3. Sample Composition and Observed Shifts Measured at 33.4°C for the Nitroform - Aromatic - Cyclohexane Systems

Samples Benzene	Moles ($x10^4$) Nitroform	Moles ($x10^4$) Aromatic	Moles ($x10^4$) Cyclohexane	C/A ($x10^2$)	Chemical Shifts (Hz w.r.t. C_6H_{12})	
					Nitroform	Aromatic
O	3.79_4	0.0	374.6	0.0	-339.65	-
K	1.57_6	1.01_1	100.0	6.94_9	-331.16	-346.93
H	1.58_2	3.11_1	100.0	18.63	-318.00	-347.25
J	1.64_9	6.37_6	99.96	31.62	-303.87	-346.99
B	1.68_8	11.14	99.96	44.06	-290.31	-346.43
C	2.01_9	33.36	99.99	66.97	-265.36	-345.58
D	3.07_2	100.0	100.0	80.49	-249.13	-345.01
E	6.10_4	299.9	100.0	86.19	-242.72	-344.62
F	1.54_9	89.95	9.98_1	88.25	-240.92	-344.96
G	3.05_2	189.9	9.96_9	88.81	-240.73	-345.10

TABLE 3-3 (contd)

Toluene

O	3.79_4	0.0	374.6	0.0	-339.65	-
J	2.72_1	3.27_8	265.8	13.59	-322.80	-337.91
A	1.37_7	5.93_6	125.1	37.63	-297.70	-337.72
B	1.49_6	18.49	131.1	63.19	-267.57	-337.07
C	1.78_1	44.04	130.1	78.21	-250.95	-336.80
D	2.56_2	125.3	125.9	87.78	-240.06	-336.83
E	5.18_4	375.5	125.4	91.57	-235.95	-337.16
F	3.15_8	281.3	31.25	92.89	-234.33	-337.52
G	2.54_9	240.0	13.00	93.24	-234.09	-

TABLE 3-3 (contd)

O-Xylene

O	3.79_4	0.0	374.6	0.0	-339.65	-
H	1.33_7	5.33_1	127.6	48.28	-281.45	-332.48
A	1.36_4	7.85_6	125.5	58.38	-271.96	-332.31
B	1.43_7	14.79	127.5	71.96	-256.51	-332.22
C	1.70_8	41.52	126.5	86.37	-238.73	-332.34
D	2.60_8	127.9	129.0	92.85	-230.74	-331.58
E	5.17_1	383.2	127.6	95.17	-227.43	-330.94
F	1.27_1	112.1	128.7	95.94	-227.19	
G	2.58_9	243.6	147.0	96.13	-227.08	

TABLE 3-3 (contd)

M-Xylene

O	3.79_4	0.0	374.6	0.0	-339.65	-
J	2.82_7	8.78_8	266.2	41.88	-292.40	-
A	1.30_4	7.80_8	125.2	58.05	-273.54	-
HA	1.44_3	13.20	128.3	69.26	-262.12	-
HB	1.48_3	14.11	134.6	69.68	-259.96	-
C	1.66_8	37.47	123.5	85.42	-241.34	-
D	2.55_6	12.68	126.9	92.78	-234.10	-
E	5.17_7	390.0	129.3	95.10	-231.35	-
F	2.57_5	228.7	25.12	95.89	-230.58	-
G	4.29_7	404.5	21.11	96.10	-231.20	-

TABLE 3-3 (contd)

P-Xylene

O	3.79_4	0.0	374.6	0.0	-339.65	-
AA	5.09_1	4.84_1	502.2	16.17	-320.77	-330.25
AB	5.03_8	9.95_6	493.3	29.14	-302.02	-330.02
AC	5.15_8	15.07	497.3	38.40	-292.16	-329.87
AD	5.19_1	26.16	514.4	51.50	-280.55	-329.62
J	1.35_1	11.24	128.1	64.55	-262.81	-329.23
B	1.43_0	13.89	125.2	69.42	-256.81	-329.07
C	1.69_5	41.89	125.8	85.53	-237.43	-328.42
D	2.61_5	130.4	129.1	92.37	-228.95	-328.11
E	5.17_1	385.5	127.6	94.79	-225.60	-328.50
F	2.26_8	232.5	259.6	95.62	-224.88	-328.86

TABLE 3-3 (contd)

Mesitylene

O	3.79_4	0.0	374.6	0.0	-339.65	-
H	1.57_6	3.09_5	99.98	46.32	-284.32	-
J	1.60_9	6.44_8	100.1	65.63	-260.53	-
B	2.07_2	13.39	125.0	76.98	-248.00	-
C	2.55_6	42.02	125.0	99.00	-231.88	-
D	1.90_7	62.55	62.5_4	94.85	-225.37	-
E	2.02_6	94.03	31.2_6	96.53	-224.24	-
F	1.51_0	90.03	10.02	97.11	-223.76	-
G	1.62_9	95.03	5.07_4	97.25	-222.85	-

TABLE 3-3 (contd)

Durene

O	3.79_4	0.0	374.6	0.0	-339.65	-
A	5.41_6	1.45_3	527.7	11.35	-324.26	-
B	5.23_0	2.60_0	516.0	19.68	-314.28	-
C	4.92_6	3.55_4	464.4	27.54	-305.10	-
D	5.07_8	5.04_4	501.1	34.51	-295.41	-
E	4.97_2	6.61_6	485.5	42.57	-285.38	-
F	5.12_4	7.59_9	499.6	45.68	-282.24	-
G	5.24_4	8.71_7	509.0	49.06	-276.88	-
H	5.35_6	10.21	521.4	52.97	-272.32	-
J	5.70_7	12.03	549.7	56.06	-268.04	-

TABLE 3-3 (contd)

Penta-methylbenzene

O	3.79_4	0.0	374.6	0.0	-339.65	-
A	5.29	0.52_6	502.6	6.81	-330.74	-
B	5.25_7	1.49_7	518.4	18.43	-317.69	-
C	5.29_6	2.56_3	510.8	29.86	-301.50	-
D	5.36_3	3.56_8	528.8	38.56	-292.65	-
E	6.17_0	5.09_9	60.48	45.55	-280.79	-
FA	6.36_2	6.62_4	609.8	53.71	-274.06	-
G	5.15_1	7.65_6	500.9	65.33	-260.16	-
H	5.11_8	7.90_6	500.2	66.45	-257.90	-

TABLE 3-3 (contd)

Hexamethylbenzene

O	3.79_4	0.0	374.6	0.0	-339.65	-
A	5.57_3	0.53_6	535.0	0.71	-328.86	-
B	5.34_3	1.53_4	511.6	20.26	-309.36	-
C	5.53_5	2.65_6	529.0	32.19	-293.31	-
D	4.86_0	3.51_3	487.5	44.39	-275.62	-
E	5.62_8	5.06_5	525.6	53.10	-263.88	-
F	5.35_0	6.72_3	499.5	65.00	-247.19	-
G	5.32_3	7.96_2	522.1	69.87	-240.72	-
H	5.07_8	8.60_9	500.5	73.52	-234.72	-
J	6.07_1	10.19	582.4	73.65	-234.52	-
J'	5.19_1	10.22	498.8	77.87	-227.91	-

TABLE 3-4. Sample Composition and Observed Shifts Measured at 33.4°C for the Haloform - Aromatic - Cyclohexane Systems

Chloroform

Samples	Moles ($x10^4$)	Moles ($x10^4$)	Moles ($x10^4$)	C/A ($x10^2$)	Chemical Shifts (Hz w.r.t. C_6H_{12})	
	Haloform	Aromatic	Cyclohexane		Haloform	Aromatic
Benzene						
O	5.17_7	0.0	506.1	0.0	-339.02	-
A	5.48_7	54.34	499.2	10.05	-329.36	-346.11
B	6.44_2	123.5	503.7	18.33	-321.19	-345.64
C	7.62_3	239.4	503.0	26.92	-312.95	-345.12
D	8.82_9	369.5	499.6	32.72	-307.28	-344.93
E	10.00	498.7	497.7	36.43	-303.66	-344.73
F	8.31_0	498.7	330.5	40.80	-299.35	-344.64
G	8.75_4	598.8	252.0	44.66	-295.51	-
H	7.17_1	569.6	139.9	47.95	-292.37	-
J	6.63_4	599.9	63.54	50.94	-289.69	-

TABLE 3-4 (contd)

P-Xylene

O	5.17_7	0.0	506.1	0.0	-339.02	-
K	5.15_2	14.29	505.8	5.03	-334.58	-329.16
C	6.20_7	98.02	520.8	23.48	-317.69	-328.57
D	6.32_4	129.2	500.6	28.47	-314.08	-328.40
E	6.94_4	166.0	509.8	32.28	-309.79	-328.31
F	7.62_3	215.3	517.2	36.34	-306.66	-328.85
G	8.03_3	271.9	505.5	40.49	-302.70	-328.22
H	8.41_0	335.1	502.9	43.79	-299.90	-328.27
J	9.18_9	412.3	495.2	46.97	-297.10	-328.13
L	5.16_0	298.0	194.0	54.19	-290.56	-328.23
M	5.48_7	383.8	163.5	57.84	-287.20	-328.45
A	5.59_6	26.63	507.8	–	–	-329.05
B	5.62_9	55.41	500.7	16.20	-324.34	-328.80

TABLE 3-4 (contd)

Bromoform

Benzene

O	5.14_7	0.0	513.2	0.0	-315.37	-
J	5.15_1	25.62	499.5	4.92_1	-310.73	-346.37
A	5.58_1	60.41	499.4	10.28	-305.40	-345.49
B	6.20_4	125.2	502.8	17.50	-298.51	-345.63
C	5.71_3	170.9	400.5	24.15	-291.83	-345.29
D	5.75_3	221.9	333.0	29.88	-286.27	-345.05
E	5.65_4	281.8	285.2	34.66	-281.15	-344.86
F	5.32_9	299.1	200.6	38.98	-277.33	-
G	6.11_7	422.7	178.3	42.91	-273.46	-344.72
H	6.26_3	499.9	120.5	46.29	-270.02	-

TABLE 3-4 (contd)

P-Xylene

O	5.14_8	0.0	513.2	0.0	-315.57	-
B	5.61_0	35.28	501.8	9.32_5	-307.56	-329.02
A	5.54_7	54.93	497.7	13.49	-300.78	-328.95
D	5.91_5	86.86	500.8	18.84	-295.24	-328.65
C	6.31_1	129.8	494.4	24.64	-289.30	-328.50
E	7.18_9	165.0	501.4	28.02	-286.09	-328.46
F	7.09_0	216.0	501.3	32.19	-281.97	-327.69
G	5.51_1	221.2	334.1	38.61	-275.79	-328.29
H	5.64_6	292.9	284.6	44.08	-268.13	-328.29
J	6.33_1	372.6	246.6	48.77	-263.96	-328.32

TABLE 3-4 (contd)

Iodoform

Benzene

A	2.01_4	0.0	196.6	0.0	-203.23	-
B	2.09_0	53.73	142.8	24.2	-182.20	-345.53
C	1.99_6	80.25	113.0	32.70	-174.84	-345.28
D	1.98_9	81.45	109.5	33.29	-174.13	-345.23
E	1.98_6	97.95	94.99	37.29	-171.03	-345.10
F	2.20_7	131.3	79.38	42.22	-166.10	-344.81
G	1.98_9	153.7	48.14	47.21	-156.96	-344.78

TABLE 3-4 (contd)

P-Xylene

O	2.01_4	0.0	196.6	0.0	-202.92	-
A	2.12_3	46.54	161.4	29.69	-175.80	-328.52
B	1.98_1	66.80	129.6	39.15	-168.56	-328.49
C	1.97_3	81.41	109.8	44.64	-162.46	-328.43
D	1.99_1	114.2	90.12	51.50	-156.83	-328.35
F	2.00_6	119.6	68.91	54.64	-153.77	-328.48
G	2.14_3	170.4	43.76	60.24	-148.64	-328.84

TABLE 3-4 (contd)

Fluoroform

Benzene

O	3.75	0.0	100.0	0.0	-248.42	-
A	0.48_4	2.82_5	100.9	3.70	-245.16	-346.62
B	0.56	5.36_2	94.69	7.02	-239.63	-346.11
C	2.38	15.67	85.00	17.49	-230.14	-345.89
D	1.62_8	23.75	74.16	25.14	-223.11	-345.64
E	3.21_5	31.35	80.82	27.51	-220.97	-345.35
F	4.65_8	61.30	50.93	42.41	-205.19	-344.86
G	2.69_3	39.55	53.02	36.85	-211.92	-344.96
H	4.87_1	53.83	31.62	45.52	-202.45	-344.73
J	9.02_6	78.38	26.20	49.14	-198.88	-344.67

TABLE 3-4 (contd)

P-Xylene

O	3.75	0.0	100.0	0.0	-248.42	-
A	6.34	4.74_4	90.97	9.46	-240.69	-328.77
B	1.17	8.64_7	90.53	17.74	-235.47	-328.64
C	2.06	10.19_6	86.99	20.20	-232.14	-328.64
D	1.87	13.30	55.78	31.60	-225.03	-328.55
E	1.67	16.26	53.11	36.25	-218.81	-328.33
F	1.47_7	18.00	50.37	39.16	-217.80	-328.21
G	3.88_9	23.66	65.00	38.38	-218.66	-328.27
H	3.17_9	50.75	58.59	53.11	-207.05	

measurements were carried out using the minimum field sweep available. Measurements could only be made for the aromatics benzene, toluene, ortho- and para-xylene. For the other homologues only immeasurably weak signals could be observed for the following reasons:-

(1) Naturally low aromatic hydrogen content coupled with

(2) low aromatic concentration found necessary and used for sample preparation and

(3) line broadening due to spin-spin coupling.

The numbers of moles of the sample constituents and the corresponding solute shifts formed the input data for an Algol computer program known as COMPLEXICON (126) which is described in Appendix B. This facilitated the search procedure, using an Elliott 803 computer, required by Creswell and Allred's method, and provided the stability constant for each system and a value for DELTA, the total apparent additional chemical shift experienced by the solute proton when transferring from the free to the fully complexed state. The results produced in this way are given in Table 3-5. The error spreads on σ_{vert} are 95% confidence limits.

3:7 Corrections of σ_{vert}

For a particular solute, the stability constants can be seen from Table 3-5 to increase systematically with increasing methyl substitution of the aromatic molecule. The σ_{vert} values also generally increase with increasing methyl substitution but do, however, do so somewhat irregularly. These screening values correspond to those for DELTA obtained using COMPLEXICON which represent the experimentally determined differences between the observed shift of the solute free in solution and that which would

TABLE 3-5. Equilibrium Constants and Uncorrected σ_{vert} values for Complex Formation of Benzene and some Methylbenzenes with Nitroform and the Haloforms @ 33.4°C.

Nitroform	K	Uncorrected σ_{vert} (p.p.m.)
with		
Benzene	8.459	1.855 ± 0.017
Toluene	14.63	1.880 ± 0.023
O-Xylene	26.48	1.949 ± 0.033
M-Xylene	26.09	1.897 ± 0.026
P-Xylene	24.12	1.987 ± 0.051
Mesitylene	37.88	1.997 ± 0.016
Durene	78.12	2.145 ± 0.018
P.M.B.	225.2	2.023 ± 0.048
H.M.B.	279.4	2.382 ± 0.020
Chloroform		
with		
Benzene	1.161	1.620 ± 0.003
P-Xylene	1.990	1.486 ± 0.009
Bromoform		
with		
Benzene	1.076	1.643 ± 0.005
P-Xylene	1.597	1.781 ± 0.031
Iodoform		
with		
Benzene	1.112	1.515 ± 0.009
P-Xylene	1.926	1.507 ± 0.019
Fluoroform		
with		
Benzene	1.418	1.671 ± 0.031
P-Xylene	2.478	1.320 ± 0.031

be observed if the solute were wholly complexed with the aromatic. Before these values for σ_{vert} can be substituted in equation 3 : 5 to obtain R1 and hence some knowledge of the detailed structure of the complexes, various corrections must be considered.

The contribution of the medium to the screening of a solute has been considered in Chapter 1 to be composed of four factors. Any of these contributions which affect the screening of the solute and solvent differently must be accounted for when determining the actual values for σ_{vert}. Because an internal reference has been used for the work now reported, $\Delta\sigma_B$ effects can be discounted. However, variations in the other three terms σ_W, σ_A, and σ_E must be accounted for and these will now be considered in detail.

σ_W The Van der Waals or Dispersion Screening Term

σ_W can be derived by a method proposed by Howard, Linder and Emerson (42).

$$\sigma_W = \tfrac{3}{4} h g \phi \quad \frac{\nu_1 \cdot \nu_2}{\nu_1 + \nu_2} \qquad 3 : 14$$

which was deduced by Stephen (127). ϕ is a proportionality constant characteristic of the nuclear species and has an approximate value in the case of bonded hydrogen of -1×10^{-12} cm^2 e.s.u.$^{-1}$ (43,128). h is Planck's constant and g is a polarisability term given by equation 3 : 15 (42).

$$g = \frac{2n^2 - 2}{(2n^2 + 1)} \cdot \frac{1}{a^3} \qquad 3 : 15$$

where n is the refractive index of the medium and a, the solute molecular radius. ν is the mean absorption frequency of the electrons in a molecule and is characterised by the subscripts 1 and 2 for the solvent and solute respectively. The appropriate values for ν are obtained from the relationship between ν and χ_m, the molar diamagnetic susceptibility (129)

$$\nu = -\frac{4mc^2}{h\,N_o\alpha}\chi_M \qquad 3 : 16$$

where N_o is Avogadro's number and α the static polarisability. For the systems studied, the calculations were carried out using the data of Table 3-6 to estimate the appropriate σ_W values. Values for 33.4°C were calculated where possible from data at standard temperatures but when refractive index extrapolations appeared erroneous the values for these were measured directly. Because the dispersion forces occur between both like and unlike molecules the effects of all interactions relevant to the screening of the solute and reference have to be considered. The effect of solute-solute interaction is ignored in view of the low concentration of this constituent used. The results of the calculations are shown in Table 3-7 from which it can be seen that the σ_W values obtained are of considerable magnitude, but the use of an internal reference which is similarly affected to the solute reduces the correction, for a particular solvent, to the order of 0.02 p.p.m. Furthermore, the effect on DELTA is even smaller, for it is only the difference in the screening corrections in the two different media (i.e. cyclohexane and aromatic) which can alter its value. A typical case is the benzene-nitroform-cyclohexane system for which the effects of the various σ_w terms are detailed below.

Cyclohexane in Cyclohexane	-0.120 p.p.m.
Nitroform in Cyclohexane	-0.102 p.p.m.
Nett Correction	-0.018 p.p.m.

TABLE 3-6. Data Used in the Calculations of Dispersion Forces, Electric Field Effects, Etc.

Refractive Indeces and Dielectric Constants

	25°C			33.4°C		
Substance	Density (gm c.c.$^{-1}$)	R.I. Na (D)	ε	Density (gm c.c.$^{-1}$)	R.I. Na (D)	ε
Cyclohexane	0.77389 (37)	1.42354 (37)	2.015 (38)	0.76591 (37)	1.4184	2.002
Benzene	0.87368 (37)	1.49790 (38)	2.274 (38)	0.8648 (37)	1.4920	2.257
Toluene	0.86220 (37)	1.49405 (37)	2.379 (38)	0.8544 (37)	1.4889	2.359
O-Xylene	0.87583 (37)	1.50282 (37)	2.555 (38)	0.8688 (37)	1.4983	2.532
M-Xylene	0.8600 (37)	1.49467 (37)	2.364 (38)	0.8525 (37)	1.4900	2.348
P-Xylene	0.85666 (37)	1.49319 (37)	2.2706 (41)	0.84934 (37)	1.4885	2.257
Mesitylene	0.8614 (39)	1.4967 (37)	2.271 (38)	0.8580 (39)	1.4909	2.258
Nitroform	1.5967 (38)	1.44511 (37)	—	1.1139 (38)	1.4423	—
Chloroform	1.4984 (37)	1.4433 (38)	4.718 (38)	1.4643 (37)	1.4378	4.573
Bromoform	2.8776 (37)	1.5948 (41)	—	2.8558 (37)	1.5893	—
Iodoform	4.008 (38)[1]					

[1] At 20°C.

TABLE 3-6 (contd)

Molar Diamagnetic Susceptibility χ_m (c.c. x 10^5) (102)

Species	
Nitroform	3.67
Chloroform	5.93
Bromoform	8.26
Iodoform	11.71
Fluoroform	3.00
Cyclohexane	6.81
Benzene	5.48
Toluene	6.61
O-Xylene	7.78
M-Xylene	7.66
P-Xylene	7.68
Mesitylene	9.23

Gas Phase Dipole Moments in Debye Units (103 and 117/9)

Nitroform	2.52$_2$ [2]
Chloroform	1.013
Bromoform	1.00
Iodoform	1.01 [2]
Fluoroform	1.645

Bond Lengths in Ånström Units (144)

$C_{AR} - C_{AR}$	1.395
C-H	1.07
C-Cl	1.77
C-Br	1.930
C-I	2.12
C-N	1.47
$N \Rightarrow O$	1.22

Van der Waals Radii in Ånström Units (117)

Chlorine	1.80	Bromine	1.95
Fluorine	1.35	Iodine	2.15
Oxygen	1.40	Hydrogen	1.2
Half thickness of Aromatic Ring	1.85		

2. Cyclohexane solution values only are available.

TABLE 3-7. **Calculated Screening Effects (σ_W) due to Dispersion Forces**

(Negative Values in p.p.m.)

Solvent / Solute	Cyclohexane	Benzene	Toluene	O-Xylene	M-Xylene	P-Xylene	Mesitylene
Cyclohexane	0.120	0.123	0.123	0.126	0.124	0.123	0.128
Benzene	0.134	0.137					
Toluene	0.113		0.116				
O-Xylene	0.100			0.106			
M-Xylene	0.098				0.101		
P-Xylene	0.097					0.100	
Mesitylene	0.089						0.095
Nitroform	0.101	0.106	0.106	0.108	0.106	0.106	0.109
Chloroform	0.173	0.176				0.177	
Bromoform	0.156	0.159				0.160	
Iodoform	0.140	0.142				0.143	
Fluoroform	0.094	0.102				0.101	

Cyclohexane in Benzene	-0.123 p.p.m.
Nitroform in Benzene	-0.106 p.p.m.
Nett Correction	-0.017 p.p.m.

The change in chemical shift due to dispersion interaction in changing solvent from cyclohexane to benzene is thus estimated to be 0.001 p.p.m. which is within experimental error. In calculating these dispersion effects the tacit assumption is, of course, made that the properties of the nitroform (or other solute) in the complex are virtually identical with that in the uncomplexed state. In view of the small size of the correction no appreciable errors are anticipated from this assumption. Insufficient data were available from the literature to calculate the dispersion forces for the higher methylbenzenes but it was not anticipated that they would be vastly different from their lower homologues.

σ_A Correction for Anisotropy of Solvent Magnetic Susceptibility

An anisotropy correction must be made, and this is done by assuming that the general anisotropy of the medium affects all the molecules to the same extent. Creswell and Allred (56) have shown that for quite differently shaped solutes the variation in solute-cyclohexane shift in benzene does not exceed ± 0.05 p.p.m. and is linear with benzene concentration. From studies on isobutane, which is similar in shape to the solutes considered here but of low electric dipole moment, they showed that the anisotropy shielding contribution to the protons of the solute molecules and cyclohexane should be similar in aromatic solvents. Schneider (130) has also shown that in a system where all but anisotropy effects can be neglected the observed chemical shifts variations on changing from a cyclohexane-type solvent to benzene for both rod-like and planar molecules are comparable with experimental error. Consequently, corrections for differing effects of medium anisotropic shielding of different solution constituents were considered unnecessary. The solute hydrogen atom in the complex, however, is in a unique position in that it lies effectively in the centre of the complex rather than on its perimeter as in the free state. It will, therefore, experience different anisotropic shieldings in the two situations. This can be accounted for by considering that on complex formation the free solute proton chemical shift is modified by removing the total anisotropic effect of the aromatic molecule about to be bound in complex (δ^{T}_{A}) and imposing the specific anisotropic effect of complex formation (σ_{vert}). Equation 3 : 10 must then be reformulated as

$$\delta_{obs\ j} = \frac{[C]_j}{[A]_j} \left(\sigma_{vert} - \sigma^{T}_{A} \right) + \delta_{free} \qquad 3 : 17$$

The values of σ^{T}_{A} can be conveniently estimated using equation 3 : 18 which was deduced by Abraham (131) and gives the total anisotropic effect of one aromatic molecule upon a proton in its vicinity.

$$\sigma^{T}_{A} = 10^{30} \frac{e^2 a^2}{mc^2} \cdot \frac{r - h}{(r + 2h)\ (r^2 + h^2)} \qquad 3 : 18$$

The aromatic molecule is considered to be a cylinder of radius r and height 2h with an equivalent magnetic dipole due to the anisotropy of the magnetic susceptibility acting along the cylinder axis. r and h represent contact separations for the haloform proton moving over the aromatic molecule and consequently must include the Van der Waals radius of the hydrogen atom and the appropriate dimensions of the aromatic ring. For benzene the calculated value for σ^{T}_{A} is +0.048 p.p.m. and for hexamethylbenzene is +0.024 p.p.m. The latter value is calculated by taking into account the shape and position of the methyl group substituents. The anisotropic shielding contributions for intermediate methylbenzenes were taken as the weighed average of the two values above, depending on the number of methyl groups present. The values are listed in Table 3-8.

σ_E Reaction Field Screening Correction Term

Because σ_E is effective only for polar molecules, due to their interaction with the surrounding medium, the resonance positions of cyclohexane and non polar aromatics will be unaffected by this mechanism. However, the effects on the solute proton at infinite dilution in cyclohexane or the aromatic could be finite and must, therefore, be considered. If the reaction field contributions to the shielding of the solute due to the aromatic and cyclohexane molecules (σ_E^B and σ_C^S respectively) are both finite and different, the observed shift for each sample must now be represented approximately by

$$\delta_{obs\ j} = \frac{[C]_j}{[A]_j} \left(\sigma_{vert} - \sigma_A^T \right) + \delta'_{free} + \left[\frac{[B]_j}{[A]_j + [B]_j + [S]_j - [C]_j} \right] \sigma_E^B + \left[\frac{[S]_j}{[A]_j + [B]_j + [S]_j - [C]_j} \right] \sigma_E^S \qquad 3 : 19$$

where δ'_{free} is the true shift of the free solute. Because the dipole moment induced in the aromatics in complex formation is generally small, contributions to the screening of the nitroform proton due to specific electric field effects in the complex should be small and no account has been taken of these.

An approximate expression of σ_E is given by (128)

TABLE 3-8. Calculated Magnetic Anisotropies for the Aromatics Used

(Positive values in p.p.m.)

Aromatic	
Benzene	0.048
Toluene	0.044
O-Xylene	0.040
M-Xylene	0.040
P-Xylene	0.040
Mesitylene	0.036
Durene	0.032
Pentamethylbenzene	0.028
Hexamethylbenzene	0.024

$$\sigma_E = -2 \times 10^{-12} E \cos \theta - 10^{-18} E^2. \qquad 3 : 20$$

where E is the reaction field at the solute and θ is the angle between the dipole axis of the solute and the X-H bond to the solute hydrogen considered. E has been defined for spherical solute molecules by Buckingham (128) using the Onsager approach (132) as:-

$$E = \frac{2(\varepsilon - 1)(n^2 - 1)\mu}{3(2 + n^2)\alpha} \qquad 3 : 21$$

and for non-spherical molecules by Diehl and Freeman (133) as

$$E = \frac{\mu}{abc} . 3. \zeta_a [1 + (n^2 - 1) \zeta_a] . \frac{(\varepsilon - 1)}{\varepsilon + \frac{n^2 \zeta_a}{1 - \zeta_a}} \qquad 3 : 22$$

In these equations, μ is the dipole moment of the solute in the gas phase, n is the refractive index of the liquid solute, α the solute polarisability and ε, the dielectric constant of the medium. a, b and c are the semi-axes of the solute ellipsoid and ζ_a is a shape factor for the solute and can be determined by the method of Ross and Sack (134).

Of the two equations for E, 3 : 22 is the most rigorous but it has been shown recently (135) that equation 3 : 21 can be used to predict the differences in shieldings in a particular solute due to the reaction field set up in different solvents. The values of σ_E computed from equations 3 : 21 and 3 : 20 for the various solutes studied are listed in Table 3-9. From these values it can be seen that σ_E^B and σ_E^S differ only slightly and only in the case of the nitroform and fluoroform samples is a correction necessary. It therefore follows that, because the sums of the mole fractions of B and S are always constant and approximately unity equation 3 : 19 will not differ significantly from a linear function. This

TABLE 3-9. Calculated Reaction Field Screening Effects (σ_E)

(Negative values in p.p.m.)

Solvent Solute	Cyclohexane	Benzene	Toluene	O-Xylene	M-Xylene	P-Xylene	Mesitylene
Nitroform	0.06121	0.07100	0.07452	0.08004	0.07415	0.07068	0.07068
Chloroform	0.02914	0.03375				0.03360	
Bromoform	0.02702	0.03146				0.03132	
Iodoform	0.02054	0.02409				0.02397	
Fluoroform	0.07768	0.08935				0.08897	

being so the equilibrium constant derived from the experimental data using COMPLEXICON will not be in significant error. Moveover, a plot of $\delta_{obs\ j}$ versus $[C]_j / [A]_j$ provided by COMPLEXICON is a line of slope $(\sigma_{vert} - \sigma_A^T)'$ and gives an approximate value for $(\sigma_{vert} - \sigma_A^T)$ that differs from the correct value by $(\sigma_E^B - \sigma_E^S)$. A corrected value for $(\sigma_{vert} - \sigma_A^T)$ can be obtained using

$$(\sigma_{vert} - \sigma_A^T) = (\sigma_{vert} - \sigma_A^T)' - (\sigma_E^B - \sigma_E^S) \qquad 3 : 23$$

and, since values for σ_A^T have been deduced using equation 3 : 18, a final corrected value for σ_{vert} may be obtained. However, before using this value with equation 3 : 5 to obtain R1, an appropriate value for d in the complex must be used. Because complex formation is postulated to depend on an electric dipole being induced in the aromatic molecule it is possible that the normal π-system in this is distorted on complex formation, and that the basic value for d (0.64Å) is modified. Consequently, any change in d on complex formation must be determined.

3:8 An Approximate Correction for π-Cloud Distortion

If distortion in the π-cloud distribution, when an aromatic nucleus becomes part of a dipole-induced complex, occurs it can be approximated roughly to a change in the value of d, the distance of the π-clouds above and below the aromatic ring. This change in distribution of π-electron density could be expected to change the shielding of the aromatic protons and, in fact, small shifts do occur which may arise from this effect.

The effect can be studied conveniently by comparing the shifts of the aromatic protons in the complexed and uncomplexed situations. For this, it is best to extrapolate the results to infinite dilution in cyclohexane in order to minimise medium effects. If the aromatic proton shift under these circumstances is δ^{A}_{free} and the corresponding value in the case of the complex is δ^{A}_{comp}, the observed shift (δ^{A}_{obs}) in a solute-aromatic-cyclohexane mixture is given approximately by

$$\delta^{A}_{obs} = x\delta^{A}_{comp} + (1 - x)\,\delta^{A}_{free} \qquad 3 : 24$$

where x is the fraction of the aromatic complexed and is given by

$$K = \frac{x}{(1 - x)Z} \qquad 3 : 25$$

where K is the association equilibrium constant for the system and Z is the mole fraction of free solute at equilibrium. δ^{A}_{free} was obtained by extrapolating a plot of mole fraction of aromatic against aromatic proton shift to zero mole fraction in cyclohexane. A similar extrapolation for a system differing from the previous one in that it contained a low constant mole fraction of solute, yielded a value for δ^{A}_{obs}; under these conditions, Z may be taken as the initial mole fraction of nitroform. The shift measurements were made relative to cyclohexane as internal reference.

To estimate changes in d it is strictly necessary to use the elliptic integral calculations of Johnson and Bovey (101) but because only small changes in d are anticipated the approximate equation 3 : 4 can be more conveniently applied. Using the experimental value for σ_{HOR}(-1.48 p.p.m.), with this equation, d is found to be 0.53 Å which differs from the best value of d (0.64 Å) by only 17%; therefore for small changes in d the former value can reasonably be used.

The procedure adopted involves first calculating δ^{A}_{comp} from equations 3 : 24 and 3 : 25. The differences (δ^{A}_{comp} - δ^{A}_{free}) is attributed to the change in π-cloud position on complex formation and is used to correct the experimental value for σ_{HOR} .

(i.e. -1.48 p.p.m.). With this new value for σ_{HOR}, equation 3 : 4 gives a new value for d and the difference between this and the original value for d is used to modify the value of 0.64 Å to what is finally used in the expression (equation 3 : 5) to determine R1.

The experimentally determined shifts (δ^{A}_{obs} and δ^{A}_{free}) and calculated modifications to d for some of the systems studied are given in Tables 3-10 (A) and 3-10 (B). From these values it can be seen that corrections for π-cloud distortion are necessary only in the case of the nitroform complexes where the infinite dilution shifts are noticeable outside experimental error. Generally, these contractions do not exceed about 0.1 Å and the corresponding decreases in R1 values (which are given in Table 3-11) due to this effect are smaller and of the order of 0.05 Å.

The fact that contraction of the π-systems is indicated by the considerations detailed above raises a point of interest as regards the nature of the interaction between the solute and aromatic. If the bonding of the two species involved charge transfer from the aromatic π-system to the solute, the π-electron density on the aromatic ring would diminish and the magnitude of the shielding arising from them would diminish i.e. the aromatic resonance line would move upfield. This increased shielding can be expected to be of quite noticeable magnitude and its absence is further confirmation of the validity of the dipole-induced dipole model used as a basis for these calculations.

3:9 Discussion

From the values obtained for R1 for each of the complexes studied, probably the most significant conclusion to be drawn is that each one approximates closely to the sum of the Van der Waals

TABLE 3-10 (A). Extrapolated Shifts (p.p.m.). of Aromatic Hydrogens in (a) pure cyclohexane and (b) cyclohexane containing 1% solute for some of the Systems* Studied

Solvent System / Aromatic in Complex	Benzene	Toluene	O-Xylene	P-Xylene
Cyclohexane	5.776	5.621	5.524	5.484
+ 1% Nitroform	5.786	5.634	5.546	5.508
+ 1% Chloroform	5.776			5.488
+ 1% Bromoform	5.777			5.490
+ 1% Fluoroform	5.778			5.480

TABLE 3-10 (B). π-Cloud deformation (contribution to d in Å) for the nitroform complexes

Benzene	-0.08_7
Toluene	-0.10_2
O-Xylene	-0.09_9
P-Xylene	-0.11_1

* The extrapolation of the iodoform values would have been meaningless because no samples could be made up containing small mole fractions of benzene or p-xylene.

TABLE 3-11. Corrected Values for σ_{vert} and Rl Values before and after π-cloud modification.

Complex Nitroform With	σ_{vert} (p.p.m.) corrected for medium screening effects	Rl (Å) π-Cloud correction Excluded	 Included
Benzene	1.913	2.928	2.88_7
Toluene	1.938	2.914	2.86_6
O-Xylene	2.009	2.874	2.82_2
M-Xylene	1.950	2.913	
P-Xylene	2.037	2.858	2.80_5
Mesitylene	2.042	2.856	
Durene *	2.177	2.786	
P.M.B. *	2.052	2.850	
H.M.B. *	2.407	2.687	
Chloroform With			
Benzene	1.683	3.072	
P-Xylene	1.531	3.182	
Bromoform With			
Benzene	1.696	3.064	
P-Xylene	1.834	2.975	
Iodoform With			
Benzene	1.567	3.155	
P-Xylene	1.550	3.168	
Fluoroform With			
Benzene	1.731	3.040	
P-Xylene	1.372	3.313	

* Uncorrected for reaction field and dispersion screening contributions.

radius of the hydrogen atom (1.2 Å) and the half thickness of the aromatic molecule (1.85 Å). This suggests that in each complex the solute proton does indeed lie, on average, in contact with the aromatic molecule and on its six-fold axis, as postulated earlier. Examination of Johnson and Bovey's isoshielding diagram (101) reveals that for a solute hydrogen to experience a shielding of ≏ 2 p.p.m. at a position other than on the six-fold axis would require considerably closer contact than indicated here. For the nitroform series, as the magnitude of the inter-molecular attractive forces increase there are corresponding small but steady decreases in R1. This can be related to the varying degree of π-cloud deformation which is proposed. This will result in an effective modification to the aromatic Van der Waals radius which leads to the decreased intermolecular separations (R1) observed. A fairly accurate estimate of the uncomplexed Van der Waals separation for a -C-H bond in contact with the plane surface of an aromatic ring can be obtained from a plot of the R1 values and the Gibbs Free Energies at 33.4°C of the nitroform complexes. Apparent absence of (see Fig.3-5) complicating factors such as steric factors, produces a fortuitous linear correlation which can be extrapolated to the $\Delta G = 0$ axis where R1 is found to be 3.1Å. Van der Waals or dispersion forces (156) are themselves dipole-induced dipole in origin and when two molecules are separated by the sum of their Van der Waals radii the energy of interaction (ΔH) is exactly balanced by the entropy term ($T\Delta S$) which encourages their re-separation.

There is the possibility that the aromatic ring proton shift changes observed for the nitroform complexes arise from the electric field of the nitroform. If this were the case, the observed shifts would not be expected to be greatly dependent on the strength of the complex, but rather on the juxtaposition of the solute and aromatic. However this is seen not to change greatly from complex to complex and in fact, in so far as the evidence available is an indication, the shift change is dependant on the strength of the complex. The main contribution to the electric field created by a nitroform molecule can be expected to arise from the nitro-groups which lie on the perimeter of the complex. Because the distances over which these contributions act vary little from complex to complex it is unlikely that the observed aromatic shifts can be interpreted solely in terms of the nitroform electric field effects and so the distortions of the π-cloud would in fact appear to be important.

These conclusions (136) and the general self-consistency of the results for the nitroform complex support the contention that the basic approach described in this chapter is not only applicable to benzene but also to the methyl, and possibly other, substituted benzenes.

For the haloforms proper, the variations in R1 that occur can not immediately be rationalised in the same manner as for the nitroform complexes. Because the complexes are far weaker, the irregular variation may be attributable to steric factors. It therefore seems likely that in rationalising these variations in terms of the strength of the complex it is incorrect to utilise K as an absolute indication of this. In fact, it would be more proper to consider the enthalpy or Free Energy of formation of the complex. This will be considered in Chapter 4.

A further useful conclusion may be drawn by comparing the uncorrected and final corrected values for σ_{vert} which are given in Tables 3-5 and 3-11 respectively. From this it is evident that the detailed corrections for medium screening effects to the uncorrected value of σ_{vert} are very small and lead ultimately to very small changes in the calculated Rl values. Because similar conclusions can be drawn concerning the effect of correcting for disturbances to the aromatic π-system it is evident that on the whole such corrections are unnecessary and little will be lost in future work from their exclusion when determining the structures of complexes of the type studied herein.

Also of interest are the values obtained for K for the various complexes. For a common aromatic constituent, K increases with increasing solute permanent electric dipole moment. The dependance between these two parameters is shown in Fig. 3-2 in which the function of K used is the natural logarithm because this is proportional to the Gibbs Free Energy of association and therefore, it may be argued, more indicative of the "strength" of the complex. Furthermore, with a particular solute LnK increases with methyl substitution of the aromatic. A direct proportionality between these, for nitroform as the solute, is demonstrated in Fig. 3-3. A similar feature for the haloforms proper may be found but at present there is insufficient data to confirm this. Regularly varying methyl substitution causes a corresponding variation in the polarisability of the aromatic molecule. If, therefore, as is probable, LnK is dependent both on solute electric moment and aromatic polarisability, considerable support is found for the dipole-induced dipole model proposed for complex formation. In this case the nature of the intermolecular interaction can be investigated more closely using a classical approach. The interaction energy of a dipole-induced dipole system of the type studied here is given (137) by

$$U = -\alpha E^2 \qquad 3 : 26$$

where α is the polarisability of the entity in which the dipole is induced and E is the electric field, exerted by the polar solute, which induces the dipole. Because the solute dipole axis is coincident with the aromatic six-fold axis the relevant electric field may be defined by

$$E = -\frac{2\mu}{R2^{3}} \qquad 3 : 27$$

and α stipulated to be the perpendicular polarisability of the aromatic ring. Consequently,

$$U = -\frac{\alpha 4\mu^{2}}{R2^{6}} \qquad 3 : 28$$

where R2 is the interdipole distance defined in Fig. 3-1. If the proposed model for complex formation is realistic it would be expected that lnK should in some way be dependent on $-\alpha 4\mu^{2}/R2^{6}$. Unfortunately, the values for R2 are uncertain, but from the values for R1 given earlier (Table 3-11) it is probable that for a particular solute they are more of less invariant with the various aromatics considered. It would, therefore, be expected that for a particular solute lnK should be dependent on $\alpha\mu^{2}$. The appropriate plots for these two terms are given in Fig. 3-4 : The values of various parameters used for this are given in Table 3-12. The plot for the nitroform results lie on a straight line passing through the origin. Similarly, the plot for the haloforms is very nearly linear. It is evident, therefore, that the value of R2 for a particular class of complex (with either nitroform or the haloforms) are very similar for all of the complexes, and more importantly that the dipole-induced dipole model can be substantiated from a classical viewpoint.

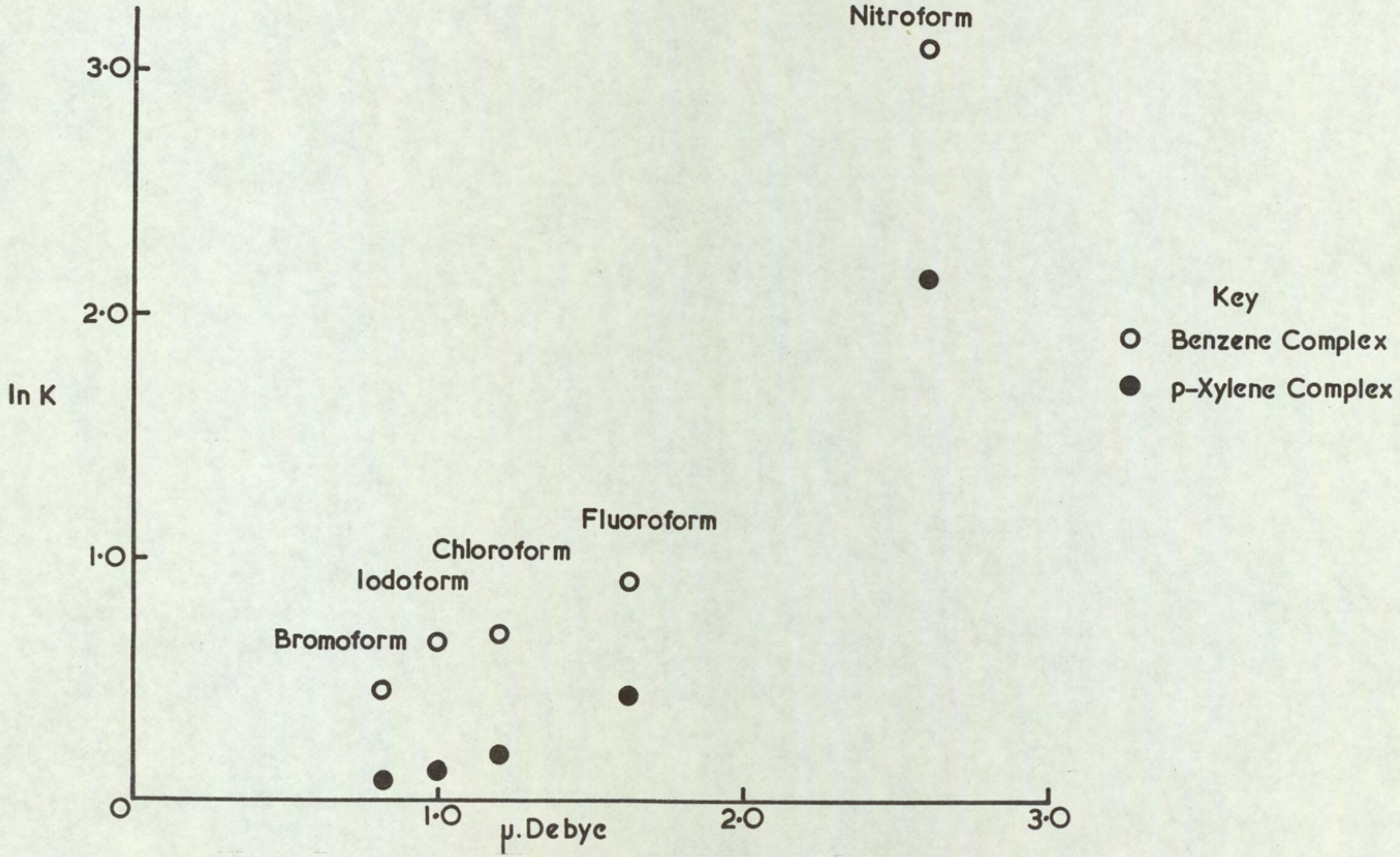

FIG 3–2 THE RELATIONSHIP BETWEEN lnK AND SOLUTE SOLUTION DIPOLE MOMENTS FOR THE BENZENE AND p-XYLENE COMPLEXES STUDIED

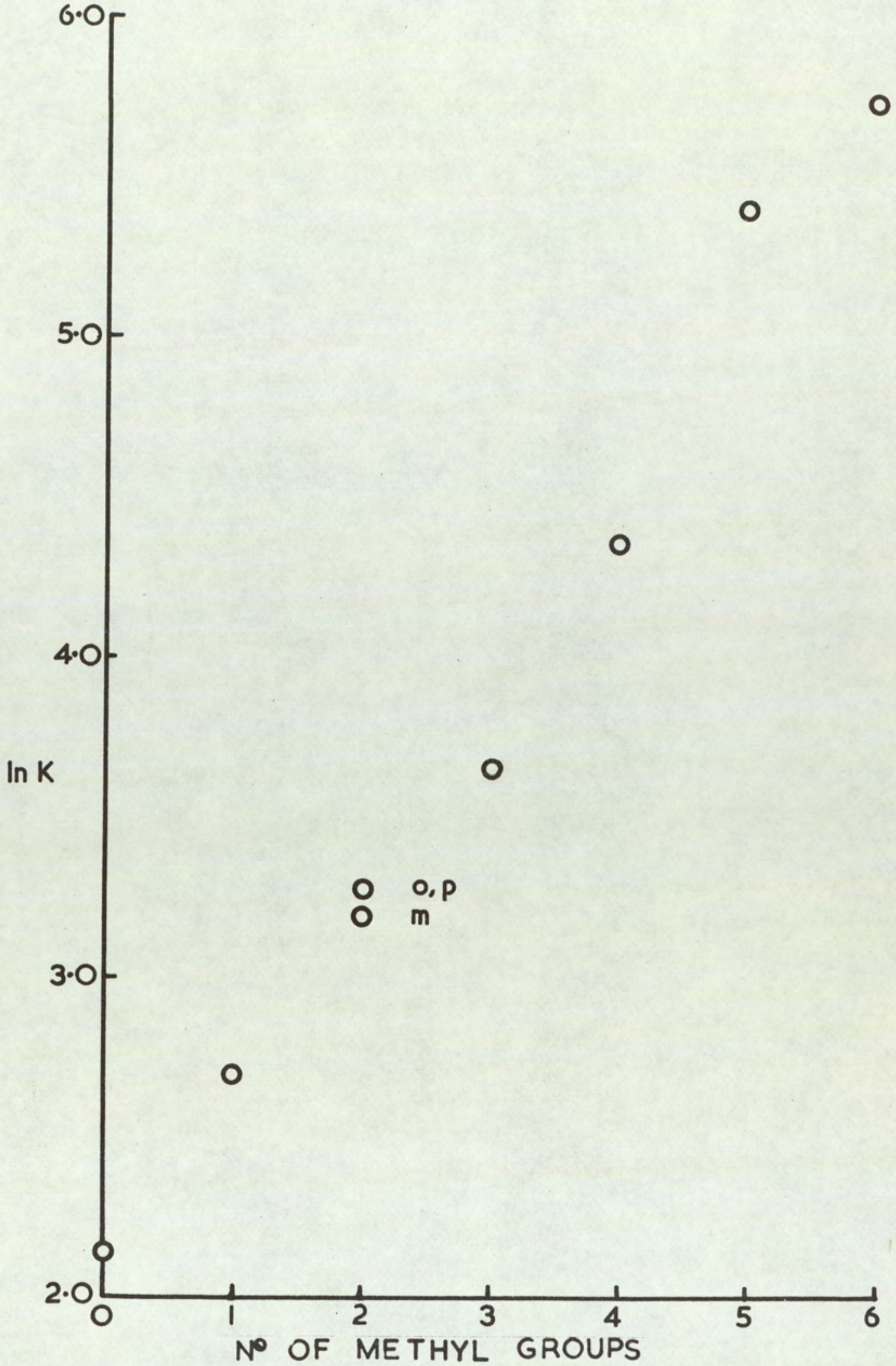

FIG 3-3 THE RELATIONSHIP BETWEEN ln K AND THE NUMBER OF METHYL GROUPS IN THE NITROFORM COMPLEXES STUDIED

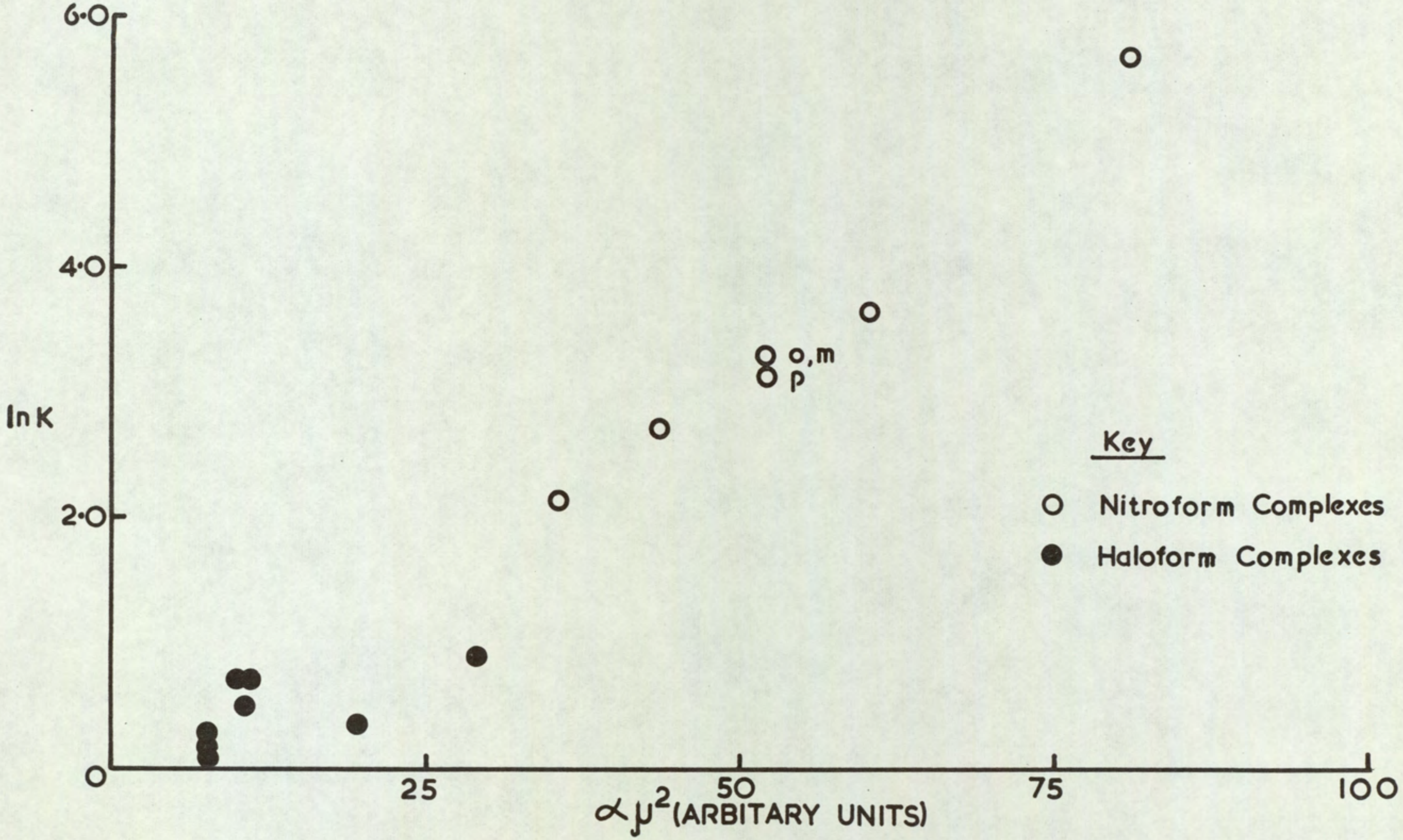

FIG 3–4 THE RELATIONSHIP BETWEEN ln K AND $\alpha\mu^2$ (THE POLARISATION TERM) FOR THE COMPLEXES STUDIED

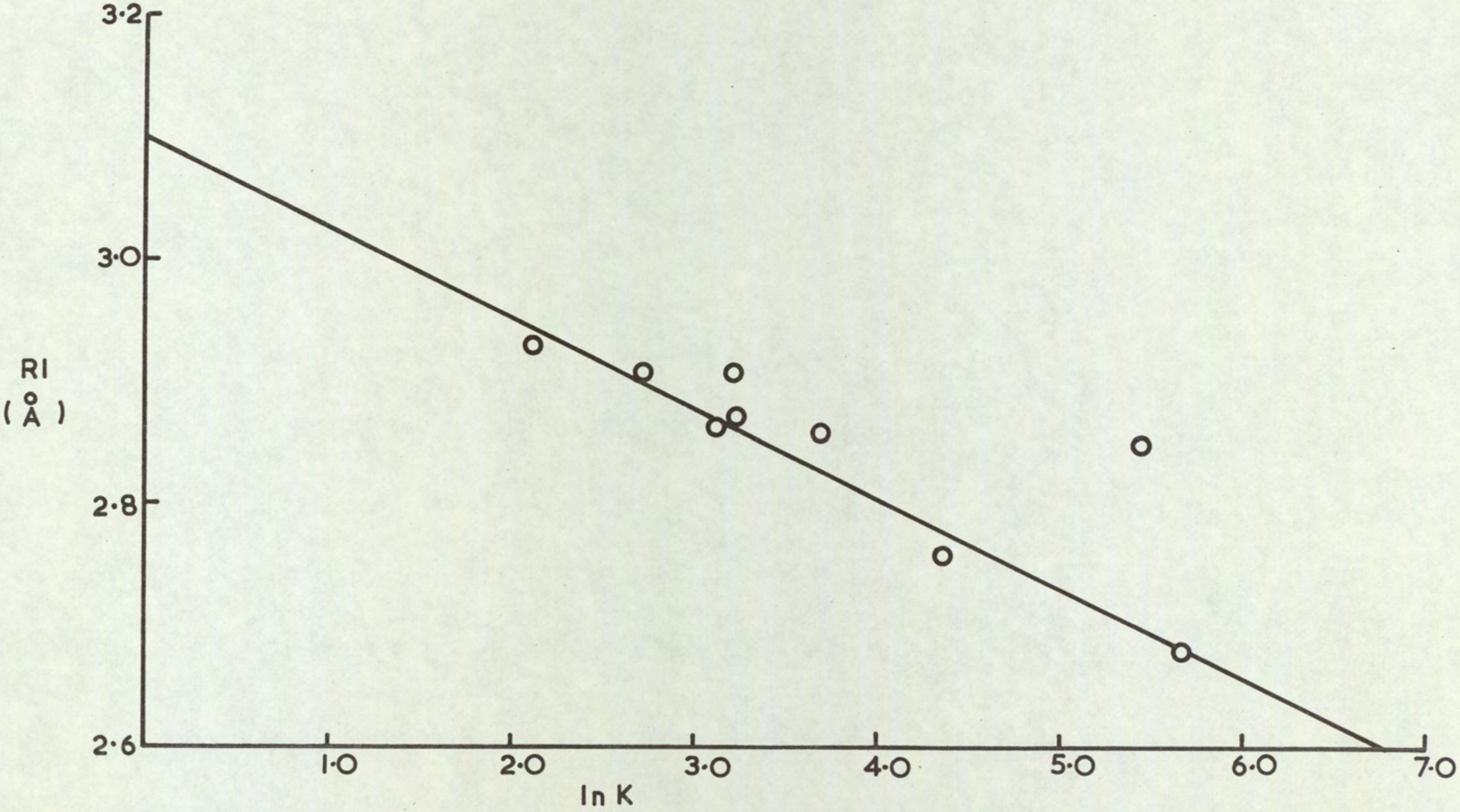

FIG 3-5 THE RELATIONSHIP BETWEEN lnK AND RI FOR THE NITROFORM COMPLEXES STUDIED

TABLE 3-12. Data Used to Plot Figs. 3-2, 3-3, and 3-4/5.

Complex	ln $K_{33.4}$	Complex	ln $K_{33.4}$
Nitroform With		Chloroform With	
Benzene	2.13	Benzene	0.166
Toluene	2.69	P-Xylene	0.688
O-Xylene	3.28	Bromoform With	
M-Xylene	3.26	Benzene	0.073
P-Xylene	3.18	P-Xylene	0.468
Mesitylene	3.63	Iodoform With	
Durene	4.36	Benzene	0.106
P.M.B.	5.42	P-Xylene	0.655
H.M.B.	5.63	Fluoroform With	
		Benzene	0.349
		P-Xylene	0.908

Some Perpendicular Polarisabilities of the Aromatic Molecules Used (139)

Aromatic	(c.c. x 10^{24})
Benzene	7.33
Toluene	9.04
o, m, p-Xylene	10.75
Mesitylene	12.47
H.M.B.	16.84

CHAPTER 4

Investigation of Complex Formation at Different Temperatures

4:1 The Basis and Value of Variable Temperature Studies

If, following the assumption of Chapter 3, the activity coefficients of the associating species in each system studied are taken to be unity, or self cancelling, in the equilibrium expressions at all temperatures, the equilibria of interest may conveniently be considered to occur in ideal solutions. If this is the case, the Gibbs Standard Free Energy change for a reaction is related to the equilibrium constant (expressed in terms of mole fractions) at a temperature T by

$$\Delta G^{\circ}_{T} = -RT\ln K_{x} \qquad 4 : 1$$

assuming negligible pressure dependance in the condensed phase. This represents the free energy change when one mole of each reactant (for the current work considered dissolved in cyclohexane) combine to produce one mole of complex at temperature T. The temperature dependance of free energies is given classically by the Gibbs-Helmholtz equation which may be written as

$$\left[\frac{\partial(\Delta G/T)}{\partial(1/T)}\right]_p = \Delta H \qquad 4 : 2$$

This may be used in combination with equation 4 : 1 to provide the expression:-

$$\frac{\partial \ln K}{\partial T} = \frac{\Delta H^{\circ}}{RT^2} \qquad 4 : 3$$

or

$$\frac{\partial \ln K}{\partial(1/T)} = -\frac{\Delta H^{\circ}}{R} \qquad 4 : 4$$

Thus if $\ln K_x$ is plotted against 1/T, the slope of the curve at any point is equal to $-\Delta H^{\circ}/R$. The value of ΔH° thus obtained, together with the corresponding value for ΔG°, deduced from equation 4 : 1, can then be used to obtain the standard entropy change for the reaction, at the temperature chosen, from the relationship:

$$\Delta G^{\circ} = \Delta H^{\circ} - T\Delta S^{\circ} \qquad 4 : 5$$

which refers to the reaction at constant temperature T.

It is evident, therefore, that by performing the N.M.R. measurements at various temperatures, and thereby obtaining values of the corresponding stability constants, the thermodynamic parameters ΔG°, ΔH° and ΔS° may readily be deduced. Apart from the value of the latter in themselves, they can be used to investigate further the credibility of the dipole-induced dipole model for complex formation which has been postulated, and to some extent already substantiated.

4:2 Experimental

The haloform samples used in the variable temperature studies were the same as those used at 33.4°C, but the original nitroform samples were replaced as indicated in Chapter 3.

The use of the variable temperature equipment presented no peculiar difficulties apart from a decrease in the signal-to-noise ratio of about 30% and a slight increase in the rate of magnetic field drift. This may have led to a marginal decrease in the accuracy of the shift measurements, which were made using the side-band technique described previously. The temperatures at which measurements were made were nominally 5°C, 15°C, 25°C, (33.4°C) and 40°C. The lower limit was determined by the freezing point of the solvent (c.a. 5°C) and the upper limit by considerations of time and the possibility of thermal decomposition of the dipolar species, particularly the nitroform, and the possibility of side-reactions.

At any preset temperature, temperature variation from sample to sample was small and with some instrument supervision could be maintained constant to within 0.1°C, although stability was more difficult to maintain at the lower temperatures. Whilst the preset temperature remained stable during the experiments, its precise value was not determinable immediately to better than 1°C. In order to remedy this, use was made of the copper constantan thermocouple, provided by the manufacturers, with its sensing head situated within 1 cm. of the R.F. coil and with its reference junction concealed in the thermostatted magnet enclosure. The e.m.f. produced by this was measured by a potentiometer and the actual temperature then obtained by reference to tables supplied.

All sample measurements were made in principle from the lowest temperature upwards to minimise any errors arising from possible solute decomposition, although certain practical considerations cut across this from time to time. The iodoform samples were, however, measured strictly in this order. The fluoroform samples were heated prior to examination to 50°C to minimise the risk of sample tube explosion in the probe. The shift measurements and molar quantities of each system were processed in the usual way with COMPLEXICON.

4:3 A Possible Source of Error in the Investigations

In view of the fact that the samples were studied at different temperatures the possibility arises of changes in the proportions of the constituents in solution, because of changes in the saturation vapour pressure of the constituents. This was thought most likely to lead to variations in the quantity of the solute species because of the wide deviation, in most cases, of the volatility of these from the solvent. To test the effect of this, the data of the benzene/chloroform/cyclohexane system at 33.4°C (the most accurately measured series) were modified by increasing and decreasing successively by 20% the numbers of moles of chloroform used in the computation by COMPLEXICON. The values of K and DELTA derived from the computations differed from the true value by less than 1% (see Table 4-1). Therefore, variations in composition with temperature change can not be expected to introduce appreciable error to the values of K and DELTA.

TABLE 4-1. Test of Solute Concentration Error on the Computation Results of COMPLEXICON for the System Benzene/Chloroform/Cyclohexane @ 33.4°C.

Parameter	Correct Results	Nbr. of moles of Chloroform Used	
		+ 20%	- 20%
K	1.1607	1.1672	1.1546
DELTA (Hz)	97.2	97.1	97.4

4:4 Results and Data Processing

The results of the measurements at various temperatures are presented in Table 4-2 to 4-18 which show the observed solute shift for each sample at each temperature investigated. The numbers of moles of the constituents used for the nitroform samples are included, since different samples to those used for the work at 33.4°C were prepared for these later investigations. The haloform samples can be identified by the letters used and the sample composition found by reference to the Tables in Chapter 3.

TABLES 4-2 to 4-18. The Numbers of Moles of the Constituents of each Sample and the Observed Chemical Shifts (in Hz) from Cyclohexane of the Solute Species at Various Temperatures.

TABLE 4-2. Benzene - Nitroform.

	Moles ($x\ 10^4$)	Moles ($x\ 10^4$)	Moles ($x\ 10^4$)	Chemical Shifts *			
	Haloform	Aromatic	Cyclohexane	@ 5°C	@ 15°C	@ 25°C	@ 40°C
O	4.99_9	0.0	499.6	-340.54	-340.20	-340.04	-339.14
A	3.10_5	4.02	295.2	-323.91	-	-328.19	-
B	2.98_6	9.20	286.7	-307.42	-312.54	-316.65	-320.90
C	3.019	14.26	296.9	-294.70	-	-305.00	-
D	3.19_8	25.71	264.6	-278.07	-283.21	-290.00	-298.30
E	3.08_5	31.31	273.6	-269.73	-280.33	-281.14	-291.11
F	3.11_2	37.57	241.6	-265.88	-271.58	-278.27	-287.08
G	2.95_3	59.98	212.0	-253.79	-260.71	-263.47	-276.34
H	2.90_7	93.56	212.0	-245.96	-250.97	-256.59	-266.08
J	3.05_9	142.6	153.1	-234.67	-	-245.57	-252.36

* Unrecorded chemical shift values arise from sample breakage or obscuration by spinning side bands.

TABLE 4-3. Toluene - Nitroform

	Moles (x 10^4)	Moles (x 10^4)	Moles (x 10^4)	Chemical Shifts			
	Haloform	Aromatic	Cyclohexane	@ 5°C	@ 15°C	@ 25°C	@ 40°C
O	4.98_9	0.0	499.6	-340.50	-340.20	-340.04	-339.14
A	3.23_7	4.60_9	310.2	-	-320.04	-323.84	-329.08
B	3.00_6	6.79_8	289.6	-290.48	-	-	-
C	3.07_9	9.67_0	287.6	-274.08	-	-306.30	-315.67
D	3.12_5	15.11	295.2	-255.66	-281.69	-290.92	-304.53
E	2.99_9	19.12	278.2	-	-273.05	-280.69	-298.70
F	3.19_1	28.53	286.1	-239.81	-262.84	-	-
G	3.03_2	49.11	248.8	-227.50	-251.07	-260.65	-272.36
H	2.92_6	82.76	214.5	-	-241.12	-249.07	-259.82
J	3.01_9	183.2	115.9	-	-232.59	-236.59	-243.15

TABLE 4-4. O-Xylene Nitroform

	Moles (x 10^4)	Moles (x 10^4)	Moles (x 10^4)	Chemical Shifts			
	Haloform	Aromatic	Cyclohexane	@ 5°C	@ 15°C	@ 25°C	@ 40°C
O	4.99_9	0.0	499.9	-340.52	-340.20	-340.04	-339.14
A	3.10_5	1.28_1	302.5	-324.03	-326.25	-329.40	-332.72
B	3.06_5	3.76_8	291.9	-302.30	-308.36	-313.81	-319.02
C	2.97_9	5.87_7	293.4	-299.31	-305.42	-313.14	-317.20
D	3.17_1	9.92_8	287.6	-265.35	–	–	–
E	3.02_6	13.05	282.3	-256.38	-265.16	-275.25	-285.02
F	2.90_6	26.98	266.4	-249.61	-258.87	-266.06	-279.33
G	3.04_6	53.16	244.1	–	–	–	–
H	3.02_6	113.1	182.8	-223.35	-229.81	-233.75	-246.83

TABLE 4-5. M-Xylene Nitroform

	Moles (x 10^4)	Moles (x 10^4)	Moles (x 10^4)	Chemical Shifts			
	Haloform	Aromatic	Cyclohexane	@ 5°C	@ 15°C	@ 25°C	@ 40°C
O	4.99_9	0.0	499.6	-340.52	-340.20	-340.04	-339.16
A	2.88_0	1.42_2	297.3	-324.43	-326.71	-329.83	-332.19
B	3.06_5	3.76_8	291.1	-300.51	-307.12	-309.74	-319.68
C	2.99_8	5.93_4	292.1	-286.49	-295.94	-	-314.31
D	2.94_0	9.23_1	291.0	-270.92	-280.94	-290.38	-299.08
H	2.99_9	50.59	248.6	-226.26	-232.97	-238.83	-249.66
J.	2.92_0	112.9	185.1	-219.38	-224.42	-228.91	-238.70

TABLE 4-6. P-Xylene Nitroform

	Moles (x 10^4)	Moles (x 10^4)	Moles (x 10^4)	Chemical Shifts			
	Haloform	Aromatic	Cyclohexane	@ 5°C	@ 15°C	@ 25°C	@ 40°C
O	4.99_9	0.0	499.6	-340.54	-340.20	-340.04	-339.14
A	3.07_9	1.49_8	302.5	-322.41	-325.22	-326.90	-330.28
B	3.13_2	4.10_7	298.7	-299.41	-305.04	-308.80	-316.50
C	2.95_3	6.16_0	278.4	-283.42	-291.52	-297.70	-306.71
D	3.05_9	9.44_8	290.3	-270.00	-278.39	-284.90	-296.01
E	2.93_3	13.47	285.4	-	-	-273.97	-
F	3.07_2	19.72	276.9	-246.08	-	-261.50	-273.99
G	2.97_9	30.35	269.6	-236.14	-243.37	-249.84	-262.18
H	3.20_4	54.90	267.3	-226.97	-233.81	-	-250.38

TABLE 4-7. Mesitylene Nitroform

	Moles (x 10^4)	Moles (x 10^4)	Moles (x 10^4)	Chemical Shifts			
	Haloform	Aromatic	Cyclohexane	@ 5°C	@ 15°C	@ 25°C	@ 40°C
O	4.99_9	0.0	499.6	-340.52	-340.20	-340.04	-339.14
A	3.18_0	1.07_3	298.1	-321.81	-325.24	-325.86	-329.63
B	2.98_2	2.60_7	300.7	-299.40	-306.94	-310.46	-317.56
C	2.97_7	43.5_6	203.8	-282.31	-289.25	-296.10	-306.67
D	3.36_7	7.22_9	317.5	-260.77	-270.28	-279.34	-294.06
E	3.35_1	10.80	319.5	-250.36	-260.98	-273.57	-282.70
F	2.96_0	13.62	282.3	-241.05	-249.38	-258.84	-271.10
G	2.99_4	21.01	276.6	-	-240.52	-249.28	-261.51
H	3.00_4	33.66	264.8	-223.16	-226.09	-238.16	-251.65
J	3.14_4	76.32	224.7	-213.06	-218.16	-224.76	-232.96

TABLE 4-18. Tetramethyl Benzene Nitroform

	Moles (x 10^4)	Moles (x 10^4)	Moles (x 10^4)	Chemical Shifts			
	Haloform	Aromatic	Cyclohexane	@ 5°C	@ 15°C	@ 25°C	@ 40°C
O	4.99_9	0.0	499.6	-340.54	-340.20	-340.04	-339.14
A	3.21_6	0.80	302.3	-	-322.88	-324.55	-328.69
B	2.80_5	1.57_9	275.5	-296.09	-302.11	-307.76	-313.70
C	2.98_9	2.62_0	293.2	-	-	-	-
D	3.03_6	4.27_1	293.6			-275.38	
E	2.94_1	5.45_1	282.9	-246.11	-255.77	-265.83	-279.26
F	4.10_9	7.60_4	391.4	-	-	-	-
G	3.14_6	10.95	295.8	-224.90	-233.28	-242.79	-256.95
H	2.86_8	17.74	291.0	-211.93	-220.59	-229.10	-241.38
J	3.01_6	38.10	255.7	-	-210.55	-216.13	-225.81

TABLE 4-9. Penta-Methyl Benzene Nitroform

	Moles (x 10^4)	Moles (x 10^4)	Moles (x 10^4)	Chemical Shifts			
	Haloform	Aromatic	Cyclohexane	@ 5°C	@ 15°C	@ 25°C	@ 40°C
O	4.99_9	0.0	499.6	-340.64	-340.20	-340.04	-339.14
A	2.94_2	0.48_3	293.1	-319.95	-324.66	-327.23	-332.09
B	3.51_8	1.10_7	340.7	-304.36	-307.60	-311.64	-317.02
C	3.04_6	0.95_8	293.1	-290.25	-297.65	-303.66	-307.93
D	3.24_8	1.44_4	296.2	-282.63	-289.63	-295.74	-303.22
E	4.85_6	2.61_8	451.5	-279.07	-286.51	-292.93	-301.20
F	3.10_6	1.80_0	291.4	-269.90	-278.34	-286.52	-294.90
G	2.85_6	2.03_9	290.8	-	-	-	-
H	2.99_9	4.36_2	285.4	-217.69	-227.44	-237.79	-253.50
J	3.05_5	6.25_3	278.9	-207.52	-215.84	-225.38	-240.28

TABLE 4-10. Hexamethyl Benzene Nitroform

	Moles (x 10^4)	Moles (x 10^4)	Moles (x 10^4)	Chemical Shifts			
	Haloform	Aromatic	Cyclohexane	@ 5°C	@ 15°C	@ 25°C	@ 40°C
O	4.99_9	0.0	499.6	-340.54	-340.20	-340.04	-339.14
A	2.89_8	0.41_4	284.3	-317.55	-319.64	-321.56	-324.42
B	2.97_5	0.93_5	290.5	-	-	-303.74	-
C	3.07_7	1.42_5	294.8	-275.72	-282.34	-288.56	-297.72
D	3.22_9	1.92_3	368.2	-263.74	-272.02	-279.64	-291.25
E	3.23_2	2.63_4	311.0	-241.84	-251.77	-261.30	-274.67
F	3.13_8	3.34_2	289.2	-222.60	-235.23	-245.41	-259.53
G	3.14_0	4.61_4	297.4	-	-231.34	-239.50	-255.73
H	2.94_1	6.64_3	262.0	-196.97	-204.21	-212.96	-227.52
J	3.30_0	12.55	297.0	-	-194.19	-200.65	-212.83

TABLE 4-11. Benzene Chloroform

	Chemical Shifts			
SAMPLE	@ 5°C	@ 15°C	@ 25°C	@ 40°C
O	-339.33	-339.36	-339.22	-339.12
A	-326.48	-327.93	-328.81	-330.02
B	-316.26	-317.99	-319.83	-322.23
C	-305.97	-308.57	-311.15	-314.27
D	-300.09	-301.00	-304.97	-308.74
E	-294.60	-298.61	-301.18	-305.08
F	-290.23	-292.87	-296.78	-300.90
G	-287.91	-290.87	-	-297.26
H	-284.65	-287.38	-289.81	-294.02
J	-281.75	-284.77	-287.34	-291.41

TABLE 4-12. P-Xylene Chloroform

O	-339.33	-339.36	-339.22	-339.12
K	-332.71	-	-335.08	-334.97
A	-	-	-	-
B	-319.02	-320.90	-323.88	-325.60
C	-310.56	-313.31	-316.53	-319.17
D	-305.74	-308.89	-310.95	-315.92
E	-302.11	-304.43	-307.64	-311.98
F	-296.81	-300.95	-301.78	-308.42
G	-289.46	-296.42	-299.73	-304.52
H	-	-293.72	-296.24	-
J	-285.50	-287.76	-292.97	-297.73
L	-	-	-287.47	-
M	-276.63	-280.24	-282.85	-289.02

TABLE 4-13. Benzene Bromoform

	Chemical Shifts			
SAMPLE	@ 5°C	@ 15°C	@ 25°C	@ 40°C
O	-315.16	-315.31	-315.46	-315.47
J	-308.78	-308.65	-310.30	-311.01
A	-301.83	-303.33	-304.48	-306.08
B	-293.59	-295.51	-296.58	-299.43
C	-285.56	-287.99	-290.12	-293.01
D	-279.01	-281.88	-283.51	-287.26
E	-273.97	-276.70	-278.90	-282.87
F	-269.31	-272.07	-274.50	-278.59
G	-264.75	-268.34	-271.29	-274.95

TABLE 4-14. Bromoform - P-Xylene

O	-315.16	-315.31	-315.46	-315.47
A	-304.29	-305.24	-306.96	-308.20
B	-294.91	-297.15	-298.90	-301.87
D	-	-	-293.79	-
E	-280.93	-284.10	-285.83	-290.84
G	-264.34	-268.65	-274.87	-277.32
H	-260.10	-264.61	-269.21	-272.69
J	-253.86	-259.48	-262.52	-268.60

TABLE 4-15. Benzene Iodoform

	Chemical Shifts			
SAMPLE	@ 5°C	@ 15°C	@ 25°C	@ 40°C
O	-	-202.90	-202.92	-203.28
A	-175.45	-178.14	-180.18	-183.20
B	-166.91	-170.51	-172.71	-176.07
C	-	-169.53	-171.79	-176.03
D	-163.68	-166.03	-168.62	-172.29
E	-158.47	-161.09	-163.52	-167.15
F	-153.94	-156.05	-158.95	-
G	-149.39	-151.82	-154.43	-158.36

TABLE 4-16. P-Xylene Iodoform

O	-	-202.90	-202.92	-203.28
A	-166.76	-170.38	-172.98	-177.35
B	-159.28	-162.46	-165.44	-170.30
C	-152.62	-156.05	-159.38	-164.44
D	-146.72	-150.16	-153.65	-158.89
F	-143.50	-147.11	-149.47	-155.88
G	-138.24	-141.63	-144.94	-150.82

TABLE 4-17. Benzene Fluoroform

	Chemical Shifts			
SAMPLE	@ 5°C	@ 15°C	@ 25°C	@ 40°C
O	-249.00	-248.81	-248.59	-248.41
A	-243.94	-244.60	-245.45	-240.09
B	-233.18	-237.61	-	-
C	-224.52	-226.72	-228.73	-231.26
D	-215.14	-218.03	-221.66	-
E	-213.34	-214.63	-218.29	-222.31
F	-196.43	-198.80	-203.51	-207.28
G	-203.22	-206.01	-209.48	-213.63
H	-193.92	-196.57	-200.53	-199.33
J	-190.19	-193.27	-196.57	-200.71

TABLE 4-18. P-Xylene Fluoroform

O	-249.05	-248.81	-248.59	-248.41
A	-237.64	-238.81	-240.23	-
B	-231.36	-233.09	-	-
C	-226.19	-228.41	-230.37	-233.10
D	-217.25	-219.92	-223.98	-226.19
E	-212.18	-214.54	-218.32	-222.05
F	-208.56	-212.00	-215.37	-219.34
G	-211.13	-214.60	-218.07	-221.33
H	-198.68	-196.79	-204.30	-208.94

The chemical shift values given in Tables 4-2 to 4-18, quoted in hertz relative to cyclohexane, are the values deduced from a least mean square treatment of the results of the side-band measurements, and whilst used for the computation involving COMPLEXICON it is not intended to imply that they are accurate to ± 0.01 Hz. The temperatures quoted are nominal and the accurate values of these are given subsequently in Table 4-19 with the values of K and DELTA derived from COMPLEXICON. The values for ΔH^{o}_{298}, ΔG^{o}_{298}, and ΔS^{o}_{298} were deduced by the procedure detailed in section 4:1 and are listed in Table 4-20. The error limits quoted on the entropy values are 95% confidence limits.

4:5 Discussion

General

The values determined for ΔG^{o}, ΔH^{o} and ΔS^{o} are of the order of magnitude expected for the formation of weak complexes of the type studied here and are consistent with the available values reported by other workers for similar complexes (140,141).

The plots of lnK against 1/T are apparently linear in all cases (see for example fig. 4 - 1) and, therefore, indicate that over the temperature range studied the enthalpy of association for each complex is independant of temperature. It is to be expected therefore, that ΔS^{o} for the complexes may also be relatively little affected by temperature. The signs of the enthalpy and entropy terms indicate, respectively, in all cases, that the formation of each complex is exothermic and is accompanied by a decrease in the entropy of the system.

Strict comparisons between published results and the values

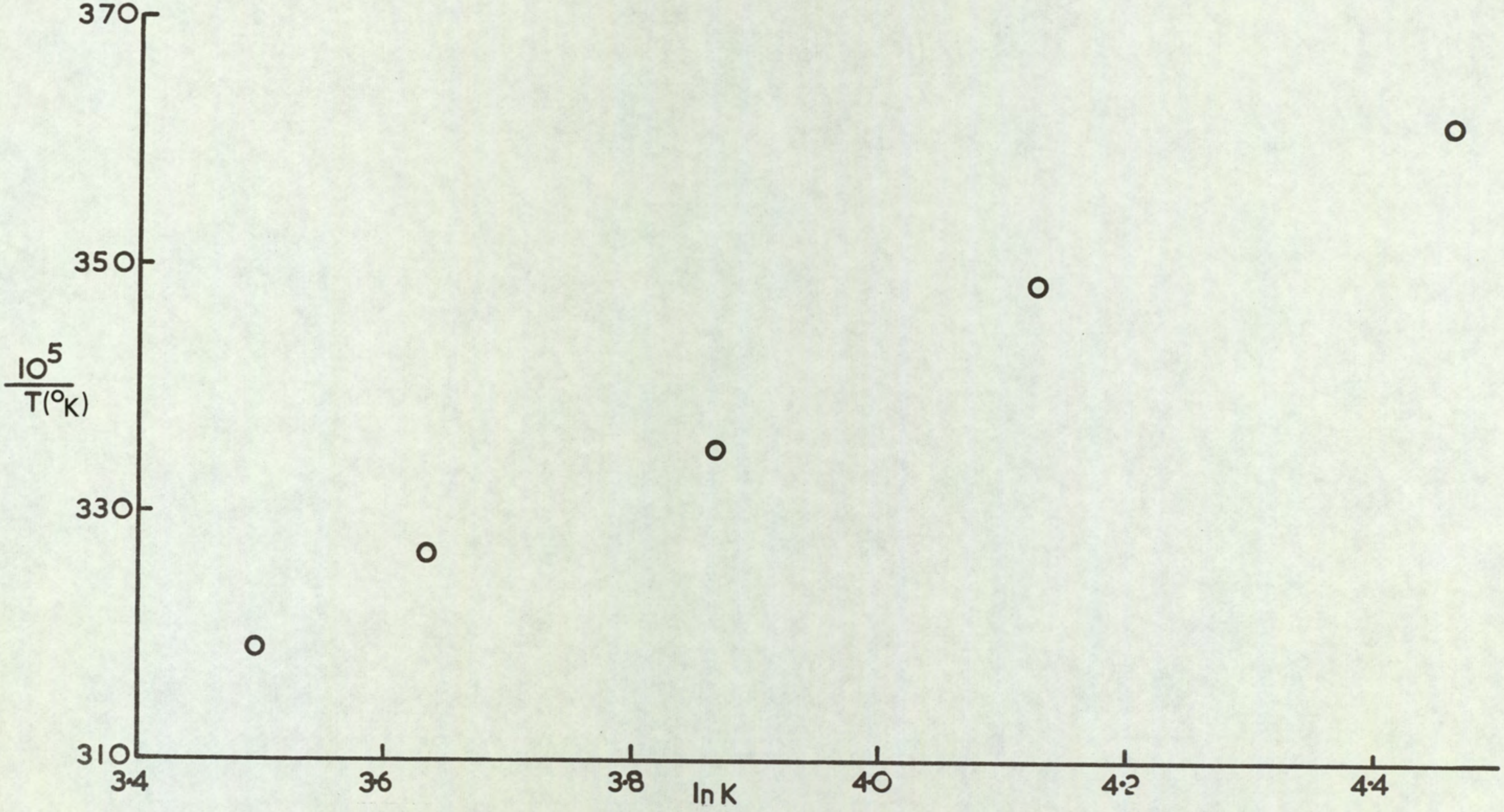

FIG 4-1 THE RELATIONSHIP BETWEEN ln K AND RECIPROCAL ABSOLUTE TEMPERATURE FOR THE MESITYLENE/NITROFORM COMPLEX

TABLE 4-19. Values of K and DELTA at the Various Temperatures of Study

Solute	Aromatic	T(^{o}C)	K	DELTA (p.p.m.)
Nitroform	Benzene	15.9	14.32	2.00
		13.8	12.51	1.90
		24.6	10.58	1.90
		40.6	7.72	1.81
	Toluene	5.5	35.8	2.26
		14.0	23.4	1.96
		23.5	17.0	1.90
		39.7	9.36	1.89
	O-Xylene	3.3	55.71	2.07
		13.9	43.82	1.97
		25.9	32.28	1.93
		40.9	28.69	1.72
	m-Xylene	3.4	47.14	2.16
		13.8	34.65	2.09
		24.8	27.49	2.05
		40.7	18.85	1.96
	p-Xylene	3.6	47.13	2.07
		13.9	37.44	2.07
		23.9	28.17	2.07
		39.7	22.21	1.90
	Mesitylene	3.5	86.68	2.20
		13.8	62.01	2.17
		25.6	47.80	2.04
		40.6	33.04	1.94

TABLE 4-19 (contd)

Solute	Aromatic	T(^{o}C)	K	DELTA (p.p.m.)
Nitroform	Durene	4.4	167.3	2.39
		13.3	125.1	2.31
		23.5	95.04	2.24
		40.8	62.69	2.14
	P.M.B.	3.6	743.1	2.44
		15.2	430.5	2.47
		23.7	269.9	2.48
		40.9	185.6	2.34
	H.M.B.	3.5	1054.0	2.52
		15.0	525.5	2.54
		23.7	352.8	2.50
		40.9	213.1	2.40
Chloroform	Benzene	3.7	1.699	1.61
		13.8	1.497	1.60
		23.7	1.292	1.63
		40.1	1.086	1.62
	P-Xylene	3.6	2.752	1.62
		13.8	2.375	1.60
		24.9	2.106	1.59
		40.7	1.738	1.54
Bromoform	Benzene	3.8	1.420	1.68
		13.8	1.263	1.66
		23.5	1.277	1.58
		39.7	0.991	1.66

TABLE 4-19 (contd)

Solute	Aromatic	T(^{c}C)	K	DELTA (p.p.m.)
	P-Xylene	3.7	1.831	1.96
		13.9	1.819	1.80
		24.6	1.662	1.73
		39.7	1.316	1.81
Iodoform	Benzene	14.5	1.361	1.49
		13.8	1.375	1.51
		23.3	1.225	1.52
		40.8	1.015	1.54
	P-Xylene	4.5	1.585	1.62
		13.7	2.205	1.61
		23.2	2.067	1.63
		40.7	1.832	1.48
Fluoroform	Benzene	3.7	2.146	1.66
		13.6	2.037	1.62
		24.3	1.690	1.63
		40.5	0.920	2.04
	P-Xylene	3.7	3.629	1.36
		13.6	2.988	1.39
		24.9	2.404	1.41
		39.9	2.253	1.30

TABLE 4-20. The Values of Thermodynamic Parameters Resulting from the Variable Temperature Studies

Solute	Aromatic	- ΔH. (K cals. moles^{-1})	- ΔS. (cals. deg^{-1} moles^{-1})	- ΔG. (K cals. moles^{-1}) @ 25°C.
Nitroform	Benzene	3.18	6.08 ± 0.17	1.37
	Toluene	6.68	16.12 ± 0.24	1.67
	O-Xylene	4.53	8.31 ± 0.26	2.05
	m-Xylene	4.19	7.51 ± 0.13	1.95
	p-Xylene	3.71	5.75 ± 0.20	1.99
	Mesitylene	4.48	7.36 ± 0.14	2.29
	Durene	4.55	6.24 ± 0.16	2.69
	P.M.B.	6.55	10.62 ± 0.58	3.38
	H.M.B.	7.25	12.54 ± 0.56	3.51
Chloroform	Benzene	2.16	6.73 ± 0.05	0.150
	P-Xylene	2.12	5.79 ± 0.06	0.435

TABLE 4-20. (contd)

Solute	Aromatic	$-\Delta H$.(K cals. moles^{-1})	$-\Delta S$.(cals. deg^{-1} moles^{-1})	$-\Delta G$.(K cals. moles^{-1}) @ 25°C
Bromoform	Benzene	1.65	5.26 ± 0.12	0.08
	P-Xylene	2.18	6.36 ± 0.42	0.29
Iodoform	Benzene	1.98	6.27 ± 0.05	0.11
	P-Xylene	1.23	2.71 ± 0.02	0.42
Fluoroform	Benzene	3.28	10.03 ± 0.07	0.29
	P-Xylene	3.47	9.86 ± 0.43	0.53

reported here are difficult because few investigations have been carried out with a view to deriving thermodynamic data, and for those that have, several employ theoretical approximations and experimental conditions which bring the reported results into question.

The only investigations which seem to have been carried out on some of the systems studied here are those of Tamres (121) who determined the heats of mixing per mole of chloroform and bromoform with benzene and m-xylene. It is of interest to attempt to draw a direct comparison between his values and the enthalpies of interaction derived from these studies. By using the known equilibrium constants for the above complexes it is possible to determine the expected degree of complex formation (in the absence of solvent) and derive a value for the heat evolved. The values so derived, together with the heats of mixing (L) are listed in Table 4-21. It is clear that little or no comparison is possible and this can be attributed to the heat effect of mixing the haloforms with the aromatic which is not considered in the present work, on the one hand, and on the other the inadequacy of using the equilibrium expression as a reliable method of determining the degree of complex formation in the absence of solvent and in the presence of a large amount of self associating solute.

TABLE 4-21. Comparison of $-\Delta H$ from this work and Actual Heats of Mixing (in cals moles^{-1}) for Some of the Systems Studied

System	$-\Delta H$ This Work	L(heat evolved) Tamres (121)
Benzene/Chloroform	727	90
Xylene/Chloroform	906	202
Benzene/Bromoform	523	34
Xylene/Bromoform	833	106

The work of Brand, Eglinton, and Tyrrell (140) is potentially of value in that N.M.R., I.R., and calorimetric data are available from three component systems very similar to those studied here, but the method of data evaluation is open to question because an inadequate approximation regarding the equilibrium expression appears to have been made. Equilibrium constants for benzoylacetylene ($C_6H_5.CO.C\equiv C\text{-}H$) complexing with benzene, toluene, p-xylene and mesitylene were determined by the two spectroscopic techniques and are listed, together with the corresponding values for ΔH°, in Table 4-22.

The calorimetric values are the differences of the heats of mixing for the solute in each aromatic and in cyclohexane and have been adjusted to allow for incomplete association under the conditions in which they were carried out (infinite dilution in the aromatic). The heat values determined by the spectroscopic techniques are not in agreement between themselves or with the calorimetric data and it appears, therefore, that confirmation of spectroscopic results by calorimetry awaits a more comprehensive and purposeful examination.

TABLE 4-22. Some Thermodynamic Data for Complex Formation between Benzoylacetylene and Some Simple Aromatic Hydrocarbons in Cyclohexane. (140)

Technique	I.R.		N.M.R.		Calorimetry
Aromatic	K_{298}	ΔH (Kcals moles^{-1})	K_{298}	ΔH (Kcals moles^{-1})	L(Kcals moles^{-1})
Benzene	0.61	-3.9	0.71	-1.8	-7.1
Toluene	1.4	-5.4	1.1	-2.1	-8.0
P-Xylene	2.4	-5.9	-	-	-
Mesitylene	3.0		-	-	-

Early work by Creswell and Allred (141), using the analytical approach presented in Chapter 3, is probably most informative, if only for comparison purposes with the results of the present work. In a study of the association of the haloforms with tetrahydrofuran, the following relationships with regard to the orders of magnitude of the enthalpies, entropies and Gibbs free energies of interaction were found:

$$\mathrm{CHCL_3} > \mathrm{CHBr_3} \bumpeq \mathrm{CHF_3} > \mathrm{CHl_3} \qquad 4 : 6$$

Moreover, it was indicated that the bond strengths for the complexes follow the order of ΔH for these. The magnitudes of the various parameters were similar to those found in the course of the present studies. However, the order corresponding to 4 : 6 for the same solutes with, say, benzene is not the same but

$$\mathrm{CHF_3} > \mathrm{CHCL_3} \bumpeq \mathrm{CHl_3} > \mathrm{CHBr_3} \qquad 4 : 7$$

This is not surprising, for two reasons. Firstly, the bonds with tetrahydrofuran and with benzene may be expected to differ in nature, particularly in view of the availability of unshared electrons in the former solvent. Secondly, different steric factors affecting complex formation with the two different solvents can operate due to the different solid angles for solute approach on complex formation. This effect would be expected to be more pronounced with benzene, and therefore the solute size would be expected to have greater significance with this solvent than with tetrahydrofuran.

It is evident that rationalisation of the thermodynamic parameters deduced for the systems studied here is helped little by reference to other reported work, and at present may only be possible on a self-consistent basis.

4:6 ΔS^o Values and some Comments on the Complex Model

From the values given in Table 4-20 for ΔS^o for the formation of the various complexes, it is immediately obvious that definite variations in these occur. To rationalise these quantitatively would be extremely difficult because a knowledge of the standard molar entropies of each of the pure compounds involved would be required for evaluation of the general expression

$$\Delta S^o_{measured} = S^o_{complex} - S^o_{aromatic} - S^o_{solute}$$

However in the case of the xylenes, comparisons of ΔS^o for the nitroform complexes may be made since values for $S^o_{liquid\ (298)}$ for the ortho, meta and para isomers have been reported as 58.91, 60.27 and 59.12 cal deg^{-1} respectively (142). $\Delta S^o_{ortho} - \Delta S^o_{para}$ is by reference to Table 4-20, - 2.56 cal deg^{-1} so that the entropy difference of the corresponding complexes is - 2.77 cal deg^{-1} which is much larger than the entropy difference for the pure aromatics and indicates the ortho to be more ordered than the para complex. Similarly, it may be argued that the entropy difference between the ortho and meta complexes is - 2.16 cal deg^{-1} and that the ortho is more ordered than the meta which is slightly more ordered than the para complex. Symmetry considerations in respect of this argument produce the same result. If real, the fact that different entropies of these three complexes are indicated, may be significant. Certainly, if the early model of the complexes with solute and solvent fixed in position is correct there would be no reason to expect different entropies for the three complexes. If, however, a different model is proposed for which the solute hydrogen remains on or very near the six-fold axis of the aromatic ring, but the remainder of the solute is allowed all possible orientations relative to the aromatic molecule, governed by molecular contact, an explanation for the entropy differences of the complexes is possible. The methyl groups would then play a steric role in complex formation since they are capable of precluding certain of the allowed orientations of the solute and solvent. Certainly in the case of ortho-xylene replusion between the methyl groups makes their exclusion volume greater than that in p-xylene which should be similar if not slightly smaller than in the meta xylene case and, so as indicated earlier, the entropy of the ortho would be expected to be less than that of the para complex. It is possible that similar arguments can explain the large $-\Delta S^{o}$ values for the penta- and hexamethylbenzene complexes but this must remain unproven until the entropies of the aromatic compounds involved become available.

4:7 Further Consideration of the Intermolecular Interaction in the Complexes.

In Chapter 3, when developing the arguments which ultimately led to the contention that in the complexes the inter molecular attraction was primarily dipole-induced dipole in origin, three points were established. Firstly, it was shown that for complexes of a common aromatic component with various solutes, ln K is dependant on the permanent electric dipole moment of the latter molecule. Secondly, with a common solute and various methylbenzenes ln K is dependant on methyl substitution and hence polarisability of the aromatic ring. Thirdly, ln K was shown to vary with $-\alpha\mu^{2}/R2^{6}$ when R2 is more or less constant.

Nevertheless, in Chapter 3 uncertainty was expressed as to which thermodynamic parameter (ΔG^{o} or ΔH^{o}) should be taken to most reasonably represent the "strength" (interaction energy) of the complexes. Other workers (141) have used ΔH^{o} to indicate bond strength but nevertheless further investigation on this point seems necessary. The problem is difficult to resolve, but some help may be obtained by considering the two models for the complex so far proposed.

The first model, in which the solute symmetry axis was proposed to be fixed and coincident with the aromatic six-fold axis, will be considered initially. In this case, the interaction energy, dependent inversely on $R2^6$, would be expected to adopt the maximum allowed value and would, therefore, be determined by molecular contact. It is difficult to conceive a mechanism whereby temperature would significantly modify this state of affairs and so, for each complex, R1 would be expected to be independent of temperature. From the results given in Table 4-19 it is evident that σ_{vert} (DELTA), and therefore R1 for a particular complex, appears in some cases to vary with temperature. Nevertheless, no overall rigorous trend is evident and for the benzene-chloroform complex, which is known to be the most accurately prepared system, the change is very small. Whilst the variations may be real, it is nevertheless possible that they may arise because of the experimental error introduced by the temperature instability of the variable temperature probe. If the R1 values for a particular complex are temperature independent, the only thermodynamic parameter that can be correlated with calculated interaction energies is ΔH^o. This could be anticipated for this complex model by consideration of the qualitative argument that the attractive forces in the complex, as calculated on the dipole-induced dipole approach, take no account of entropy factors which are necessarily implicit in ΔG^o but not ΔH^o. If ΔH^o is taken as the critical thermodynamic parameter reflecting the intermolecular attraction, correlations with solute dipole moment (constant aromatic), aromatic perpendicular polarisability (constant solute) and $\alpha\mu^2$ interaction energy with changes in R2 assumed negligible) are found (Figs. 4 - 2, 4 - 3 and 4 - 4 respectively) which are similar to those found previously with ln K .

It is interesting to note the relationship between Rl and ΔH^o (Fig. 4 - 5) for the various complexes studied. This shows a definite trend throughout, although of course the precise disposition of force fields active in the different solutes may differ. The values of Rl used are those measured at 33.4°C because these are likely to be the most accurate values. The plot confirms the suggestions made in Chapter 3 that the higher the interaction energy the more highly compressed is the aromatic π-system. It can also be seen that values of Rl greater than the distance (3.05 Å) corresponding to molecular contact are possible, even for systems where steric factors should be unimportant. In fact it is evident that before specific molecular interaction can be considered negligible, Rl must be greater than c.a. 3.5 Å. In this case the molecules would be completely separated and the interaction energy would be smaller than obviously possible. However, the corresponding plot of ΔG^o with Rl (Chapter 3) shows that when $\Delta G^o = 0$, Rl is c.a. 3.1 Å which is eminently more reasonable. Moreover, Fig. 3 - 4 shows a reasonable correlation between ln K (ΔG^0) and $q\mu^2$.

In view of this it appears necessary to revert to ΔG^o as the critical parameter reflecting complex strength, even though the choice of ΔH^o would on the whole appear to be more logical. Certainly for the nitroform complexes, the variation of ΔG^o with aromatic polarisability is more regular than that of ΔH^o. Similarly the variation is more systematic when considering any of the solutes with benzene and p-xylene. The main drawback to adopting ΔG^o to indicate complex strength, is that it is temperature dependent and includes an entropy term that is not formally

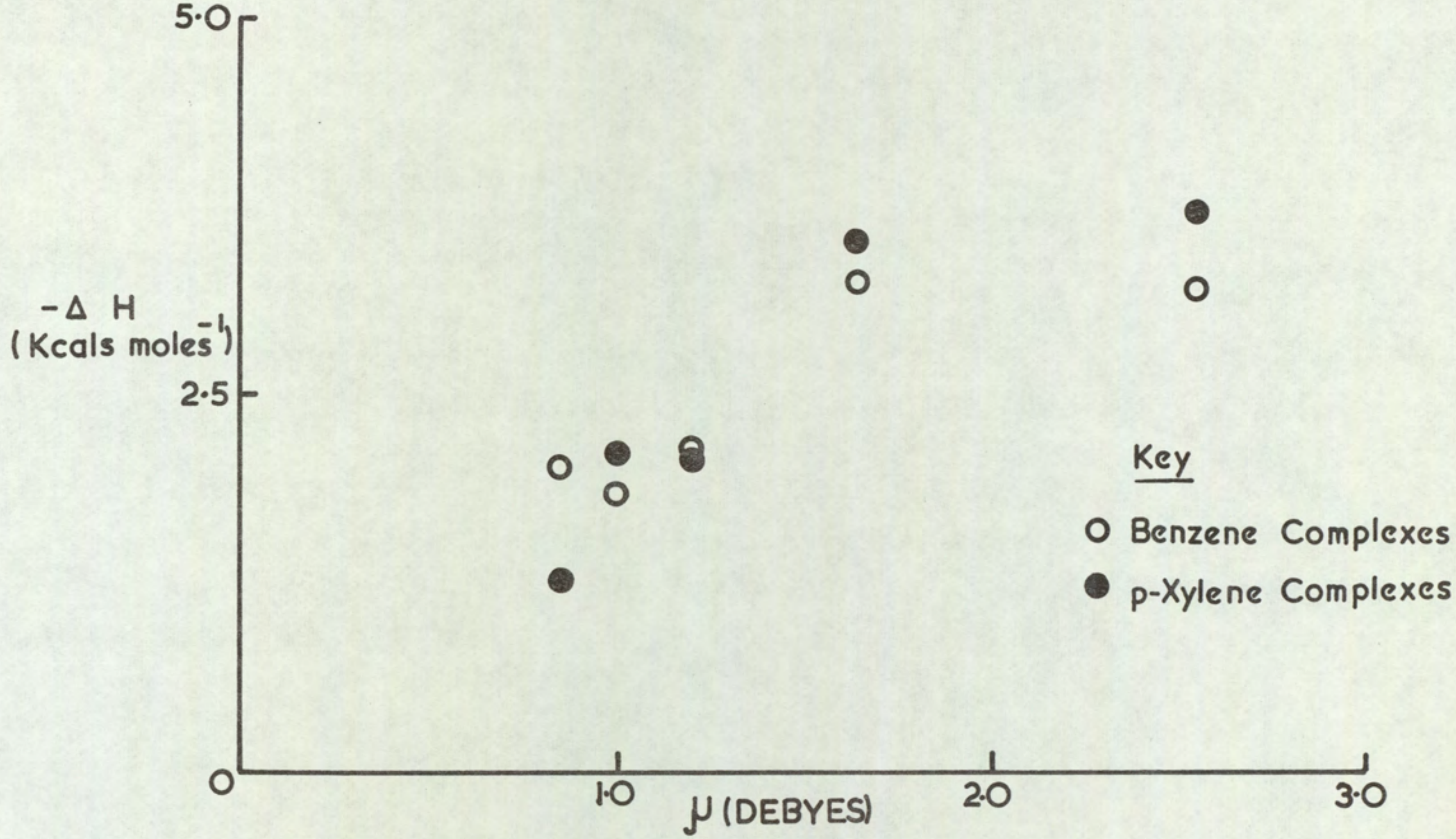

FIG 4-2 THE RELATIONSHIP BETWEEN ENTHALPY OF ASSOCIATION AND SOLUTE SOLUTION DIPOLE MOMENT FOR THE BENZENE AND p-XYLENE COMPLEXES STUDIED

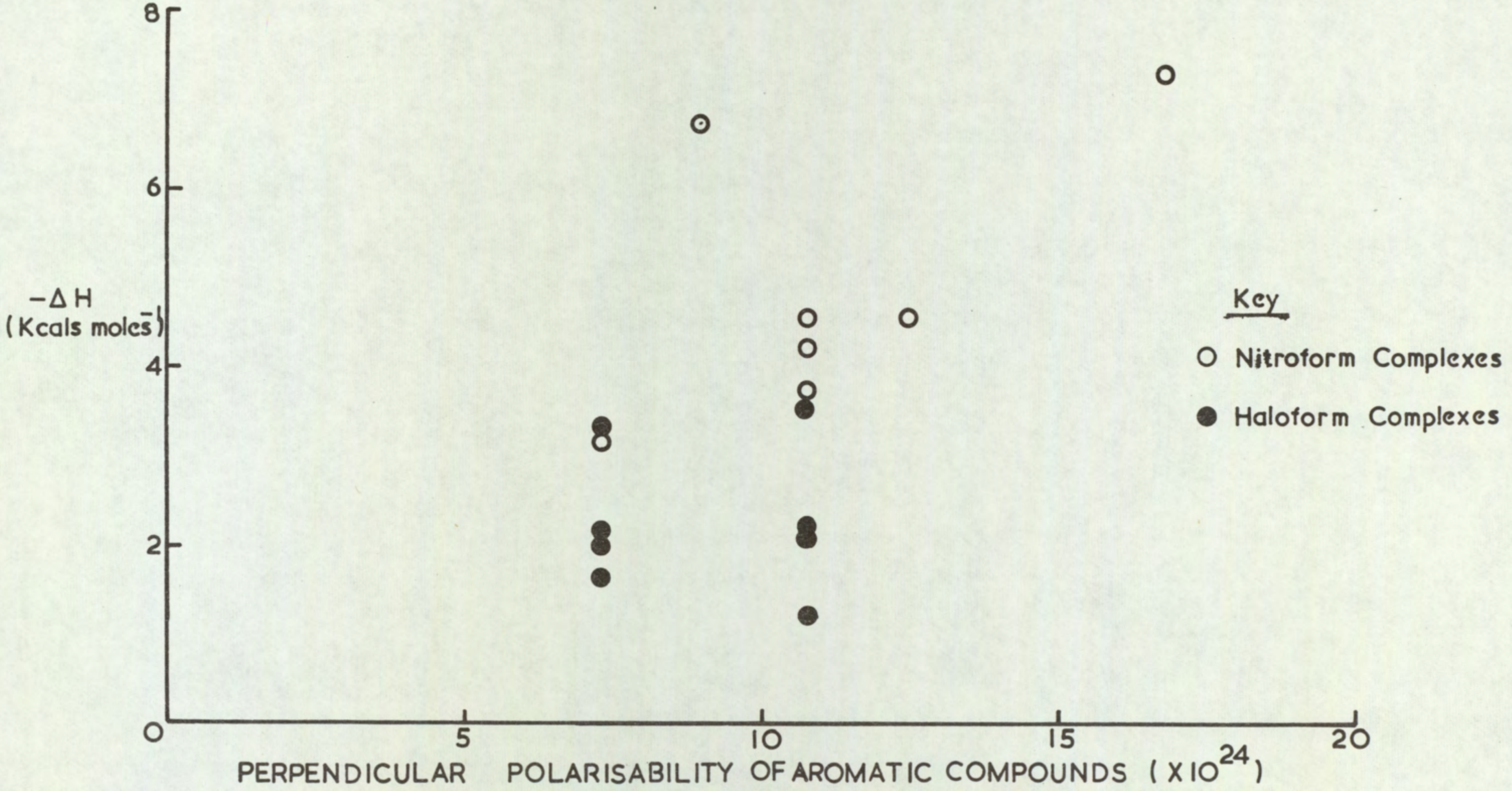

FIG4-3 THE RELATIONSHIP OF PERPENDICULAR POLARISABILITY OF THE AROMATIC SPECIES TO THE ENTHALPY OF INTERACTION OF EACH COMPLEX

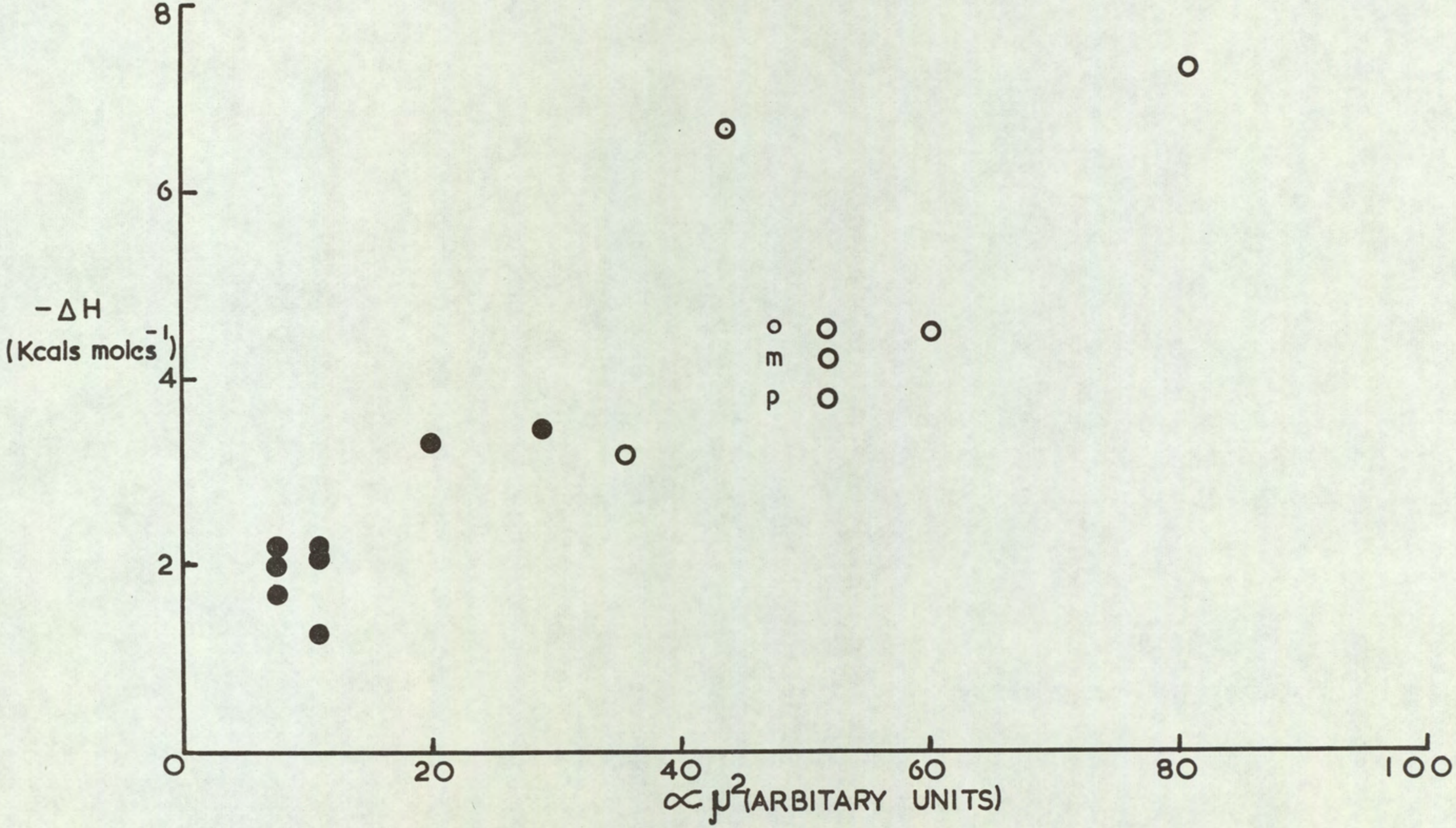

FIG 4- 4 THE RELATIONSHIP OF ENTHALPY OF ASSOCIATION TO $\propto \mu^2$ (THE POLARISATION TERM) FOR THE COMPLEXES STUDIED

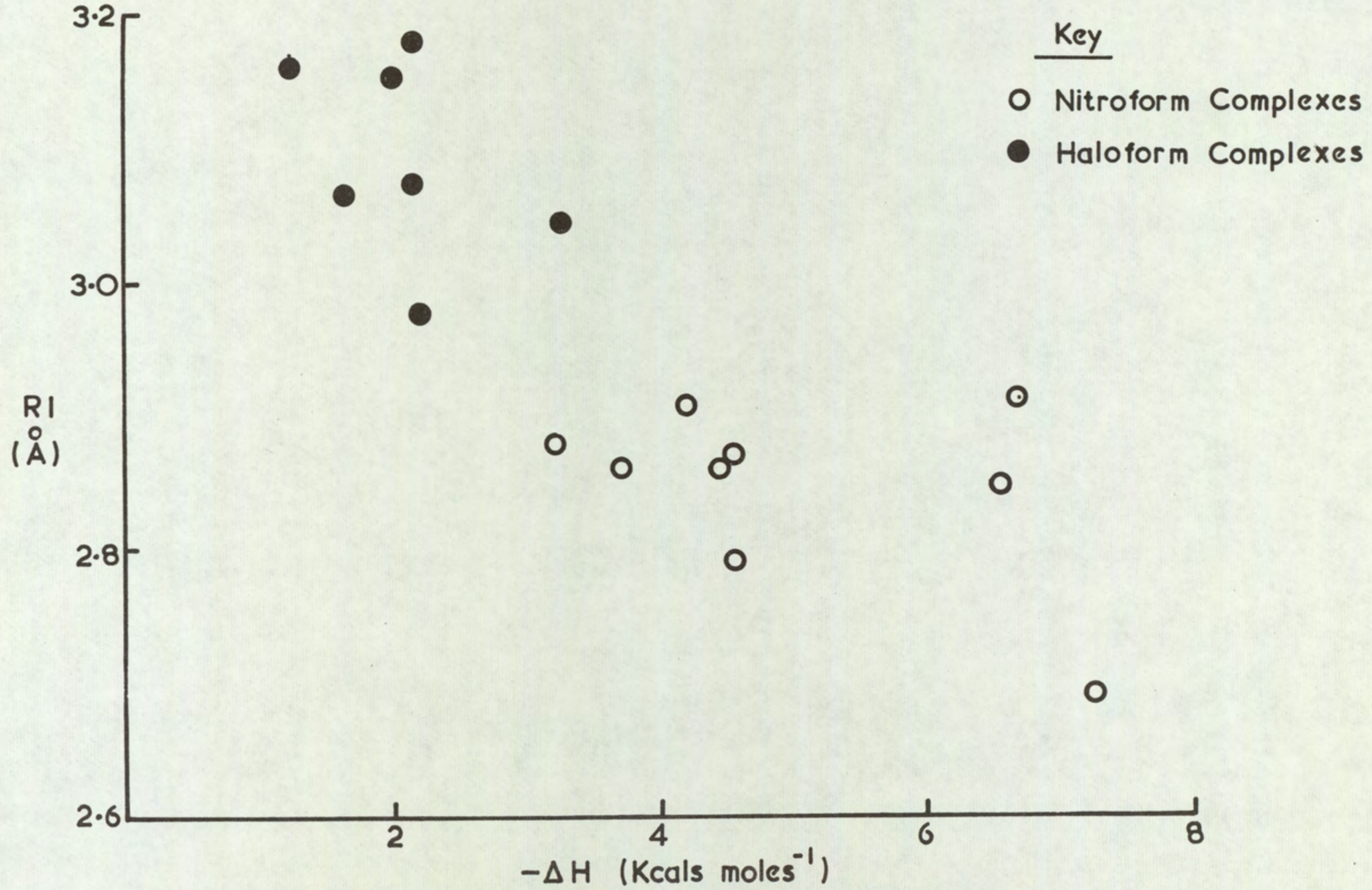

FIG 4-5 THE RELATIONSHIP BETWEEN RI AND ENTHALPY OF ASSOCIATION FOR THE COMPLEXES STUDIED

considered on the simple dipole-induced dipole approach to interaction energy. The apparent anomaly may perhaps be resolved by considering the non-rigid model for the complex. On the basis of this it is possible that the interaction energy can be temperature dependent, because R2 can be varied, with or without R1 being varied. This is possible because the different allowed orientations of solute and solvent will differ energetically and more of these will become adopted as the temperature increases. Even if the solute were fixed in position, and hence R1 remains constant, the time averaged picture of the mobile complex (or of all allowed different structures) to a simple fixed model will result in differing values for R2. As the temperature increases greater deviation from aromatic six-fold axial symmetry will be allowed with the result that the effective value of R2 will decrease and the interaction energy increase. In other words the mean binding energy must change due to the instability caused by wobbling excitation. If this is the correct model, it is not difficult to appreciate why both ΔG^o and ΔH^o can be correlated with the interaction energies as calculated approximately. For the fixed model this (U) is $-q\mu^2/R2^6$ and must be temperature independent, whereas it may be temperature dependent and should be represented by $U + \Delta U$, the latter term accounting for the change in R2. When ΔH^o was correlated with U the assumption was made that changes in R2 were negligible and therefore implicitly that $\Delta U = 0$. So far as correlations with ΔG^o are concerned it is evident that in fact the total interaction energy for all configurations of the mobile model should be used. To a rough approximation this may be equated to $U + \Delta U$, of which the first term is similar to ΔH^o and temperature independent, and the second term to $T\Delta S^o$ (the entropy indicating deviations from the single model) which is temperature dependent.

Consequently, if variations in R2 with temperature for one system, and between different systems, are assumed to be negligible correlations of ΔG^{o} with the simple interaction energy are to be expected.

ΔH^{o}, taken as an indication of bond strength, does not appear to adequately explain all of the experimental data and necessitates a rigid model for the complex with temperature independent interaction energy. On the other hand, ΔG^{o} requires a mobile or time averaging complex for which the interaction energy can be temperature dependent. It appears on the whole that ΔG^{o} may represent, perhaps fortuitously, the complex interaction energy better than ΔH^{o}. Certainly the choice of the former has one principal advantage. This is that it can be used to explain the fact that R1 can have values greater than 3.05 Å. Considerations of ΔH^{o} and the rigid model would indicate, as mentioned earlier, that R1 should be less than or equal to 3.05 Å depending on aromatic π-cloud distortion. Whilst this may in fact be the normal criterion, ΔG^{o} and the mobile model will allow configurations in which the solute symmetry axis departs from the aromatic six-fold axis. If this is so, the solute hydrogen could be lifted from contact with the aromatic, resulting in increased R1 values. Alternatively, the solute hydrogen may remain in contact with the aromatic molecule but move from the six-fold axis. The result on time average will be to relatively deshield the proton so that R1 appears to be larger than 3.05 Å.

4:8 Conclusion

The thermodynamic data resulting from the variable temperature investigations are consistent with the formation of weak molecular complexes. Furthermore, they have been used to investigate, and to some extent substantiate, the dipole-induced dipole explanation proposed for the molecular interaction. In the course of this, it was necessary to propose two models for the complexes. The first of these is such that the solute and solvent are fixed in orientations with the solute symmetry axis coincident with the aromatic six-fold axis. The second model can be considered in two ways. Either the solute and solvent have different allowed orientations which are adopted in different complexes and these are all effectively time averaged, or each complex is non-rigid such that the solute 'wobbles' relative to the solvent in an allowed region. On the whole the second model, which ever way it is conceived, allows better rationalisation of the experimental data. The adoption of this model requires that the aromatic methyl groups, and therefore implicitly the solute, play a significant role in determining the nature of the complexes.

CHAPTER 5

The Determination of the Effective Dipolar Centres of Some of the Solutes Studied

5:1 The General Approach

The evidence presented in Chapters 3 and 4 is consistent with the initial postulate that the type of interaction present in the complexes studied is essentially that of a dipole-induced dipole. This conclusion is further confirmed by the fact that the vast majority of measurements made of the dipole moments of the solutes involved, measured in aromatic solvents, indicate that the observed moment is larger than its value in an inert solvent and this can be attributed, in view of the results reported here, to the presence of solute-aromatic complexes in addition to the uncomplexed solute molecules. While it has been acknowledged that some degree of association does exist (104) no attempt appears to have been made to determine its extent or compensate for it. With the equilibrium constants now available, such a correction can be attempted and a more realistic value of the dipole moment of the complex obtained.

If either of the models for the complex, discussed in Chapter 4, is correct the geometry can be depicted as in Fig. 3 - 1 with the CHX_3 dipole, fixed in one case or on time average in the other, lying symmetrically along the six-fold axis of the aromatic ring, with the hydrogen atom nearest the ring. In this case, the distance along this axis from the centre of the π-electron cloud to the effective centre of the CHX_3 dipole is given by r in

$$\mu_{IND} = \frac{2\mu \nu (\varepsilon + 2)}{3 \varepsilon r^3} \qquad 5 : 1$$

This is the equation of Frank (105) with $\Theta = 0^\circ$ and the distance r which is the inter-dipole distance may be equated to R2 of Fig. 3 - 1, if the assumption is made that the effective centre of the induced dipole remains in the aromatic carbon ring plane. μ_{IND} is the value of the dipole induced in the aromatic molecule, ν is the perpendicular polarisability of the aromatic molecule and μ is taken to be the value of the solute dipole moment in a non interacting solvent (cyclohexane in this case). ε is the dielectric constant of the medium at the temperature in question (usually 25°C). The equation will be considered in greater detail in a later section.

A necessary condition, which has received some justification earlier, is that charge transfer from the aromatic is absent and μ_{IND} arises solely from the localised distortion of the π-cloud and σ-bonding structure and not from a migration of charge involving the solute molecule. The problem to be resolved is the determination of a reliable value for μ_{IND}, particularly as the changes in dipole moment observed are only an order of magnitude greater than experimental error.

5:2 The Basic Method for Determining Dipole Moments

The basic considerations which lead to the determination of dipole moments were laid down by Mosotti, Clausius, and Debye (143) The former, by considering the effect of an applied electric field on a unit charge in a small spherical cavity, derived an expression relating the dielectric constant (ε) to its polarisability (α), its molecular weight (M) and density ρ via a term P called the molar polarisation.

$$P = \frac{\varepsilon - 1}{\varepsilon + 2} \cdot \frac{M}{\rho} = \frac{4}{3} \pi N \alpha \qquad 5 : 2$$

where N is Avogadro's number. This relationship applies to non-polar molecules, and for such cases Maxwell derived the relationship

$$\varepsilon = n_{\infty}^{2} \qquad 5 : 3$$

where n_{∞} is the refractive index for radiation of long wavelength.

For some solute molecules the molar polarisation is found to be temperature dependent, and these no longer obey the Mossotti-Clausius equation, nor the Maxwell relationship. Debye showed that this is because these solutes possess permanent electric dipole moments. To account for this he reformulated the total molar polarisation of a molecule possessing a permanent moment μ_e as

$$P = \frac{\varepsilon - 1}{\varepsilon + 2} \cdot \frac{M}{\rho} \cdot = \frac{4}{3}\pi N + \frac{4\pi N}{3} \frac{\mu_e^{2}}{3kT} = P_d + P_o \qquad 5 : 4$$

The total polarisation is thus the sum of the distortion polarisation P_d, composed of electronic P_E and atomic contributions P_A, and the orientation polarisation P_o. When measurements are made with visible radiation the oscillations are so rapid that only distortions of the electrons (P_E) can be detected by influencing the refractive index, whereas with infra-red radiation the nuclei are also affected and $P_E + P_A$ can be obtained. In neither case can the molecular permanent electric dipole orient itself with the electric field, and so no information concerning P_o is forthcoming. However, dielectric constants are measured by employing an oscillating electric field of typical frequency 1 MHz. In this case the period of oscillation is greater than the relaxation time of the polar molecule and hence information is obtained that allows P_o to be determined and so finally μ_e from

$$\mu_e = \left(\frac{9kTP_o}{4\pi N}\right)^{\frac{1}{2}} \qquad 5 : 5$$

To determine dipole moments, several methods are available, but the one of concern here is the method used for dilute solution of polar solutes in a non-polar medium. In such a solution, the total polarisation is the sum of the polarisation contributions of the constituents.

$$P_{1,2} = x_1 P_1 + x_2 P_2 = \frac{\varepsilon - 1}{\varepsilon + 2} . \frac{x_1 M_1 + x_2 M_2}{\rho} \qquad 5 : 6$$

where x_1 and x_2 are the mole fractions of the solvent and solute respectively. P_1 and $P_{1,2}$ can be evaluated by measurement of the dielectric constant and density of the pure solvent and dilute solution respectively, and hence a value for P_2, the total polarisation of the solute is obtainable. A series of measurements are extrapolated to infinite dilution of the solute to obtain a value free from solute-solute interaction effects. The measurement of the refractive index with the Na_D line yields the electron polarisation and after a correction for atomic polarisation usually by assuming $P_A \simeq 0.05.P_E$, a value for P_o the orientation polarisation can be obtained which leads to a value for μ_e by substitution in equation 5 : 5 which is more usually expressed as

$$\mu_e = 0.01281\sqrt{P_o T} \qquad 5 : 7$$

5:3 A Method for Estimating the Inter-Dipole Distances in the Complexes Examined.

For some of the solute-aromatic systems examined extensive dipole moment measurements have been made. However, for any one system the values reported cover a wide range. After critical examination of the data the values quoted in Table 5-1 are considered most reasonable and will be used hereafter. These all refer to infinite dilution of the solute in the chosen solvent. Because of this it is necessary to decide on a physical interpretation of the solution composition under these conditions, i.e. whether the solute is free or bound in complex.

Other workers have suggested (138) that at infinite dilution the solute is fully complexed. This seems unlikely because this interpretation would imply that the solute cannot undergo exchange with different aromatic molecules and that it would be associated with only one aromatic molecule with no free time of exchange. If it is assumed that the infinite dilution criterion is a specific example of solution composition, which is governed by the general equilibrium expression given in Chapter 3, the equation relevant to the dipole moment measurements is

$$K = \frac{C\,(A + B - C)}{(A - C)\,(B - C)} \qquad 5 : 8$$

with $S = 0$. If, in fact, the solute is considered to be all complexed $A = C$ and $K = \infty$ which is inconsistent with the basic assumption. However, if the fraction of solute complexed is x

$$K = \frac{Ax(A + B - xA)}{(A - xA)\,(B - xA)} \qquad 5 : 9$$

so that at infinite dilution when $B \gg A$

$$K = \frac{x}{1 - x} \qquad 5 : 10$$

Consequently, it would seem reasonable to interpret the infinite dilution situation such that the solute can be considered to be free, with dipole moment μ_{INERT}, and complexed, with moment $\mu_{INERT} + \mu_{IND}$, in the proportion $(1 - x):x$. μ_{IND} is taken to arise solely from the aromatic molecule. The assumption is made that the value of μ_{INERT} in benzene is identical to the value of μ_{INERT} in cyclohexane. Because the polarisabilities of these two solvents are similar this assumption will not introduce appreciable error. The total orientation polarisation of the solute can therefore be regarded as arising from two components in the manner indicated by equation 5 : 6.

$$P_{o,\ TOTAL} = x P_{o,\ COMPLEX} + (1 - x)\, P_{o,\ INERT} \qquad 5 : 11$$

from which may be deduced, via equation 5 : 7 the relationship

$$\mu^2_{AROMATIC} = x\mu^2_{COMPLEX} + (1 - x)\, \mu^2_{INERT} \qquad 5 : 12$$

Hence

$$\mu_{COMPLEX} = \left[\frac{\mu^2_{AROMATIC} - (1 - x)\,\mu^2_{INERT}}{x}\right]^{\frac{1}{2}} \qquad 5 : 13$$

The difference between $\mu_{COMPLEX}$ and μ_{INERT} is taken to be μ_{IND} which can be substituted into equation 5 : 1 to obtain R2.

At this stage equation 5 : 1 must be considered in detail because the physical model adopted for the effect can modify the way the equation is used. Initially, the polar solute of moment μ_{INERT}, can be considered to induce a moment μ_{IND} in a non-polar aromatic of perpendicular polarisability ν, and not to contribute to the dielectric properties of the complex. The induced moment is given classically by

$$\mu_{IND} = \nu . F \qquad 5 : 14$$

where F is the intensity of the electric field acting on the aromatic molecule and is given by

$$F = \frac{\varepsilon + 2}{3} . E \qquad 5 : 15$$

where ε is the medium and hence aromatic dielectric constant. E, the electric field in the dielectric medium, is related to the field E_o arising from the polar solute in vacuo by

$$E = \frac{E_o}{\varepsilon} \qquad 5 : 16$$

For the complex with molecular orientations as proposed earlier

$$E_o = \frac{2 . \mu_{INERT}}{r^3} \qquad 5 : 17$$

for a dipole-induced dipole separation r. Consequently, from equations 5 : 14 to 5 : 17, equation 5 : 1 is obtained i.e.

$$\mu_{\text{IND}} = \frac{2\nu\mu_{\text{INERT}}(\varepsilon + 2)}{3\varepsilon r^3}$$

If, as is desired here, the field due to the polar molecule is considered to arise from a point dipole within the solute it could be argued that the dielectric constant for the medium has contributions from both solute and solvent. In equation 5 : 1, ε should perhaps be replaced, to a first approximation, by the arithmetic mean of the solute and solvent dielectric constants. It should, therefore, be pointed out that this has not been done for the subsequent calculations but the assumption that ε refers to the aromatic alone, as made by Frank and also Walker et.al., has been retained.

It might be argued further, that since R2 - R1 is required ultimately and R1 has been deduced for the complex in the presence of cyclohexane, equation 5 : 1 should be modified accordingly to obtain R2. However, it can then be pointed out that for the model proposed for the complex, even in cyclohexane, the latter is unable to interpose between solute and aromatic and therefore cannot be considered to modify ε or any other parameter in equation 5 : 1. This equation has, therefore, been used simply according to the definition of Frank.

5:4 Application of the Method

By assuming the validity of equation 5 : 8 for two component systems and of the applicability of the equilibrium constants to these (at 25° - Chapter 4), the proportions of the solutes considered in the complex state at infinite dilution in various aromatic solvents, were found. The results for the solvents for which relevant dipole moment data are available are presented in Table 5-2. From these values the solution dipole moments of the complexes were determined and these are also given in Table 5-2. Using the appropriate values for the dielectric constants and perpendicular polarisabilities, which are listed in Tables 3-6 and 3-12 of Chapter 3, values for R2, shown in Table 5-3, were obtained. These, together with the corresponding values of R1, deduced earlier, enabled the positions of the solute point-dipoles to be deduced by reference to the values of R2 - R1 which are given in Table 5-3.

5:5 Discussion

The values of R2 - R1 given in Table 5-3 indicate the distance along the solute symmetry axis, from the centre of the hydrogen atom, at which the molecular point dipole can be considered to be located. It can be seen from Fig. 5 - 1, illustrating the relevant dimensions of the solutes, that for each of these,(144) the position determined for the dipolar origin lies well within the physical confines of the molecule. Furthermore, whilst it is difficult, because of the number of steps and approximations in the approach, to define the accuracy of these values, particularly for chloroform where μ_{IND} is very small for both systems, it is evident that in each case the dipolar origin lies, as to be expected, well towards the more electronegative end of the molecule. In addition, there is a regular trend in the R2 - R1 values which indicates that in the series ($CH(NO_2)_3$, $CHCl_3$, $CHBr_3$, CHI_3) the dipolar centre lies progressively closer to the solute hydrogen atom. This may be a function of the decreasing electronegativity and increasing polarisability of the substituents.

It might have been hoped that the R2 - R1 values for a particular solute with different aromatic solvents, would be very

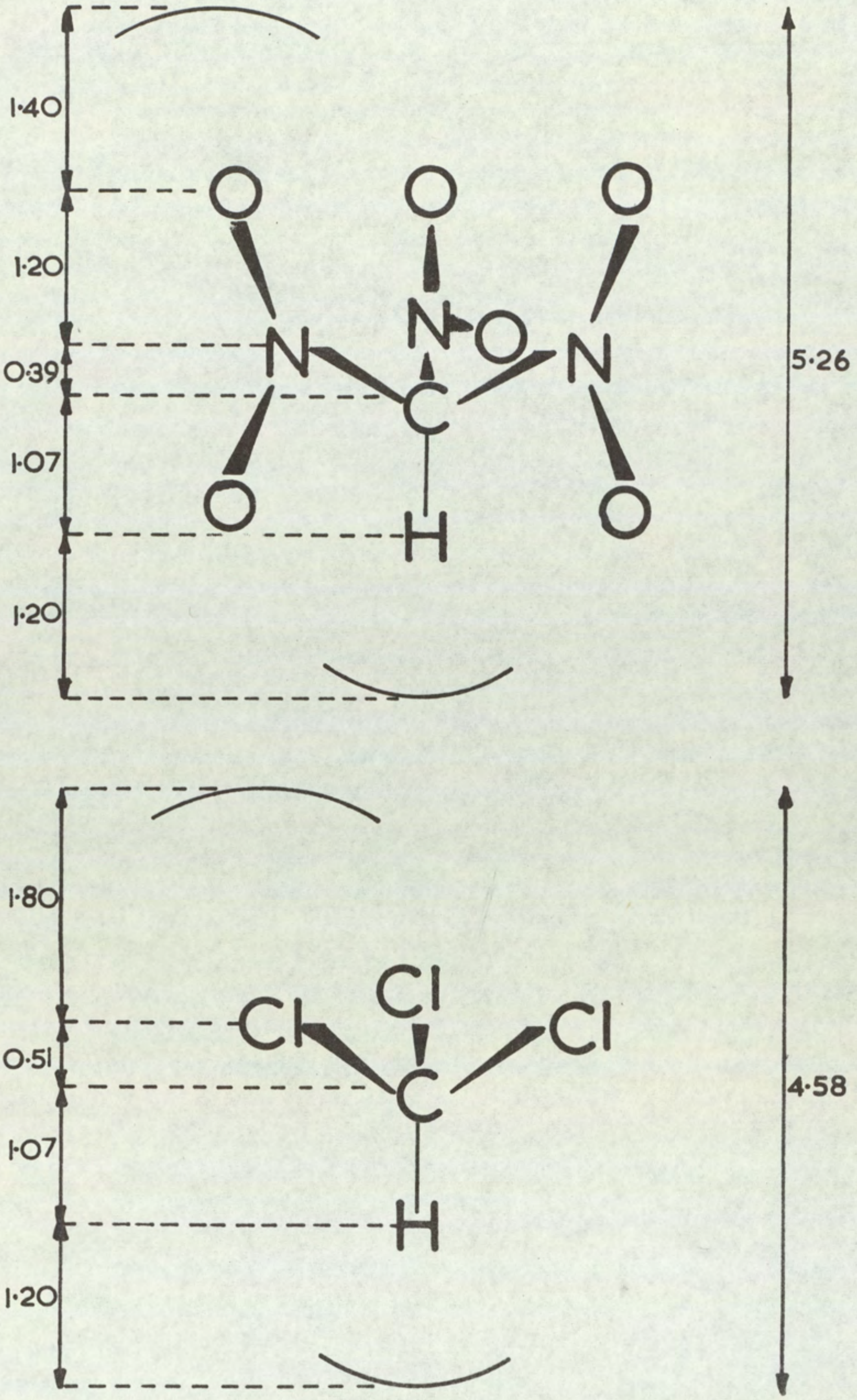

FIG. 5-1. SOME DIMENSIONS OF THE SOLUTES STUDIED. THE DIAGRAMS ARE NOT TO SCALE. ALL DISTANCES ARE IN Å.

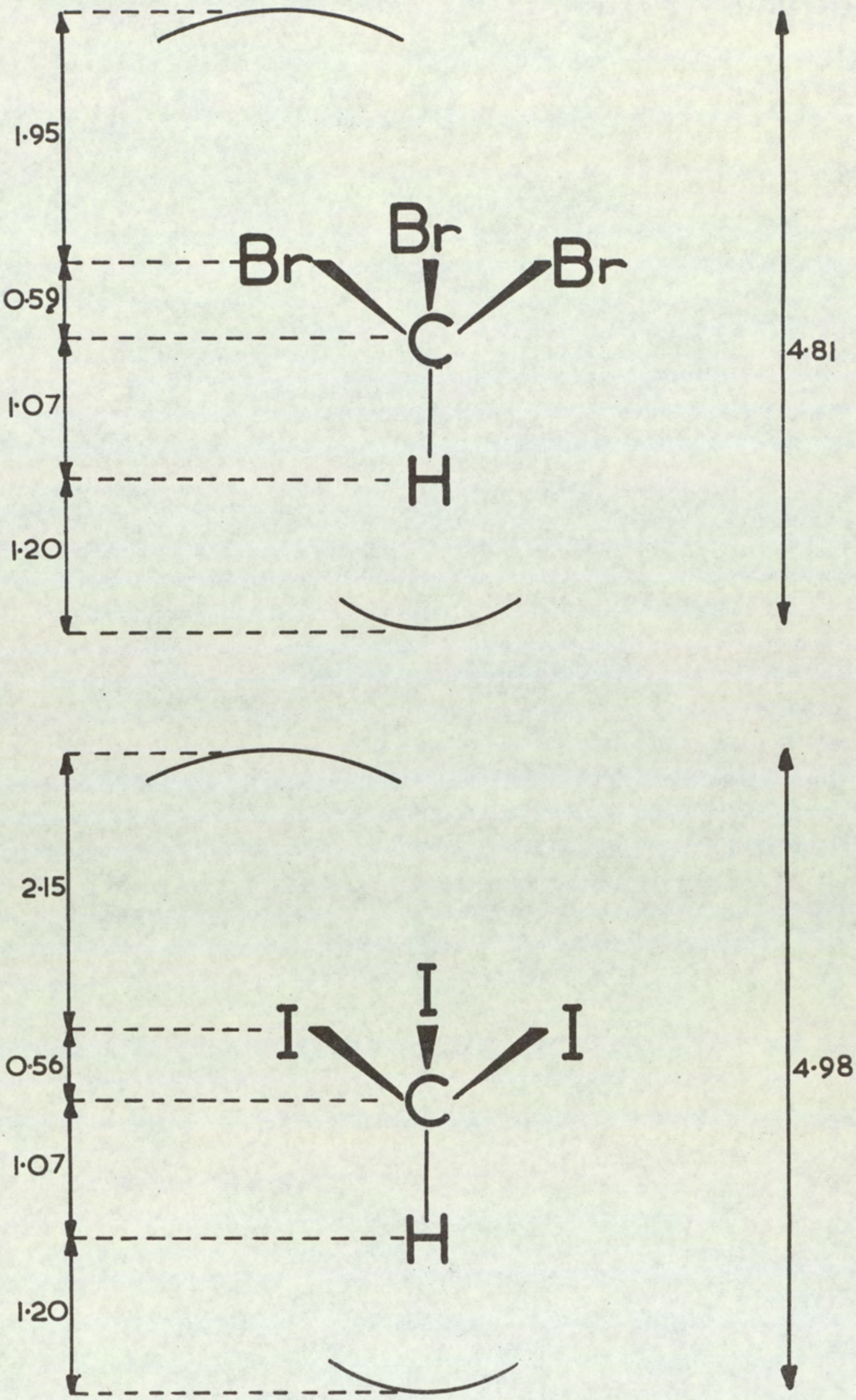

FIG. 5-1 [CONTINUED]

TABLE 5-1. The Solution Dipole Moments of the Solutes. (103)

Solute	Inert Solvent	Benzene	P-Xylene	Mesitylene
Nitroform	2.52_2	2.61	2.73_5	3.00
Chloroform	$1.06/1.19_6$*	1.22	1.25_3	—
Iodoform	0.82_3	0.86_1	0.89_9	—
Bromoform	1.00_4	1.04	1.07_6	—

* These values indicate the limits of the most reasonable range of values.

TABLE 5-2. The Estimated Proportions of the Solutes Present in the Complex State in Aromatic Solvents at 25°C at infinite dilution and the Estimated Values of the Complex Dipole Moments

System	Fraction Solute in Complex (x)	μ_e of Complex (Debye)
Benzene Nitroform	0.91	2.64
P-Xylene Nitroform	0.97	2.74
Mesitylene Nitroform	0.98	3.01
Benzene Chloroform	0.56	1.23
P-Xylene Chloroform	0.68	1.28
Benzene Bromoform	0.56	1.07
P-Xylene Bromoform	0.62	1.12
Benzene Iodoform	0.55	0.89_1
P-Xylene Iodoform	0.57	0.95_2

TABLE 5-3. The Calculated Values of R2 and the Estimated Distances of the Effective Dipolar Centres (Å)

Complex	R2	R2 - R1
Benzene Nitroform	5.82	2.89
P-Xylene Nitroform	5.39	2.53
Mesitylene Nitroform	4.33	1.47
Benzene Chloroform	3.86/6.87 *	0.79/3.80
P-Xylene Chloroform	4.02/5.77 *	0.84/2.59
Benzene Bromoform	5.19	2.13
P-Xylene Bromoform	4.89	1.98
Benzene Iodoform	4.81	1.65
P-Xylene Iodoform	4.42	1.40

* These values correspond to the range of dipole moments referred to in the footnote to Table 5-1.

similar. This would be particularly true if the rigid model discussed in Chapters 3 and 4 were valid. Certainly the values are similar, and any differences may well be attributable to error both in experimentation and theoretical approach. Superficially, nevertheless, the values appear consistently to decrease with increasing aromatic methyl substitution. If this variation is significant it can most readily be explained in terms of the mobile or 'wobbling' model discussed in Chapter 4. For this, motion which allows the greatest deviation from the rigid model will, on time average, result in a situation interpreted on the rigid model basis with the smallest effective value for R2. Consequently the decrease in value of R2 - R1, obtained from the complexes of a particular solute with aromatics progressively substituted with methyl groups, must be attributed to the fact that the X end of CHX_3 must spend increasingly greater times closer to the plane of the aromatic ring because of increasing steric interactions of the methyl group with the solute. This may be explained if the solute contribution to the entropy of a benzene complex is the same or less than that of the methyl benzenes.

5:6 Conclusion

The method for estimating solute dipolar centres presented in this chapter appears to be promising. It is clear that the N.M.R. method involved in this is sufficiently well developed to provide meaningful locations for the solute hydrogen above a simple aromatic molecule. On the other hand, the dipole moment side of the method requires considerably more precise measurements before values for R2 can be determined reliably and before improvements to the theoretical approach to R2 are justified.

The accumulative evidence in this and preceeding chapters indicates that the mobile model is preferable to the rigid model explanation of the structure of the complexes. In the present studies it has been assumed that the solute hydrogen lies on average on the aromatic six-fold axis. Confirmation of the average geometry of a complex can be supplied by determining the screenings (DELTA) for two or more magnetically dissimilar nuclei in a solute. Of those studied here, this is potentially feasible for fluoroform by employing both ^{1}H and ^{19}F measurements. However, a major obstacle arises to the latter type of measurement because of the difficulty of securing a simple fluorocarbon for internal reference purposes that does not itself complex with the aromatic molecule.

APPENDIX A

THE AUTOMOUSE

This device consists of a separate unit mounted on the operating console of the spectrometer and was designed as a plug-in accessory to it. The connecting cables are all screened to ensure freedom for the N.M.R. signals from electrical interference, particularly from the mains supply to the timers. These form the nub of the circuitry (see fig. A1) and were arranged in a closed electrical loop. After initiation, the timers operate indefinitely in sequence, their relays opening and closing the necessary spectrometer circuits.

The complete sequence of events is as follows:-

(a) The spectrometer is switched from normal operation by operating the manual switches S1, S2 (a and b) and S3, in order to place them in the positions indicated in fig. A-1. When closed these switches effectively bye-pass the timers and return the N.M.R. signals to the spectrometer. S2(b) is open for normal operation but during the use of the AUTOMOUSE, switches in a dummy load.

(b) The operation of the timer loop is initiated with timer C1 which operates for a selected period of from 5 to 120 seconds. During this time, the N.M.R. signal, taken from the front-panel sensitivity control, is fed to the integrator via this control using the normal R10 circuitry. The length of time used at this stage determines the final S/N improvement. If the input signal consists only of noise there is little nett accumulation of charge on the integrator condenser whatever the time period used. An N.M.R. signal, however, even if present to a minute extent, over a period of time can emerge above the transient fluctuations of noise.

(c) After the specified time period, the relay in C1 opens and its trigger pulse causes C2 to operate. This switches out the dummy load across the pen recorder unit output and allows the accumulated integrator signal to pass to the pen drive motor which causes the pen to move to a new position corresponding to the integrated signal. The time for this event is about 0.5 seconds after which the pen is again isolated from the recorder and integrator, being replaced by the dummy load, and remaining at the last position on the chart paper.

(d) The trigger pulse from C2 causes the relay of C3 to close for a fraction of a second and this causes the recorder drum to rotate a short distance and simultaneously sweep the field of the spectrometer.

(e) The final step of the sequence is the cancellation of the integral by C4 which is connected across the integral cancel button on the front panel, after which the sequence automatically recommences.

Because the pen is inactivated immediately after it has recorded the integrated signal it traces out on the chart paper the envelope of all the accummulated signals and this is the normal absorption signal. It is necessary initially to detect an inverted absorption signal in order that conventional spectra are presented finally.

An example of the performance of the device when compared with the best spectrum that can be obtained in the normal manner is illustrated in Figs. A2 and A3. The conditions of A.2 were:

R.F. Power	$10^2.5$ µV
R.F. Gain	0.5
Sensitivity	8
Sweep Rate	8 units per minute (≡ 24 Hz/minute)
Time Constant	1.5 second plus 4KHz selective filter
Phase Detector Gain	2

The mouse spectrum conditions were:-

R.F. Power	$10^2 . 6.3$ μV
R.F. Gain	0.5
Sensitivity	2
Sweep Rate	32 units per minute *
Time Constant	0.1 seconds

* This was the normal chart drum speed which only operated once every 30 seconds. The actual nett sweep speed was about 30 second per hertz of swept frequency.

It is interesting to note that, in spite of the higher power level used on the slow integral scan, saturation effects do not appear to be conspicuous.

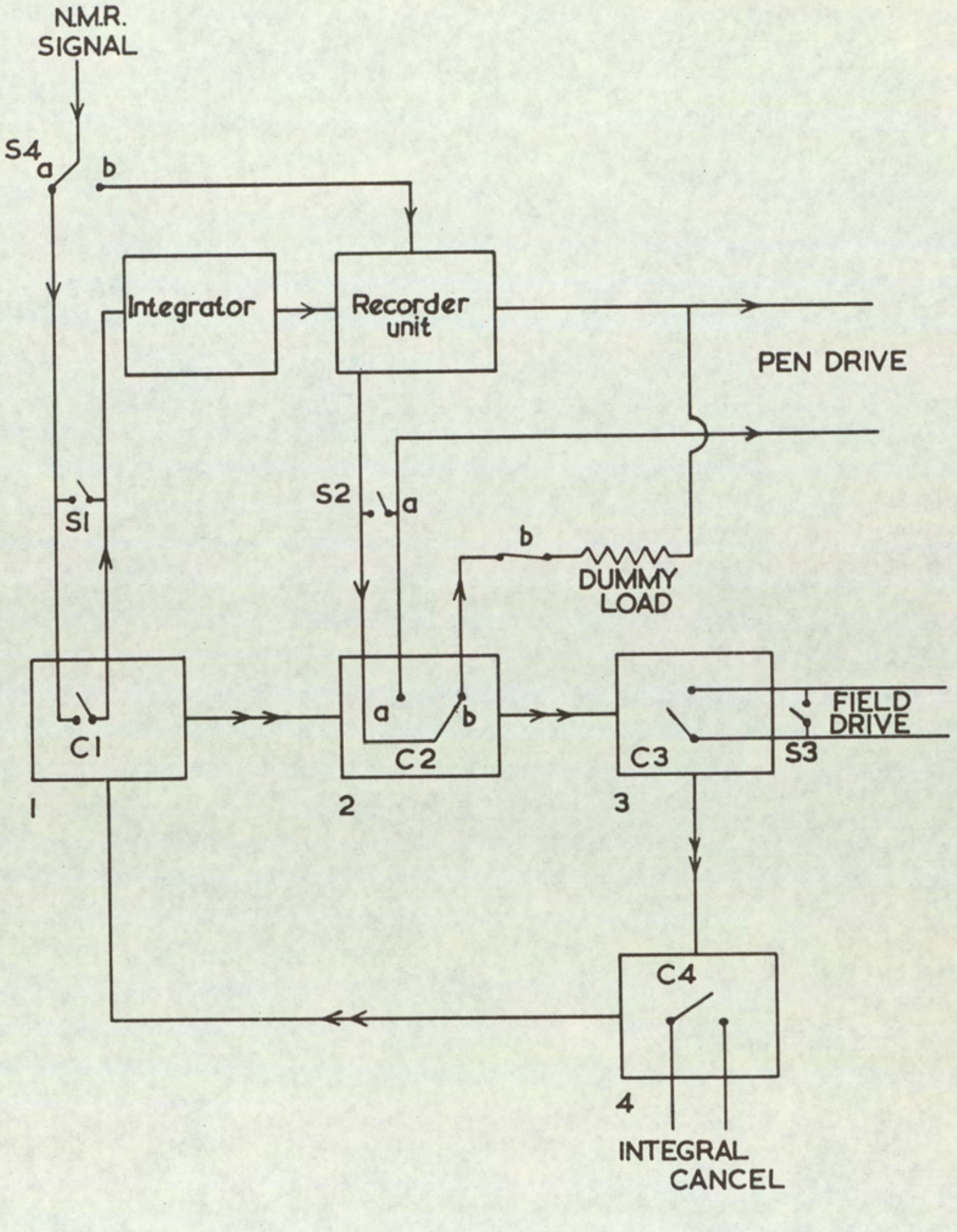

FIG. A.I. BLOCK DIAGRAM OF THE INTEGRAL SWEEP DEVICE (MOUSE)

(→ N.M.R. SIGNAL ↠ TRIGGER PULSE)

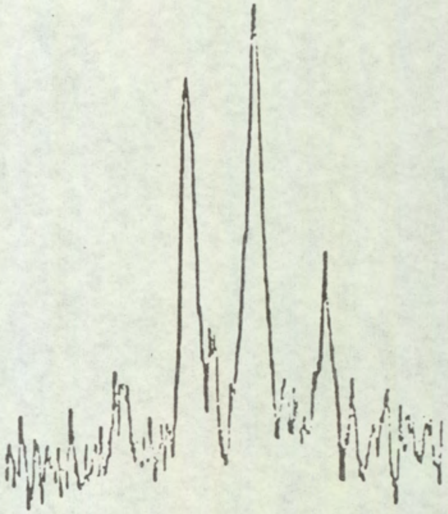

FIG A·2 NORMAL BEST SPECTRUM

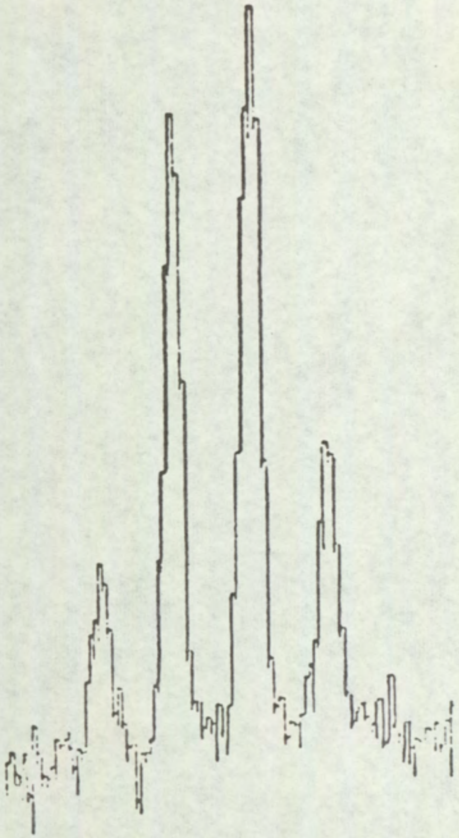

FIG A·3 30 SECONDS MOUSE SPECTRUM

APPENDIX B

A Computer Program for Evaluating Equilibrium Constants from Nuclear Magnetic Resonance Chemical Shift Data

As explained in Chapter 3 the method for equilibrium constant determination developed by Creswell and Allred does not lead directly to an explicit value for K, and an iterative routine for determining both this and DELTA is necessary. For greater accuracy and speed it was necessary to carry out the calculations on a computer. This reduced the time necessary for calculation from about 1 week to 10 minutes and gave an answer that was reliable to a few per cent in most cases.

The program to do this, known as COMPLEXICON is in the Elliott dialect of the programming language Algol 60 and was run on an Elliott 803 computer. The basis of the method is that the limiting values of the range of K the equilibrium constant for the association, within which the true value is thought to lie, is supplied to the computer. This then chooses values for K within the range and calculates values for $[C]_j \ / \ [A]_j$ less than or equal to unity for each sample of the series. The regression line for the plot of $[C]_j \ / \ [A]_j$ upon $\delta_{obs \ j}$ for each K value is calculated by the method of least squares and the sum of the squares of the residual values of $[C]_j \ / \ [A]_j$ upon this line is also calculated. The latter function, known as SUMSQ(K) is minimised by the method of trisection, upon the values of K using an iterative Algol procedure MINX (145). When this error function is at a minimum the current value of K corresponds to that giving the best straight line for equation 3:9. This part of the program was developed in collaboration with Mr. P. D. Groves of this department.

In the computation there is no enforcement of the calculated line through the point ($\delta_{obs\ j} = \delta_{free}$, $[C]_j\ /\ [A]_j = 0$), because of the influence of medium screening effects discussed in Chapter 3.

The input data for the program are as follows:-

(i) An identification reference.

(ii) The number of solutions being studied.

(iii) Experimental values of $[A]_j$, $[B]_j$, $[S]_j$, and $\delta_{obs\ j}$.

(iv) Three numbers identified by UPPER, LOWER and ACCY. The first two of these indicate the upper and lower trial values for K, between which the correct value is anticipated. The third number gives the smallest interval in adjacent values of K between which it is considered necessary to perform the computation MINX. In the event of the best value for K being outside the expected range UPPER to LOWER, errors may arise because

(i) there is no value for $[C]_j\ /\ [A]_j$, less than unity,

(ii) the procedure MINX falsely chooses UPPER or LOWER as the value of K corresponding to the minimum of SUMSQ(K).

The program contains routines for the detection of errors of this sort and will indicate their occurrence by printing an appropriate message on an on-line teleprinter together with a request for new values for the limits UPPER and LOWER. The computer then waits for these to be supplied, whereupon the computation is recommenced.

The output provides the following information:-

(i) The identification reference.

(ii) The input values of $[A]_j$, $[B]_j$ and $[S]_j$, the corresponding values of $[C]_j\ /\ [A]_j$ evaluated from the final K value, and the input values of $\delta_{obs\ j}$; all tabulated in the manner of Tables 3-3 and 3-4.

(iii) The values chosen for UPPER, LOWER and ACCY.

(iv) The selected value of K and the slope ($\delta_{\text{complex}} - \delta_{\text{free}}$ known as DELTA) and intercept (δ_{free} known as DFREE) of the corresponding line representing equation 3 : 9.

(v) The estimated residual variance (s^2) and standard deviation(s) of the final $[C]_j \;/\; [A]_j$ values where

$$S^2 = \frac{n}{n-2} \sum_{j=1}^{n} \left([C]_j \;/\; [A]_j - \overline{[C]_j \;/\; [A]_j} \right)^2 \qquad \text{B : 1}$$

n is the number of samples investigated and $\overline{[C]_j \;/\; [A]_j}$ the least squares value.

As a further check on the consistency of the experimental measurements and to eliminate points grossly in error it is possible, if desired, to use an on-line graph plotter to compare visually the calculated regression line of $[C]_j \;/\; [A]_j$ on $\delta_{\text{obs } j}$ with the corresponding experimental points. The Algol Plotter Package supplied by Elliott Brothers (London) Ltd., is utilised for this purpose. A copy of the program is inserted into the pocket at the rear of this thesis.

REFERENCES

1. W. Pauli: Naturwiss., 12, 741 (1924).

2. I. I. Rabi, S. Millman, P. Kusch, and J. R. Zacharias: Phys. Rev., 55, 526 (1939).

3. O. Stern: Z. Phys., 7, 249 (1921).

3a. W. Gerlach and O. Stern: Ann. Phys. Leipzig: 74, 673 (1924).

4. E. M. Purcell, H. C. Torrey, and R. V. Pound: Phys. Rev., 69, 37 (1946).

5. F. Bloch, W. W. Hansen, and M. E. Packard: Phys. Rev., 69, 127 (1946).

6. E. U. Condon and G. H. Shortley, "Theory of Atomic Spectra", Cambridge University Press, New York, 1953.

7. J. Schwinger: Phys. Rev., 51, 648 (1937).

8. H. S. Gutowsky and D. W. McCall: Phys. Rev., 82, 748 (1951).

9. E. L. Hahn, and O. E. Maxwell: Phys. Rev., 84, 1246 (1951).

10. F. Bloch: Phys. Rev., 105, 1206 (1957).

11. N. Bloembergen: "Nuclear Magnetic Relaxation". W. A. Benjamin, New York, 1961.

12. F. Bloch: Phys. Rev., 70, 460 (1946).

13. R. K. Wangsness and F. Bloch: Phys. Rev., 89, 728 (1953).

14. F. Bloch: Phys. Rev., 102, 104 (1956).

15. G. V. D. Tiers: J. Phys. Chem., 65, 1916 (1961).

16. G. E Pake: J. Chem. Phys., 16, 327 (1948).

17. R. Kubo and K. Tomita: J. Phys. Soc. Japan, 9, 888 (1954).

18. N. Bloembergen, E. M. Purcell, and R. V. Pound: Phys. Rev., 73, 679 (1948).

19. W. A. Anderson: Phys. Rev., 104, 850 (1956).

20. J. T. Arnold, S. S. Dharmatti, and M. E. Packard: J. Chem. Phys., 19, 507 (1951).

21. J. A. Pople, W. G. Schneider, and H. J. Bernstein: "High Resolution

Nuclear Magnetic Resonance". Mc.Graw-Hill Book Company, Inc., New York, New York.

22. G. V. D. Tiers, J. Phys. Chem., 63, 1379 (1959).
23. A. Saika and C. P. Slichter: J. Chem. Phys., 22, 26 (1954).
24. N. F. Ramsey: Phys. Rev., 78, 699 (1950).
25. H. M. McConnell: J. Chem. Phys., 27, 226 (1957).
26. J. A. Pople: Proc. Roy. Soc., A239, 541 (1957).
27. H. M. McConnell: J. Chem. Phys., 41, 3906 (1957).
28. T. P. Das and R. Bersohn: Phys. Rev., 104, 476 (1956).
29. C. P. Slichter, "Principles of Magnetic Resonance", Harper and Row, New York, New York, Pg. 69.
30. B. R. McGarvey: J. Chem. Phys., 27, 68 (1957).
31. M. J. Stephen: Proc. Roy. Soc., A243, 264 (1957).
32. J. Homer and D. Callaghan: J. Chem. Soc., A,439 (1968).
33. J. A. Pople: J. Chem. Phys., 24, 1111 (1956).
34. L. Pauling: J. Chem. Phys., 4, 673 (1936).
35. W. G. Proctor and F. C. Yu: Phys. Rev., 77, 717 (1950).
36. W. C. Dickinson: Phys. Rev., 77, 736 (1950).
37. J. A. Pople: Proc. Roy. Soc., A239, 550 (1957).
38. P. T. Narasimhan and M. T. Rogers: J. Chem. Phys., 31, 1302 (1959).
39. J. Homer and D. Callaghan: J. Chem. Soc., A, 518 (1968).
40. A. D. Buckingham, T. Schaeffer, and W. G. Schneider: J. Chem. Phys., 32, 1227 (1960).
41. P. Laszlo and J. I. Musher: J. Chem. Phys., 41, 3906 (1964).
42. B. B. Howard, B. Linder, and M. T. Emerson: J. Chem. Phys., 36, 485 (1962).
43. A. A. Bothner-By: J. Mol. Spect., 5, 52 (1960).
44. W. G. Proctor, and F. C. Yu: Phys. Rev., 81, 20 (1951).

45. W. E. Quin and R. E. Brown: J. Chem. Phys., <u>21</u>, 1605 (1953).

46. N. F. Ramsey: "Nuclear Moments", Wiley, Inc., New York, 1953.

47. N. F. Ramsey and E. M. Purcell: Phys. Rev., <u>85</u>, 143 (1952).

48. N. F. Ramsey: Phys. Rev., <u>91</u>, 303 (1953).

49. H. M. McConnell: J. Chem. Phys., <u>24</u>, 460 (1956).

50. M. Karplus: J. Chem. Phys., <u>30</u>, 11 (1959).

51. M. Karplus, D. H. Anderson, T. C. Farrar, and H. S. Gutowsky: J. Chem. Phys., <u>27</u>, 597 (1957).

52. H. S. Gutowsky, D. W. McCall, and C. P. Slichter: J. Chem. Phys., <u>21</u>, 279 (1953).

53. H. M. McConnell, and C. H. Holm: J. Chem. Phys., <u>27</u>, 68 (1957).

54. J. I. Kaplan: J. Chem. Phys., <u>28</u>, 278 (1958).

55. M. Takeda, and E. O. Stetskal: J. Amer. Chem. Soc., <u>82</u>, 25 (1960).

56. C. J. Creswell, and A. L. Allred: J. Phys. Chem., <u>66</u>, 1469 (1962).

57. A. L. Bloom, and M. A. Packard: Science, <u>122</u>, 738 (1955).

58. M. E. Rose: Phys. Rev., <u>53</u>, 715 (1938).

59. M. J. E. Golay: Rev. Sci. Instruments, <u>29</u>, 313 (1958).

60. W. A. Anderson: Rev. Sci. Instruments, <u>32</u>, 241 (1961).

61. F. Bloch: Phys. Rev., <u>94</u>, 496 (1954).

62. W. A. Anderson, and J. T. Arnold: Phys. Rev., <u>94</u>, 497 (1954).

63. J. I. Kaplan: J. Chem. Phys., <u>27</u>, 1426 (1957).

64. B. A. Evans, and R. E. Richards: J. Sci. Instruments, <u>37</u>, 353 (1960).

65. A. P. McCann, F. Smith, J. A. S. Smith, and J. D. Thwaites: J. Sci. Instruments, <u>39</u>, 349 (1962).

66. The Handbook of the Perkin-Elmer R10 High Resolution N.M.R. Spectrometer.

67. G. Slomp: Rev. Sci. Instruments, 30, 1024 (1959).

68. H. Primas, and H. H. Günthard: Rev. Sci. Instruments, 28, 510 (1957).

69. M. E. Packard: Rev. Sci. Instruments, 19, 435 (1948).

70. R. B. Williams: I.S.A. Proc., 4, 163 (1958).

71. E. B. Baker, and L. W. Burd: Rev. Sci. Instruments, 28, 313 (1957).

72. H. Primas: 5th European Congress on Molecular Spectroscopy, Amsterdam (1961).

73. R. Freeman, and D. H. Whiffen: Mol. Phys., 1160 (1962).

74. R. Bradford, C. Clay, and E. Strick: Phys. Rev., 84, 157 (1951).

75. B. A. Jacobsohn, and R. K. Wangsness: Phys. Rev., 73, 942 (1948).

76. Varian Associates Staff, "N.M.R. and E.P.R. Spectroscopy", Pergamon Press, Oxford, 1960.

77. L. C. Allen, and L. J. Johnson: J. Amer. Chem. Soc., 85, 2668 (1963).

78. H. Primas, R. Arndt, and R. Ernst: Z. Instr., 68, 55 (1960).

79. M. M. Crutchfield: 4th OCEANS Conference, Pittsburgh, 1963.

80. C. M. Huggins, G. C. Pimentel, and J. N. Shoolery: J. Chem. Phys., 23, 1244 (1955).

81. L. W. Reeves, and W. G. Schneider: Can. J. Chem., 35, 251 (1957).

82. G. J. Korinek, and W. G. Schneider: Can. J. Chem., 35, 1157 (1957).

83. A. A. Bothner-By, and R. E. Glick: J. Chem. Phys., 26, 1651 (1957).

84. A. D. Cohen, and C. Reid: J. Chem. Phys., 25, 790 (1956).

85. T. Schaefer, and W. G. Schneider: J. Chem. Phys., 32, 1218 (1960).

86. J. C. Davis, Jr., and J. S. Pitzer: J. Phys. Chem., 64, 886 (1960).

87. L. Pauling: J. Chem. Phys., 4, 673 (1936).

88. J. I. Musher: J. Chem. Phys., 43, 4081 (1965).

89. G. M. Barrow, and E. A. Yerger: J. Amer. Chem. Soc., 76, 5247 (1954).

90. C. M. Huggins, and G. C. Pimental: J. Chem. Phys., 23, 896 (1955).

91. R. C. Lord, B. Nolin, and H. D. Stidham: J. Amer. Chem. Soc., 77, 1365 (1955).

92. E. Beckman, and O. Faust: Z. physik. Chem., 89, 247 (1914).

93. D. P. Earp, and S. Glasstone: J. Chem. Soc., 1709 (1935).

94. M. J. Copley, G. F. Zellhoefer, and C. S. Marvel: J. Amer. Chem. Soc., 60, 1337 (1938).

95. J. H. Hildrebrand, and R. L. Scott: "Solubilities of Non-Electrolytes", Reinhold, New York, N.Y. 1950.

96. W. Gordy, and S. C. Stanford: J. Chem. Phys., 9, 204 (1941).

97. R. Parshad: Indian J. Phys. 16, 1307 (1942).

98. L. A. K. Staveley, W. I. Tupman, and K. R. Hart: Trans. Faraday Soc., 51, 323 (1955).

99. J. D. Lambert, J. S. Clarke, J. F. Duke, C. L. Hicks, S. D. Lawrence, D. M. Morris, and M. G. T. Shore: Proc. Roy. Soc. (London), 249A, 414 (1959).

100. Z. Pajak: Compt. Rend., 249, 1211 (1959).

101. C. E. Johnson, and F. A. Bovey: J. Chem. Phys., 29, 1012 (1958).

102. J. W. Emsley, J. Feeney, and L. H. Sutcliffe, "High Resolution Nuclear Magnetic Resonance Spectroscopy", Pergamon, Oxford, 1965, vol. 1.

103. A. L. McClellan: "Table of Experimental Dipole Moments". W. H. Freeman & Co., London, 1963.

104. R. P. Young, A. Holt, and S. Walker: Tetrahedron, 20, 2351 (1964).

105. F. C. Frank: Proc. Roy. Soc., A152, 171 (1936).

106. M. J. S. Dewar, and C. C. Thompson: Tetrahedron, Suppl. No. 7, 97 (1966).

107. F. A. Cotton and G. Wilkinson: "Advanced Inorganic Chemistry", Interscience Publishers, Wiley, New York, N.Y., U.S.A. 1962.

108. A. Audsley, and F. R. Goss: J. Chem. Soc., Suppl. Issue No.1 S228 (1949).

109 J. Ronayne and D. H. Williams: Chem. Commun., 20, 712 (1966).

110. R. E. Merrifield and W. D. Phillips: J. Amer. Chem. Soc., 80, 2778 (1958).

111. N. M. D. Brown, R. Foster, and C. A. Fyfe: J. Chem. Soc., B5, 406 (1967).

112. R. W. Taft, S. Ehrenson, I. C. Lewis, and R. E. Glick: J. Amer. Chem. Soc., 81, 5352 (1959).

113. P. L. Corio, and B. P. Dailey: J. Amer. Chem. Soc., 78, 3043 (1956).

114. A. A. Bothner-By and R. E. Glick: J. Amer. Chem. Soc., 78, 1071 (1956).

115. H. Spiesecke, and W. G. Schneider: J. Chem. Phys., 35, 731 (1961).

116. J. Timmermans: "Physico Chemical Constants of Pure Organic Compounds", Elsevier, New York, N.Y. (1950)

117. "Handbook of Chemistry and Physics" The Chemical Rubber Publishing Co., Cleveland, U.S.A., 1966.

118. "Dictionary of Organic Compounds". Eyre and Spottiswoode Ltd. London 1965.

119. United States National Bureau of Standards Circular No. 357.

120. J. S. Waugh, and R. W. Fessenden: J. Amer. Chem. Soc., 79, 846 (1957).

121. M. Tamres: J. Amer. Chem. Soc., 74, 3375 (1952).

122. J. V. Hatton, and W. G. Schneider: Canad. J. Chem., 40, 1285 (1962).

123. H. S. Gutowsky, and A. Saika: J. Chem. Phys., 21, 1688 (1953).

124. C. F. Jumper, M. T. Emerson, and B. B. Howard: J. Chem. Phys., 35, 1911 (1961).

125. A. I. Vogel: Longmans, London 1961.

126. P. D. Groves, P. J. Huck, and J. Homer: Chem. and Ind., 915 (1967).

127. M. J. Stephen: Mol. Phys., 1, 223 (1958).

128. A. D. Buckingham: Canad. J. Chem., 38, 300 (1960).

129. F. London: Z. Phys., 63, 245 (1936).

130. W. G. Schneider: J. Phys. Chem., 66, 2653 (1962).

131. R. J. Abraham: Mol. Phys., 4, 369 (1961).

132. L. Onsager: J. Amer. Chem. Soc., 58, 1486 (1936).

133. P. Diehl and R. Freeman: Mol. Phys., 4, 39 (1961).

134. I. G. Ross and R. A. Sack: Proc. Phys. Soc., B63, 893 (1950).

135. J. Homer: Tetrahedron: 23, 4065 (1967).

136. J. Homer and P. J. Huck: J. Chem. Soc., (A), 277 (1968).

137. A. E. Moelwyn-Hughes: "Physical Chemistry" Pergamon London. 1957.

138. K. M. Baker and B. R. Davis: J. Chem. Soc., B, 261 (1968).

139. C. G. Le Fèvre and R. J. W. Le Fèvre: Rev. Pure and Applied Chem., 5, 261 (1955).

140. J. C. D. Brand, G. Eglinton, and J. Tyrrell: J. Chem. Soc., 5914 (1965).

141. C. J. Cresswell and A. L. Allred: J. Amer. Chem. Soc., 85, 1723 (1963).

142. M. H. Everdell: J. Chem. Ed., 44, 538 (1967).

143. P. Debye: Phys. Z., 13, 97 (1912).

144. "Tables of Interatomic Distances and Configurations of Molecules and Ions". The Chemical Society, London 1958.

145. J. Boothroyd: Computer Bulletin, 9, 104 (1965).

REPRINTED FROM CHEMISTRY AND INDUSTRY, 1966, pp. 1488—1490

A Device for Improving the Signal to Noise Ratio of N.M.R. Spectra

By P. J. Huck and J. Homer

Department of Chemistry, University of Aston in Birmingham, Birmingham, 4

The problem of detecting weak N.M.R. signals has, in recent years, been overcome by two techniques. One improves the signal to noise ratio (S/N) using a computer of average transients[1,2] to sum a number of normal spectra. The alternative method employs slow spectral scan with high gain, suitably low R.F. level to avoid saturation and adequate filter to reduce the response of the detection and presentation systems to spectrometer noise.[3] While providing reliable and improved spectra the additional equipment for the first technique is costly. Use of the second method is often limited because few spectrometers provide suitable gain, filtering and scan facilities and may, therefore, require extensive modification to benefit fully from this technique.

Recently, a third method has been reported[4] which enables noise time-averaging and signal enhancement using equipment which is simple and inexpensive to construct. It is, however, subject to limitations of both theoretical and practical nature. The method involves continuous slow spectral scan during which the spectrometer integrator is repeatedly activated and discharged for fixed time intervals. When the integrator is operative the recorder pen follows the accumulating signal and on cancellation returns to the initial spectrum baseline. Ideally the spectrum is recorded as a series of vertical lines whose envelope corresponds to the S/N improved spectrum. Even though the spectrum may be scanned slowly the successive deflections in practice represent an averaged signal from a finite width of the spectrum. Only by signal accumulation at fixed points in the spectrum and, therefore, necessarily scanning in small steps, can an enhanced signal be accurately produced. From the original idea by Crutchfield,[5] Mayo and Goldstein[6] have developed a device, working on these principles, to enhance the sensitivity of a Varian Associates A-60 spectrometer.

Although not recorded in the open literature it has been known for some time that workers* in the field have made further developments for signal to noise improvement which, though analogous to those previously reported,[4,6] produce spectra of conventional appearance. The principle of the more elegant of these techniques involves successively, integration at a fixed point in the spectrum, reading only the final integrated signal, stepwise scan and integral cancellation; each operation being carried out for an accurately known and constant time.

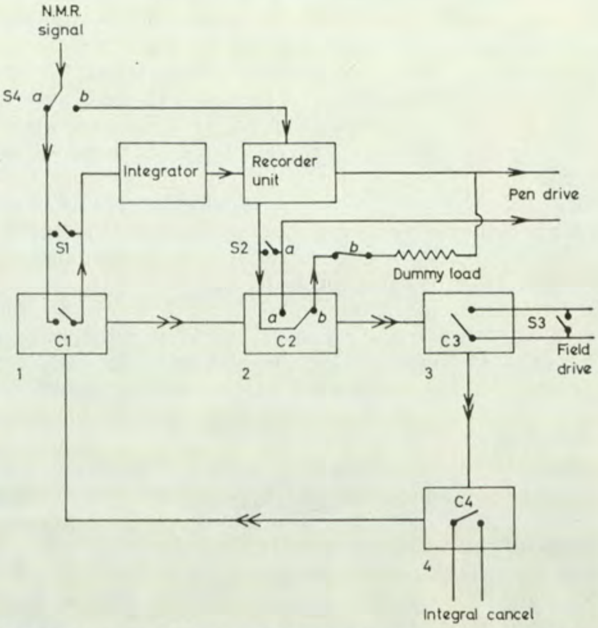

FIG. 1.—*Schematic diagram for stepped-sweep and spectral point integration techniques. Contacts C1, C2, C3 and C4 are shown in their normal positions and switches S1, S2, S3 and S4 set for spectral point integration*

We have modified a Perkin-Elmer R10 60 Mc./sec. instrument to perform repeatedly these operations controlled by commercial timing equipment. The schematic diagram for the system is shown in Fig. 1 and the behaviour of the relays governing the successive basic operations in Fig. 2. The timing equipment (Venner Electronics Ltd, Timing Units Type ETDR with fast reset time of 0·1 sec. and timing accuracy of 2%) is housed in a separate console designed as a plug-in accessory to the spectrometer and connected to it by screened coaxial cables. The complete sequence of operations is (*a*) signal integration on closure of contacts C1 for a time T_1 (5–120 secs.), (*b*) recording the accumulated signal on closure of

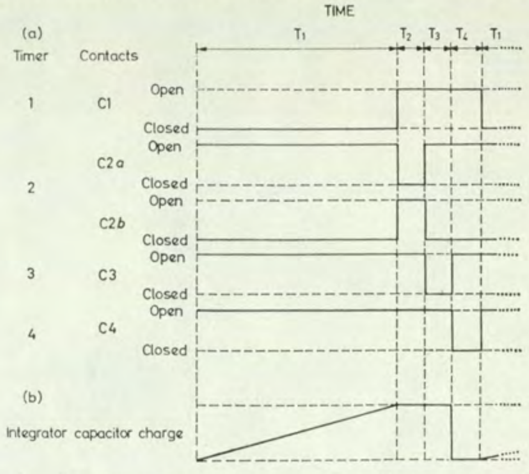

FIG. 2.—(*a*) *Timer contact sequence and* (*b*) *integrator charge variation for the spectral point integration technique*

---

*The authors wish to acknowledge the work of M. M. Crutchfield, A. V. Robertson, W. F. Beach and A. W. Douglas in the development of these techniques. They also thank Professor W. G. S. Parker for the provision of facilities and his interest in this work. One of them (P. J. H.) is grateful to the University of Aston in Birmingham, for a Research Assistantship.

C2a for time T_2 (0·1–3 secs.), (*c*) spectral span on closure of C3 for time T_3 (0·1–10 secs.) at any of the normal spectrometer sweep rates and (*d*) cancellation of the integrated signal by closure of C4 for time T_4 (0·1–3 secs.). Immediately after recording the signal, C2*b* closes and replaces the pen drive circuit by a dummy load across the recorder-amplifier output and so maintains the pen at a point on the chart corresponding to the previous integrated signal. The inclusion of switches S1, S2 (*a* and *b* ganged) and S3 (Fig. 1) provides separate control over the integration, reading and scanning operations and, thereby, increases the versatility of the device. For example, with all three switches closed (S2*b* open) the spectrometer may be used either conventionally with the timers inoperative or, when operative, in a manner analogous to that described previously.[4]

In normal spectrometer mode (integrator off, S4*b* closed) with S2*a* and S3 open, the timing system may be used to simulate the slow sweep necessary for heavily filtered spectra; T_1 is chosen to allow the appropriate reduction in sweep rate and enable complete response of the pen (C2*a* closed) to the heavily filtered signal. To record spectra of conventional appearance and improved S/N by integration the spectrometer is adjusted for normal operation and the phase of the detection system changed by 180°. This is also necessary for the recently reported method.[4] S1, S2*a* and S3 are then opened and the timing loop initiated with the required times T_1–T_4. Accurate phasing for the absorption mode is necessary as is thermal stability of both integrator d.c. amplifier and sample. While the phase detector pedestal voltage need not be accurately backed off (Y-axis set zero control) the d.c. amplifier feedback must be optimised to produce a flat baseline.

A typical "best" normal spectrum of the methylene proton resonance of ethylbenzene, 1% v/v in carbon tetrachloride, is shown in Fig. 3*a*. Fig. 3*b* illustrates the same resonance under purposefully noisy conditions. The S/N can be increased from that in Fig. 3*b* either by the use of reduced filter bandwidth and sweep rate or by the point integration technique. By using the former method the S/N improvement (F) is a function of the square root of the factor by which the bandwidth is reduced. The sweep rate must also be reduced to the same extent to maintain the signal distortion parameter[3] at the previous optimum low value. For the latter technique F is proportional to the square root of the point integration time providing saturation effects are avoided. Fig. 3*c* illustrates a S/N improvement relative to Fig. 3*b* using reduced bandwidth and sweep rate. By using the timing system to simulate even slower sweep rates higher F values may be obtained if suitable bandwidths are available. Fig. 3*d* shows the improvement over Fig. 3*b* of a point integration spectrum with a relatively short point integration time. Fig. 3*e* illustrates the benefit of longer point integration times and gives some indication of the improvement possible over Fig. 3*a*.

While both point integration and reduced-bandwidth slow-sweep methods give S/N improvements consistent with those expected an important advantage of the former is that it requires only minor

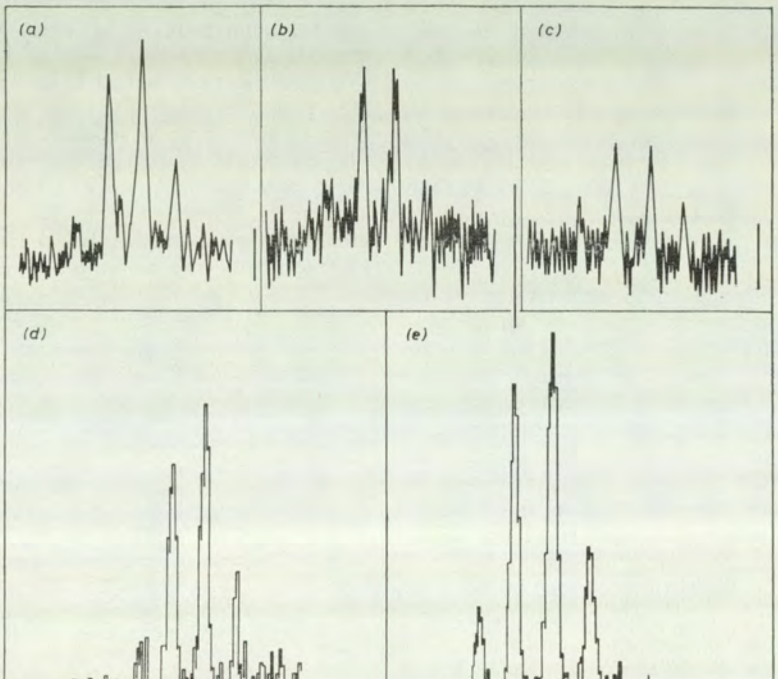

FIG. 3.—60·004 Mc/sec. *methylene proton resonance spectra of* 1% v/v *ethylbenzene in* CCl_4. *The vertical lines following spectra* (*a*), (*b*) *and* (*c*) *are associated noise samples*

modifications to the spectrometer whereas for the latter they may be extensive. One further practical advantage of the former method has been found empirically. This is that R.F. level and possible associated saturation effects appear to influence the production of good S/N spectra by the point integration method less critically than by the reduced-bandwidth slow-sweep method. Further study of the significance of this is in progress.

References

[1] Jardetzky, O., Wade, N. G. & Fischer, J., *Nature, Lond.*, 1963, **197,** 183
[2] Allen, L. C. & Johnson, L. F., *J. Am. Chem. Soc.*, 1963, **85,** 2668
[3] Primas, H., Arndt, R. & Ernst, R., *Z. Instr.*, 1960, **68,** 55
[4] Brown, S. E., Maguire, D. A. & Perrin, D. D., *Chem. & Ind.*, 1965, 1974
[5] Crutchfield, M. M., reported at 4th OCEANS Conference, Pittsburgh, 2 February, 1963
[6] Mayo, R. E. & Goldstein, J. H., *Rev. Sci. Instr.*, 1964, **35,** 1231

PRINTED BY RICHARD MADLEY LTD., 54 GRAFTON WAY, LONDON, W.1, ENGLAND

REPRINTED FROM CHEMISTRY AND INDUSTRY, 1967, pp. 915—917

A Computer Programme for Evaluating Equilibrium Constants from Nuclear Magnetic Resonance Chemical Shift Data

By P. D. Groves, P. J. Huck and J. Homer

Department of Chemistry, The University of Aston in Birmingham, Gosta Green, Birmingham 4

Studies of association resulting in the formation of 1:1 molecular complexes in solution, may be performed readily by spectroscopic methods. A particularly powerful technique for investigations in this field is nuclear magnetic resonance spectroscopy. A prerequisite for the successful implementation of the technique for this specific purpose is that some spectral parameter of one of the reactant species should be modified as a direct result of complex formation. Creswell and Allred[1] have shown that chemical shifts can conveniently provide adequate information for studies of this kind.

The formation of a 1:1 molecular complex (A...B) from two compounds A and B which are precluded from normal chemical reaction may be represented by

$$A + B \rightleftharpoons A\ldots B.$$

Because exchange of A and B between free and complex situations normally occurs more rapidly than the nuclear resonance absorption any nucleus of either A or B will not exhibit discrete resonances characteristic of the two possible magnetic environments but will instead show a single resonance band.[2,3] The observed shift ($\delta_{\mathrm{obs.}}$) of, for example, A is the weighted average of the shifts characteristic of the associated and unassociated molecules, *i.e.*, $\delta_{\mathrm{complex}}$ and δ_{free} respectively, which are normally assumed to be independent of the concentration of A and A ... B within the ranges of concentration studied. The relationship between these parameters is given by

$$\delta_{\mathrm{obs.}} = \frac{[\mathrm{C}]}{[\mathrm{A}]}.\,\delta_{\mathrm{complex}} + \frac{[\mathrm{A}] - [\mathrm{C}]}{[\mathrm{A}]}.\,\delta_{\mathrm{free}} \quad \ldots\ldots \quad \text{(i)}$$

where [A] is the number of moles of A initially present and [C] the number of moles of complex at equilibrium. Because [C] cannot be determined directly the straightforward evaluation of $\delta_{\mathrm{complex}}$ from equation (i) is not possible. If, however, the concentrations of complex present in a series of samples with different initial concentrations of A and B can be found it is evident, by rearranging equation (i) to (ii),

$$\delta_{\mathrm{obs.\,j}} = \frac{[\mathrm{C}]_{\mathrm{j}}}{[\mathrm{A}]_{\mathrm{j}}}\,(\delta_{\mathrm{complex}} - \delta_{\mathrm{free}}) + \delta_{\mathrm{free}} \quad \ldots\ldots\ldots \text{(ii)}$$

that both $\delta_{\mathrm{complex}}$ and δ_{free} can be evaluated from a plot of the observed shift ($\delta_{\mathrm{obs.j}}$) versus $[\mathrm{C}]_{\mathrm{j}}/[\mathrm{A}]_{\mathrm{j}}$. The subscript j refers to the "j*th*" sample. For experimental convenience the studies are best performed on three-component systems in which one component is a non-bonding solvent. To determine the quantity of complex formed in each solution the equilibrium constant K governing its formation is required. K can be defined as

$$\mathrm{K} = \frac{[\mathrm{C}]_{\mathrm{j}}\,([\mathrm{A}]_{\mathrm{j}} + [\mathrm{B}]_{\mathrm{j}} + [\mathrm{S}]_{\mathrm{j}} - [\mathrm{C}]_{\mathrm{j}})}{([\mathrm{A}]_{\mathrm{j}} - [\mathrm{C}]_{\mathrm{j}})\,([\mathrm{B}]_{\mathrm{j}} - [\mathrm{C}]_{\mathrm{j}})} \quad \ldots\ldots\ldots \text{(iii)}$$

the concentration of each species being expressed as a mole fraction. $[\mathrm{A}]_{\mathrm{j}}$, $[\mathrm{B}]_{\mathrm{j}}$ and $[\mathrm{S}]_{\mathrm{j}}$ are respectively the number of moles of A, B and the solvent S initially present and $[\mathrm{C}]_{\mathrm{j}}$ the number of moles of the complex at equilibrium. Even though $[\mathrm{A}]_{\mathrm{j}}$, $[\mathrm{B}]_{\mathrm{j}}$ and $[\mathrm{S}]_{\mathrm{j}}$ are known the value of $[\mathrm{C}]_{\mathrm{j}}$ can only be estimated from an assumed value of K. The normal method of determining $\delta_{\mathrm{complex}}$, and also K, is to plot $\delta_{\mathrm{obs.j}}$ for a series of samples against the corresponding $[\mathrm{C}]_{\mathrm{j}}/[\mathrm{A}]_{\mathrm{j}}$ values estimated from assumed values for K; the resulting plot can only be linear if the correct value for K is chosen. The evaluation of $[\mathrm{C}]_{\mathrm{j}}$ from equation (iii) using an assumed value for K results in two values for each sample because equation (iii) is quadratic in $[\mathrm{C}]_{\mathrm{j}}$. The only physically meaningful values are, however, those for which $0 \leqslant [\mathrm{C}]_{\mathrm{j}}/[\mathrm{A}]_{\mathrm{j}} \leqslant 1$ and consequently, only these values are chosen for appropriate inclusion in the plot of $[\mathrm{C}]_{\mathrm{j}}/[\mathrm{A}]_{\mathrm{j}}$ with $\delta_{\mathrm{obs.j}}$. The benefit of adopting the above procedure is evident from the resulting concurrent evaluation of both $\delta_{\mathrm{complex}}$ and K and furthermore, from the possibility of evaluating ΔS° and ΔH° for complex formation from chemical shift measurements at various temperatures. It can, therefore, prove profitable to undertake the laborious manual computation involved in this procedure and plot the appropriate trial graphs until the best visual fit to a straight line is obtained. However, when many systems are being studied this is both time consuming and tedious. Consequently, we have written a computer programme which enables the rapid evaluation of $\delta_{\mathrm{complex}}$, δ_{free} and K.

The programme, known as COMPLEXICON, is in the Elliott dialect of the programming language Algol 60 and has been run on an Elliott 803 computer. The basis of the method is that the computer is programmed to choose values for K within predetermined limits and calculate the corresponding values of $[\mathrm{C}]_{\mathrm{j}}/[\mathrm{A}]_{\mathrm{j}}$ less than or equal to unity. The regression line for $[\mathrm{C}]_{\mathrm{j}}/[\mathrm{A}]_{\mathrm{j}}$ upon $\delta_{\mathrm{obs.j}}$ for each K value is calculated by the method of least squares and the sum of the squares of the residual values of $[\mathrm{C}]_{\mathrm{j}}/[\mathrm{A}]_{\mathrm{j}}$ upon this line is also calculated. The latter function, known as SUMSQ (K), is minimised by the method of trisection, using an iterative Algol procedure MINX.[4] When this error function is at a minimum the current value of K corresponds to that giving the best straight line for equation (ii).

In the computation the criterion, apparently implicit in equation (ii), that the best straight line should pass through the point ($\delta_{\text{obs.j}} = \delta_{\text{free}}$ $[C]_j/[A]_j=0$), has not been enforced because it has been shown[5] that the intercept of a plot of $\delta_{\text{obs.j}}$ against $[C]_j/[A]_j$ is not necessarily δ_{free}. For some systems the intercept can provide a shift which differs from δ_{free} by a small amount which is constant for a particular system and is due to medium screening effects.

The input data for the programme are as follows:—

(i) An identification reference.

(ii) The number of solutions being studied.

(iii) Experimental values of $[A]_j$, $[B]_j$, $[S]_j$ and $\delta_{\text{obs.j}}$.

(iv) Three numbers identified by UPPER, LOWER and ACCY. The first two of these indicate the upper and lower trial values for K, between which the correct value of K is anticipated. The third number gives the smallest interval in adjacent values of K between which it is considered necessary to perform the computation of MINX. In the event of the best value for K being outside the expected range UPPER to LOWER, errors may arise because

(i) there is no value for $[C]_j/[A]_j$ less than unity,

(ii) the procedure MINX falsely chooses UPPER or LOWER as the value of K corresponding to the minimum of SUMSQ (K).

The programme contains routine for the detection of errors of this sort and will indicate their occurrence by printing an appropriate message on an on-line teleprinter together with a request for new values for the limits UPPER and LOWER. The computer will then wait for these to be input whereupon the computation is recommenced.

The output provides the following information:—

(i) The identification reference.

(ii) The input values of $[A]_j$, $[B]_j$ and $[S]_j$, the corresponding values of $[C]_j/[A]_j$ evaluated from the final K value, and the input values of $\delta_{\text{obs.j}}$.

(iii) The values chosen for UPPER, LOWER and ACCY.

(iv) The selected value of K and the slope (δ_{complex}-δ_{free} known as DELTA) and intercept (δ_{free} known as DFREE) of the corresponding line representing equation (ii).

(v) The estimated residual variance (s^2) and standard deviation (s) of the final $[C]_j/[A]_j$ values where

$$s^2 = \frac{n}{n-2}\sum_{j=1}^{n}\left([C]_j/[A]_j-\overline{[C]_j/[A]_j}\right)^2,$$

```
    £BENZENE CHLOROFORM 33C ? 10                                    (Reader one)
O   5.1768@–4   0.0           5.0605@-2   –339.02
A   5.4868@–4   5.4338@–3     4.9924@–2   –329.36
B   6.4417@–4   1.2349@–2     5.0367@–2   -321.19
C   7.6228@–4   2.3944@–2     5.0299@–2   –312.95
D   8.8291@–4   3.6952@–2     4.9958@–2   –307.28
E   1.0002@–3   4.9869@–2     4.9773@–2   –303.66
F   8.3097@–4   4.9872@–2     3.3046@–2   –299.35
G   8.7537@–4   5.9878@–2     2.5199@–2   –295.51
H   7.1705@–4   5.6955@–2     1.3991@–2   –292.37
J   6.6344@–4   5.9987@–2     6.3544@–3   –289.69

3.0     0.0     0.0001                                              (Reader two)
```

FIG. 1.—*Typical input data. The amounts of each of the species present are expressed in moles and the chemical shifts in c./sec.*

```
COMPLEXICON II
BENZENE CHLOROFORM 33C
                        NUMBERS OF MOLES
 SAMPLE       A             B              S              C/A         DELTA OBS
    1     5.1768@–04    0.0000@+00    5.0605@–02    0.0000@+00     –339.02
    2     5.4868@–04    5.4338@–03    4.9924@–02    1.0058@–01     –329.36
    3     6.4417@–04    1.2349@–02    5.0367@–02    1.8339@–01     –321.19
    4     7.6228@–04    2.3944@–02    5.0299@–02    2.6928@–01     –312.95
    5     8.8291@–04    3.6952@–02    4.9958@–02    3.2729@–01     –307.28
    6     1.0002@–03    4.9869@–02    4.9773@–02    3.6438@–01     –303.66
    7     8.3097@–04    4.9872@–02    3.3046@–02    4.0814@–01     –299.35
    8     8.7537@–04    5.9878@–02    2.5199@–02    4.4670@–01     –295.51
    9     7.1705@–04    5.6955@–02    1.3991@–02    4.7964@–01     –292.37
   10     6.6344@–04    5.9987@–02    6.3544@–03    5.0956@–01     –289.69

ESTIMATED RANGE OF K
UPPER VALUE: 3.000
LOWER VALUE: .0000
ACCY:         .0001

RESULTS
K = 1.1612
DELTA = 97.206C/S.
DFREE = –339.06C/S.
ESTIMATE OF VARIANCE:  .00000
STANDARD DEVIATION:   .00092
```

FIG. 2.—*Typical output data from the punch. The results are also output by the teleprinter.*

n is the number of samples investigated and $\overline{[C]_j/[A]_j}$ the least squares value. As a further check on the consistency of the experimental measurements it is possible, if desired, to use an on-line graph plotter to compare visually the calculated regression line of $[C]_j/[A]_j$ on $\delta_{obs.j}$ with the corresponding experimental points. The Algol Plotter Package supplied by Elliott Brothers (London) Ltd is utilised for this purpose.

Figures 1, 2 and 3 exemplify typical input, output and graph plotter output information. The experimental data for these illustrations were obtained for benzene-chloroform-cyclohexane systems using a Perkin-Elmer R10 spectrometer operating at 60·004 Mc./sec. and 33°C. Chemical shifts were measured relative to cyclohexane using the conventional side-band technique. The modulation signals for this were derived from a Muirhead-Wigan D-890-A oscillator and their frequencies measured with a Venner 3336 counter.

Copies of the programme are available from the authors.

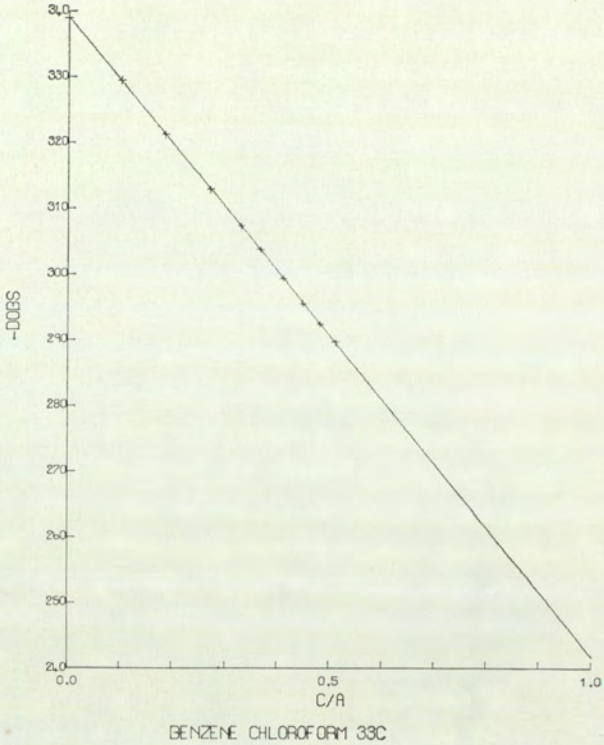

FIG. 3.—*Typical graph plotter output obtained using a California Computer Products Inc. Digital Incremental Plotter model* 565. *The plotted points* X *correspond to the values of* $[C]_j/[A]_j$ *and* $\delta_{obs.}$ *given in* Fig. 2. *The bold line is the best least squares fit to equation* (ii).

References

[1] Creswell, C. J. & Allred, A. L., *J. Phys. Chem.*, 1962, **66,** 1469

[2] Huggins, C. M., Pimentel, G. C. & Shoolery, J. N., *J. chem. Phys.*, 1955, **23,** 1244

[3] Gutowsky, H. S. & Saika, A., *J. chem. Phys.*, 1953, **21,** 1688

[4] Boothroyd, J., *Computer Bulletin*, 1965, **9,** 104

[5] Homer, J. & Huck, P. J., Unpublished results.

PRINTED BY RICHARD MADLEY LTD., 54 GRAFTON WAY, LONDON, W.1, ENGLAND

Molecular Complexes. Part I. Proton Magnetic Resonance Studies of Complexes of Nitroform with Benzene and with Some Methylbenzenes

By **J. Homer** and **P. J. Huck**, Department of Chemistry, The University of Aston in Birmingham, Birmingham 4

Reprinted from

JOURNAL
OF
THE CHEMICAL SOCIETY

SECTION A
Inorganic, Physical, and Theoretical Chemistry

1968

Molecular Complexes. Part I. Proton Magnetic Resonance Studies
Complexes of Nitroform with Benzene and with Some Methylbenzene

By **J. Homer** and **P. J. Huck**, Department of Chemistry, The University of Aston in Birmingham, Birmingha

Equilibrium constants for the formation of complexes of nitroform with benzene and with some methylbenzene determined from the nitroform proton resonance shifts and their dependence on the concentration of the arom in nitroform–aromatic–cyclohexane systems. The difference in proton shielding in the free and complexed n form is determined and used to calculate the separation of the nitroform hydrogen and the plane of the arom ring in each complex. The values obtained compare favourably with those estimated from hydrogen and arom Van der Waals radii.

THE formation and nature of complexes of aromatic compounds with molecules having electric dipole moments have been of interest for some time. Complexes which are relatively easy to study are those formed from haloforms and similar molecules, with mononuclear aromatic compounds. These complexes have been studied by investigating the significant changes which occur in the n.m.r.[1-7] and infrared [7-9] spectra of haloforms and other polar molecules when they are dissolved in aromatic solvents; other techniques have also been used (see ref. 10). In many cases, however, n.m.r. can most profitably be chosen for these investigations because of the relative sensitivity of the analysis and the wealth of information which can be obtained. Although this type of complex formation has been established [11] no attempt has been made to determine accurately any intermolecular distances in the species formed. This Paper reports n.m.r. investigations of the complexes formed between nitroform and benzene and also some methylbenzenes.

It is to be expected that nitroform–aromatic complexes are formed similarly to the well known chloroform–benzene complex.[10,11] However, little information is available regarding the nature of the intermolecular bond in species of this type. In fact because no rigorous description of the precise nature of the bond has b[illegible]tablished it is generally referred to simply as a hydrogen bond. However, Abraham [4] has tentatively suggested that the bond is essentially similar to other hydrogen bonds and that the aromatic π-electrons behave similarly to the unpaired electrons of common donor atoms. In addition to suggesting that the bond is primarily electrostatic in nature, he attributes its lack of stability to the weak ionic character of the C–H bond of the polar species. Significantly, absorptions typical of charge transfer were absent in the u.v. spectra of the complex systems studied by him. He inferred, therefore, that charge transfer was unimportant in the formation of t complexes. The nitroform complexes forming the b of the investigations reported currently do, howe have u.v. absorptions which could be associated v charge transfer. The intensities of the bands in spectra increase with increasing equilibrium const but in no case does the extinction coefficient rise t value generally associated with charge transfer. Beca of this and the fact that Dewar and Thompson [12] h pointed out that even when 'charge-transfer spect are observed they are not necessarily indicative of t charge transfer, this mechanism can be conside insignificant in this type of complex formation. T conclusion may also be the n.m.r. evidence which presented later and shows that, while there can be m fications to the effective location of the arom π-electrons on complex formation, this is an in rather than an inter-molecular process. To provid basis for the subsequent discussion we propose that complex formation the nitroform approaches the matic ring along its six-fold axis and that the elec fields associated with the permanent electric di moment of the former molecule induce an elec moment in the polarisable aromatic molecule to f the basis for the electrostatic bonding between participant species. Justification for this dipole-indu dipole mechanism for complex formation can be infer from the work of Young, Holt, and Walker.[13] In complex, the six aromatic π-electrons remain fir associated with the aromatic molecule but the regior maximum π-electron density may be modified complex formation.

In his treatment of the magnetic screening produ by the circulation of aromatic π-electrons Popl considered the electrons to move in the carbon pl and provide a ring current with an effect equivalent that of a single-point magnetic dipole acting at centre of the ring and perpendicular to it. If t

---

[1] J. E. Anderson, *Tetrahedron Letters*, 1965, 4713.

[2] A. A. Bothner-By and R. E. Glick, *J. Chem. Phys.*, 1957, **26**, 1651.

[3] J. A. Pople, W. G. Schneider, and H. J. Bernstein, 'High Resolution Nuclear Magnetic Resonance,' McGraw-Hill, New York, 1959.

[4] R. J. Abraham, *Mol. Phys.*, 1961, **4**, 369.

[5] J. V. Hatton and R. E. Richards, *Mol. Phys.*, 1960, **3**, 253.

[6] J. V. Hatton and R. E. Richards, *Trans. Faraday Soc.*, 1961, **57**, 28.

[7] J. C. D. Brand, G. Eglinton, and J. Tyrrell, *J. Chem. Soc.*, 1965, 5914.

[8] C. M. Huggins and G. C. Pimentel, *J. Chem. Phys.*, 1 **23**, 896.

[9] M. Tamres, *J. Amer. Chem. Soc.*, 1952, **74**, 3375.

[10] C. J. Creswell and A. L. Allred, *J. Phys. Chem.*, 1962, 1469.

[11] L. W. Reeves and W. G. Schneider, *Canad. J. Ch* 1957, **35**, 251.

[12] M. J. S. Dewar and C. C. Thompson, *Tetrahedron*, Su No. 7, 1966, 97.

[13] R. P. Young, A. Holt, and S. Walker, *Tetrahedron*, 1 **20**, 2351.

[14] J. A. Pople, *J. Chem. Phys.*, 1956, **24**, 1111.

tment is extended to a two-point dipole system, esenting more closely the accepted electronic cture with two regions of high electron density above below the carbon plane, the shielding contribution) to the aromatic protons is given by

$$\sigma_{\text{hor}} = \frac{+\,3e^2a^2\cos^2\theta}{2mc^2(R^2+d^2)^{3/2}} \cdot [3d^2/(R^2+d^2)-1] \quad (1)$$

re R is the distance of the aromatic protons from the re of the ring of radius a, $2d$ is the separation of the dipoles, and $\cos^2\theta = \frac{1}{3}$ is a term allowing for all ible orientations of the aromatic molecule relative to applied field. Waugh and Fessenden [15] adopted an roved approach to the problem and deduced a more rous expression by determining the magnetic field ne proton due to currents in circular wires in terms liptic integrals. In a similar manner, Johnson and ey [16] have shown that by taking the separation of the conducting loops, representing the regions of imum π-electron density, as 0·918 ring radii (*i.e.*, Å) the calculated shifts for a wide range of aromatic ecules are in excellent agreement with the observed es. Using the value $d = 0{\cdot}64$ Å in equation (1) bles the magnitude of the aromatic proton deshield- to be calculated with quite reasonable accuracy and fies the use of this simple equation for subsequent ussions in this Paper.

recent publication [17] gives a comprehensive list of calculated shielding contributions to nuclei at ous orientations relative to benzene due to two rete but equivalent π-electron ring currents in this ecule. Consequently, by determining the additional ding of a proton or protons in a suitable polar ecule due to the formation of a complex with an natic molecule, it should be possible to determine e accurately the position of the proton or protons ive to the aromatic ring. If in the case of nitroform simple model proposed for the association is correct, change in the nitroform proton resonance shift on plex formation should be due primarily to the ectron screening along the aromatic six-fold axis. effect (σ_{vert}) can be formulated simply and isely by

$$_{\text{ert}} = \frac{e^2a^2}{2mc^2} \left\{\frac{1}{[(R_1-d)^2+a^2]^{3/2}} + \frac{1}{[(R_1+d)^2+a^2]^{3/2}}\right\} \quad (2)$$

re R_1 is the distance of the nitroform proton from aromatic ring along the six-fold axis. σ_{vert} Can etermined experimentally as the difference between nitroform proton shifts in the complex (δ_{comp}) and sociated (δ_{free}) situations. Whilst the latter shift be measured directly in a normal non-bonding ent such as cyclohexane the former shift cannot be measured because of the possibility of incomplete complex formation of the nitroform even in the aromatic alone as solvent. To account for equilibrium conditions and obtain meaningful values for δ_{comp} and δ_{free} the procedure proposed by Creswell and Allred [10] involving three-component systems was used in these investigations. This procedure allows a non-bonding solvent to be used as the third component and so benefits the investigation in three ways. First, the solvent can be chosen to act as a suitable internal reference for shift measurements. Secondly, it allows solid dipolar and solid aromatic materials to be examined. Thirdly, it allows the concentration of the polar solute to be maintained at a low and constant value so that the effects of possible self association of the solute can be minimised.

The equilibrium constant based on mole fractions for the association

$$\text{CX}_3\text{H} + \text{Aromatic} \rightleftharpoons \text{CX}_3\text{H}\cdots\text{Aromatic}$$

in an inert solvent is given by

$$K = \frac{[\text{CX}_3\text{H}\cdots\cdots\text{Aromatic}]}{[\text{CX}_3\text{H}]\,[\text{Aromatic}]} = \frac{[\text{C}]_j([\text{S}]_j+[\text{A}]_j+[\text{B}]_j-[\text{C}]_j)}{([\text{A}]_j-[\text{C}]_j)([\text{B}]_j-[\text{C}]_j)} \quad (3)$$

where in any sample j of a system $[\text{A}]_j$, $[\text{B}]_j$, and $[\text{S}]_j$ are the initial numbers of moles of CX_3H, aromatic, and solvent respectively, and $[\text{C}]_j$ is the number of moles of the complex formed at equilibrium. In a sample j the observed CX_3H proton shift is given by

$$\delta_{\text{obs(j)}} = \frac{[\text{C}]_j}{[\text{A}]_j}\,\delta_{\text{comp}} + \frac{[\text{A}]_j-[\text{C}]_j}{[\text{A}]_j}\,\delta_{\text{free}} \quad (4)$$

or alternatively

$$\delta_{\text{obs(j)}} = \frac{[\text{C}]_j}{[\text{A}]_j}(\delta_{\text{comp}}-\delta_{\text{free}}) + \delta_{\text{free}} \quad (5)$$

Consequently, for a series of samples with different initial concentrations of the constituent species the plot of $\delta_{\text{obs(j)}}$ with $[\text{C}]_j/[\text{A}]_j$ will be linear and of gradient σ_{vert}. Because $[\text{C}]_j$ cannot be determined directly, trial values for K are chosen to evaluate $[\text{C}]_j/[\text{A}]_j \geqslant$ zero and $\leqslant 1$ from equation (3) which can then be plotted with $\delta_{\text{obs(j)}}$. Only when the correct value for K is chosen will the plot be linear and represent equation (5). σ_{vert} Can then be obtained and substituted in equation (2) together with appropriate values for d and a to determine R_1.

The proton resonance measurements were made at 60 Mc./sec. and 33·4° using a Perkin-Elmer R10 spectrometer. Chemical shifts were measured relative to the internal reference solvent cyclohexane, using the conventional side-band technique, to an estimated accuracy of ±0·002 p.p.m. The modulation signals were derived from a Muirhead–Wigan D-890-A oscillator and their frequencies determined using a Venner 3336

J. S. Waugh and R. W. Fessenden, *J. Amer. Chem. Soc.*, **79**, 846.

C. E. Johnson and F. A. Bovey, *J. Chem. Phys.*, 1958, **29**,

[17] J. W. Emsley, J. Feeney, and L. H. Sutcliffe, 'High Resolution Nuclear Magnetic Resonance Spectroscopy,' Pergamon, Oxford, 1965, vol. 1.

counter. Each shift was measured six times to minimise random errors and the average taken to represent $\delta_{\text{obs(j)}}$. For each system, ten samples were prepared each containing a constant low mole fraction of nitroform. The concentrations of the aromatic and cyclohexane were chosen to cover as large a nitroform proton-shift range as possible. Nitroform was prepared by the method described by Walker *et al.*[13] and used immediately. High purity cyclohexane was distilled from sodium and stored over the same metal. The other materials were 'AnalaR' where possible and their purities were established by g.l.c. The numbers of moles of each constituent of each sample of a system, together with the appropriate observed nitroform shift, were processed on an Elliott 803 computer using the program COMPLEXICON[18] developed in this Department and the best values for K and σ_{vert} were obtained thereby.

Nitroform was chosen as the polar molecule in these investigations because it possesses a relatively large electric-dipole moment and could, therefore, be expected to have larger equilibrium constants with a particular aromatic molecule than would the more conventional members of the CHX_3 class of compounds such as chloroform or bromoform. Benzene was used initially to test the validity of the theoretical approach but, in order to determine if the basic procedure is more generally applicable, substituted benzenes were also used. Methyl substituents were used exclusively in order to minimise possible complicating intermolecular interactions. A large range of K values was anticipated with the aromatic molecules chosen, and so the systems were expected to provide a stringent test for possible variation in R_1 for different situations. The mole fraction of nitroform was kept low and constant at about 0·01 to minimise the effects of self-association and complicating intermolecular screening contributions which are likely to occur at higher concentrations. The value indicated also represents the lowest concentration at which accurate shift measurements could be made.

TABLE 1

Equilibrium constants and uncorrected σ_{vert} values for complex formation of nitroform with benzene and various methylbenzenes

Aromatic	K	Uncorrected σ_{vert} (p.p.m.)
Benzene	8·46	1·855
Toluene	14·63	1·880
o-Xylene	26·48	1·950
m-Xylene..................	26·09	1·897
p-Xylene	24·12	1·987
Mesitylene	37·88	1·997
Durene	78·11	2·145
Pentamethylbenzene ...	225·25	2·024
Hexamethylbenzene ...	279·40	2·383

Table 1 presents the experimentally determined equilibrium constants and the uncorrected values obtained for σ_{vert}. The equilibrium constants can be seen to increase systematically for the symmetrical aromatic molecules. The σ_{vert} values generally increase increasing methyl substitution but do so somev irregularly. Before these values for σ_{vert} can be stituted in equation (2) to obtain R_1, various correct must be considered. Buckingham, Schaefer, Schneider[19] have attributed to the medium a scree contribution to the solute which can be defined by

$$\sigma_{\text{solvent}} = \sigma_B + \sigma_W + \sigma_A + \sigma_E$$ (

σ_B Is the screening contribution arising from the mec bulk susceptibility, σ_W that due to the Van der Waa dispersion forces between the solute and sol molecules, σ_A that arising from the magnetic anisotı of the medium, and σ_E that produced by the ele field induced in the medium by the polar solute. of these contributions which affect the screening o solute and reference differently must be accountec when determining actual chemical shifts. Becaus internal reference was used for the work now repoı σ_B effects can be discounted.

The dispersion interaction screening constant, arises from time-variant electric dipoles present i molecules which produce electric fields tempor polarising adjacent molecules and thereby altering screening of nuclei in these molecules. Values fo can be deduced using the procedure proposed by How Linder, and Emerson.[20] To calculate the magnituc σ_W in the systems investigated, the reference (c hexane) and nitroform were each considered as solu cyclohexane and in the aromatic. The calcul shielding contributions for each of these solute–sol interactions for the lower methyl-substituted ben systems are given in Table 2 together with other tributions which could be required for addit corrections considered later. Insufficient data available in the literature to calculate the contribu for the higher methyl-substituted benzene systems can be seen from Table 2 that whilst the indivi values cover a significant range the difference bet the calculated screening of the solute and referen the concentration range from almost pure cyclohe to almost pure aromatic never exceeds a 0·002 p.p.m. which is considered to be within ex mental error. Consequently, corrections for σ_W unnecessary.

When considering possible corrections arising the bulk magnetic anisotropy of the molecules for the medium it should be appreciated that whils molecules in the solution should experience the shielding effects and so obviate the necessity anisotropy shielding corrections, it is possible differently shaped solute molecules in the system be affected to different extents. Creswell and All have shown that for quite differently shaped mol the variation in solute–cyclohexane shift is not gı

---

[18] P. D. Groves, P. J. Huck, and J. Homer, *Chem. and Ind.*, 1967, 915.

[19] A. D. Buckingham, T. Schaefer, and W. G. Schneid *Chem. Phys.*, 1960, **32**, 1227.

[20] B. B. Howard, B. Linder, and M. T. Emerson, *J. Chem.* 1962, **36**, 485.

TABLE 2

lculated shielding contributions ($-\sigma_W$) in p.p.m. arising from dispersion interactions in some solute–solvent systems

Solute \ Solvent	Cyclohexane	Benzene	Toluene	*o*-Xylene	*m*-Xylene	*p*-Xylene	Mesitylene
yclohexane	0·120	0·123	0·123	0·126	0·124	0·123	0·128
enzene	0·134	0·138					
oluene	0·113		0·116				
Xylene	0·100			0·106			
-Xylene	0·098				0·101		
Xylene	0·097					0·100	
esitylene	0·089						0·095
itroform	0·102	0·106	0·106	0·109	0·106	0·106	0·109

ı ±0·05 p.p.m. and is linear with benzene contration in benzene–cyclohexane solvent mixtures. thermore, from studies of isobutane, which is similar hape to the haloforms but has a low dipole moment, y show that the anisotropy shielding contributions the protons of haloform-type molecules and cycloane should be similar in aromatic solvents. sequently, corrections for variations in the ent anisotropic shielding of differently shaped ite molecules can be considered unnecessary. Howr, the nitroform hydrogen atom in the complex is in nique position in that in the complex it is effectively ed in the centre of a molecular system rather than he molecular boundary as in the non-bonded state. vill, therefore, experience different anisotropic shields in the two situations. This can be accounted for considering that on complex formation the free oform proton-shift (δ_{free}) is modified by removing total anisotropic effect of the aromatic molecule ut to be bonded in the complex ($\sigma_A{}^T$) and imposing specific anisotropic effect of complex formation $_{\text{rt}}$). Equation (5) must then be reformulated as

$$\sigma_{\text{obs(j)}} = \frac{[C]_j}{[A]_j}\,(\sigma_{\text{vert}} - \sigma_A{}^T) + \delta_{\text{free}} \qquad (7)$$

$_E$ Gives the contribution to the shielding of the polar ite arising from the polarisation of this solute by the tric field induced by it in the medium. The proton ts of cyclohexane and the non-polar aromatics are ffected by this mechanism but the effects on the oform proton at zero concentration in cyclohexane aromatic could be finite and must, therefore, be sidered. If the reaction field contributions to the lding of the solute due to the aromatic and cycloane molecules are both finite and different, the erved shift for each sample must now be represented

$${}_{\text{obs(j)}} = \frac{[C]_j}{[A]_j}\,(\sigma_{\text{vert}} - \sigma_A{}^T) + \delta' \text{ free} + \sigma_E{}^B\left[\frac{[B]_j}{[A]_j + [B]_j + [S]_j - [C]_j}\right] + \sigma_E{}^S\left[\frac{[S]_j}{[A]_j + [B]_j + [S]_j - [C]_j}\right] \qquad (8)$$

ead of either equation (5) or equation (7). The tric-field contributions to the shielding of the nitroform hydrogen due to the aromatic and cyclohexane present are $\sigma_E{}^B$ and $\sigma_E{}^S$, respectively; δ'_{free} is the true shift of the free nitroform. Because the dipole moment induced in the aromatics on complex formation is generally small [13] contributions to the screening of the nitroform proton due to specific electric-field effects in the complex should be small and no account is taken of these.

A procedure for calculating σ_E for spherical molecules has been proposed by Buckingham,[21] and for non-spherical molecules by Diehl and Freeman.[22] It has been shown recently [23] that in order to predict the differences in shielding in a particular solute due to the reaction fields set up in different solvents, it is adequate to consider the solute as spherical. The values of σ_E, for nitroform with cyclohexane and the aromatics studied, computed using the approach of Buckingham, are listed in Table 3. From these values it can be seen that $\sigma_E{}^B$ and $\sigma_E{}^S$ do not appear to differ significantly and so, because the sums of the mole fractions of B and S are always constant and approximately unity, equation (8) will not deviate significantly from a linear function. Consequently, a plot of $\delta_{\text{obs(j)}}$ versus $[C]_j/[A]_j$ provides a line which has a slope that can be equated to $(\sigma_{\text{vert}} - \sigma_A{}^T)'$ and gives an approximate value for $(\sigma_{\text{vert}} - \sigma_A{}^T)$ that differs from the correct value by $\sigma_E{}^B - \sigma_E{}^S$. It can be seen from Table 3 that for the systems studied $\sigma_E{}^B - \sigma_E{}^S$

TABLE 3

Some reaction field and molecular magnetic anisotropic contributions to the screening of nitroform

Solvent	$-\sigma_E$ (p.p.m.)	$\sigma_A{}^T$ (p.p.m.)
Cyclohexane	0·061	
Benzene	0·071	0·048
Toluene	0·075	0·044
o-Xylene	0·080	0·040
m-Xylene	0·074	0·040
p-Xylene	0·071	0·040
Mesitylene	0·071	0·036
Durene	*	0·032
Pentamethylbenzene	*	0·028
Hexamethylbenzene	*	0·024

* Insufficient data in the literature precluded the calculation of these values.

---

[21] A. D. Buckingham, *Canad. J. Chem.*, 1960, **38**, 300.

[22] P. Diehl and R. Freeman, *Mol. Phys.*, 1961, **4**, 39.

[23] J. Homer, *Tetrahedron*, 1967, **23**, 4065.

does not exceed 0·02 p.p.m. A corrected value for $\sigma_{\text{vert}} - \sigma_A{}^T$ can be obtained using

$$\sigma_{\text{vert}} - \sigma_A{}^T = (\sigma_{\text{vert}} - \sigma_A{}^T)' - (\sigma_E{}^B - \sigma_E{}^S) \qquad (9)$$

and $\sigma_A{}^T$ can be estimated using the equation

$$\sigma_A{}^T = 10^{30}\,\frac{e^2a^2}{mc^2}\,\frac{r-h}{(r+2h)\,(r^2+h^2)^{3/2}} \qquad (10)$$

which was deduced by Abraham.[4] For this equation the aromatic molecule is considered to be a cylinder of radius r and height $2h$ with an equivalent dipole due to the anisotropy of the molecular magnetic susceptibility acting along the cylinder axis. r and h Represent contact separations for the nitroform hydrogen moving over the benzene molecule and consequently must include the Van der Waals radius of the proton and the appropriate dimensions of the aromatic ring. For benzene the calculated value for $\sigma_A{}^T$ is $+0{\cdot}048$ p.p.m. and for hexamethylbenzene $\sigma_A{}^T$ is calculated as $+0{\cdot}024$ p.p.m. by taking into account the shape and position of the methyl groups. The anisotropic shielding contribution for intermediate methylbenzenes such as mesitylene is taken as the weighted average of the values obtained for benzene and hexamethylbenzene depending on the number of methyl group substituents. The values obtained in this way are given in Table 3. Each of the values for $\sigma_{\text{vert}} - \sigma_A{}^T$ determined using equation (9) can be corrected for anisotropy effects using the appropriate values for $\sigma_A{}^T$ to obtain the final corrected values for σ_{vert} which are listed in Table 5.

TABLE 4

Values of $\delta^A{}_{\text{obs}}$ and $\delta^A{}_{\text{free}}$ (p.p.m. relative to cyclohexane) and estimates of π-cloud deformation in some nitroform-aromatic complexes

Aromatic	$\delta^A{}_{\text{obs}}$	$\delta^A{}_{\text{free}}$	π-Cloud deformation (contribution to d in Å)
Benzene	−5·786	−5·776	$-0{\cdot}08_7$
Toluene	−5·635	−5·621	$-0{\cdot}10_2$
o-Xylene	−5·546	−5·525	$-0{\cdot}09_9$
p-Xylene	−5·508	−5·485	$-0{\cdot}11_1$

When substituting the final corrected value for σ_{vert} into equation (2) to obtain R_1 an appropriate value for d in the complex must be used. The value of 0·918 ring radii used by Johnson and Bovey [16] can be taken as the basis for the calculations. However, because complex formation is postulated to depend on an electric dipole being induced in the aromatic molecule, it is possible that the normal aromatic π-system is distorted on complex formation and that the basic value for d is modified. Consequently, any change in d on complex formation must be determined. This is done conveniently by comparing the chemical shift of the aromatic protons in the complex with that in the free aromatic molecule. In order to minimise medium effects, the shifts should be determined at infinite dilution in cyclohexane. If the aromatic proton shift at infinite dilution in cyclohexane alone as solvent is $\delta^A{}_{\text{free}}$ and the corresponding value in the case of the complex is $\delta^A{}_{\text{comp}}$ the observed shift ($\delta^A{}_{\text{obs}}$) in a nitrofo aromatic–cyclohexane mixture is given approximatel

$$\delta^A{}_{\text{obs}} = x\,\delta^A{}_{\text{comp}} + (1-x)\,\delta^A{}_{\text{free}} \qquad (1$$

where x is the fraction of the aromatic complexed a given by

$$K = \frac{x}{(1-x)Z} \qquad (1$$

where Z is the mole fraction of free nitroform at ec brium. $\delta^A{}_{\text{free}}$ Can be obtained by extrapolating a of mole fraction of aromatic against aromatic pr shift to zero mole fraction in cyclohexane alone as sol A similar extrapolation for a system differing from previous one in that it contains a low constant fraction of nitroform yields a value for $\delta^A{}_{\text{obs}}$; u these conditions Z may be taken as the initial fraction of nitroform. Shift measurements can be relative to cyclohexane as internal reference. U equation (1), the generally accepted value of − p.p.m.[3,15] for σ_{hor} in the case of benzene affords an app mate value for d. $\delta^A{}_{\text{comp}}$ Can be determined equation (11) and the difference between this and is used to refine the basic value for σ_{hor} for subseq substitution in equation (1) to give another value f The actual values obtained for d in this way are u portant although they are close to the value use Johnson and Bovey.[16] However, the difference bet the two values for d can be taken as an estimate o displacement of the effective centres of the π-elec on complex formation and can be used to correct basic value of 0·918 ring radii for d accordingly.

Of the systems studied here reasonable correction π-cloud deformation were only made for the methylated aromatic compounds. Only in these did the concentrations of aromatic used provide adec ring-proton signal strength over a sufficiently wide centration range to permit enough accurate measurements to obtain meaningful infinite dil shifts. The experimentally determined shifts and $\delta^A{}_{\text{free}}$) and calculated modifications to d for of the systems studied are given in Table 4. From values it can be seen that in each case a slight traction of the π-system occurs. Overall, these tractions do not exceed about 0·01 Å and the c sponding decreases in R_1 values due to this effec smaller and of the order of 0·05 Å. These deduc are dependent on the assumption that the differe observed between $\delta^A{}_{\text{obs}}$ and $\delta^A{}_{\text{free}}$ are due entirel π-cloud deformation and that medium screening ef are unimportant. This is substantiated by the fact the change in chemical shift of the aromatic hydro appears to be purely dependent on the strength o complex (inferred from the values found for K). ever, whilst bulk medium effects may be unimpo the screening effects of the complexed nitroform influence the observed aromatic proton shifts.

---

[24] 'Handbook of Chemistry and Physics,' The Che Rubber Publishing Co., Cleveland, U.S.A., 1966.

effects would be expected to be small and if they nored the values observed for δ^{A}_{comp} and δ^{A}_{free} may, ference to equation (1), be taken to be indicative of d contraction. Charge transfer from the aromatic e nitroform hydrogen atom therefore appears un- since this would decrease the π-density in the atic hydrogens. The foregoing theory which de- s on there being two regions of maximum π-electron ty with no complete charge transfer occurring rs, therefore, to be valid.

e values obtained for R_1 in the nitroform–aromatic lexes studied are given in Table 5. In each case the value approximates to the sum of the Van der Waals radii [24] of the hydrogen atom (1·2 Å) and the π-cloud of the aromatic molecule (1·85 Å). This suggests that in the complex the nitroform adopts a position in which its hydrogen atom is on the aromatic six-fold axis and in contact with the aromatic molecule. It is apparent, however, that as the magnitude of the intermolecular attractive forces in the complexes increase there are corresponding small but steady decreases in R_1. This must be associated with the varying degree of aromatic π-cloud deformation and a resulting effective modification to the aromatic Van der Waals radius which leads to decreased intermolecular contact separations represented by R_1.

TABLE 5

ected values for σ_{vert}, and R_1 values for nitroform–aromatic complexes

omatic in the complex	σ_{vert} (p.p.m.) corrected for medium screening effects	R_1 (Å) π-Cloud correction Excluded	Included
ne	1·913	2·93	$2{\cdot}88_7$
ne	1·938	2·91	$2{\cdot}86_6$
ene	2·009	2·87	$2{\cdot}82_2$
lene..................	1·950	2·91	
ene	2·037	2·86	$2{\cdot}80_5$
lene	2·043	2·86	
e	2·177 *	2·76	
methylbenzene ...	2·052 *	2·85	
nethylbenzene ...	2·407 *	2·68	

Uncorrected for reaction field and dispersion screening contributions.

The procedure described above shows considerable promise for determining the structures of transient molecular complexes formed in solution. However, it must be recognised that any thermodynamic constants which are determined using this method, may be subject to error because the three component systems studied are unlikely to be perfect mixtures, as has been assumed.

The authors thank Professor W. G. S. Parker for his interest in this work and for the provision of facilities. One of them (P. J. H.) is grateful to the University of Aston in Birmingham for a Research Assistantship.

[7/644 *Received, May 3rd, 1967*]

P.J.HUCK

Ph.D. 1968

ERRATA

Table 3 - 6
Page 81/2

Reference 37 should be 116
" 38 " " 117
" 39 " " 118
" 41 " " 104

The refractive indeces at 33.4°C were measured in the laboratory.

The values of the dielectric constants at 33.4°C are extrapolations from the data in reference 117.

The static polarisability, α , and refractive index , n , of fluoroform were calculated from the molar refraction of fluoroform estimated from atomic contributions. (117) The molar volume of fluoroform was determined from the density in the solid state at -100°C.

(1.52 gm. c.c.$^{-1}$) (117).

P. J. HUCK PH.D. 1968

```
H
COMPLEXICON II'
BEGIN COMMENT PROGRAM FOR EVALUATING COMPLEXITY CONSTANTS FROM
N.M.R. DATA P.D.GROVES/ASTON UNIV./SEPT.1966.PRIOR INPUT OF
803 PLOTTER PACKAGE REQUIRED'
   INTEGER I,NO,RR'
   REAL UPPER,LOWER,ACCY,FVAL,K,P,Q,R,T,C1,C2,DELTA,DFREE,MM,CC'
   INTEGER ARRAY REF(1:50)'
   READER(1)' RR:=1' INSTRING(REF,RR)' READ NO'

   BEGIN ARRAY AA,BB,C,S,DOBS,CA(1:NO)'

      REAL PROCEDURE SIGMA(X,I,N)' INTEGER I,N' REAL X'
      BEGIN REAL SUM' SUM:=0'
         FOR I:=1 STEP 1 UNTIL N DO SUM:=SUM+X'
         SIGMA:=SUM'
      END OF SIGMA'

      PROCEDURE LSQ(Y,X,M,C,I,N)' REAL Y,X,M,C' INTEGER I,N'
      BEGIN REAL DENOM' ARRAY A,B(1:N)'
         FOR I:=1 STEP 1 UNTIL N DO
         BEGIN A(I):=X**2' B(I):=X*Y'
         END'
         DENOM:=N*SIGMA(A(I),I,N)-SIGMA(X,I,N)**2'
         C:=(SIGMA(Y,I,N)*SIGMA(A(I),I,N)-SIGMA(X,I,N)*SIGMA(B(I),I,N))
         /DENOM'
         M:=(N*SIGMA(B(I),I,N)-SIGMA(X,I,N)*SIGMA(Y,I,N))/DENOM'
      END OF LSQ'

      PROCEDURE CALCCA(CA,I,N)' INTEGER I,N' ARRAY CA'
      BEGIN REAL Q,R,T,C1,C2'
         SWITCH SS:=ALARM,START' GOTO START'
 ALARM:PRINT PUNCH(3),££L?UNSATISFACTORY VALUE OF K.K=?,
          SAMELINE,K,££L?CHOOSE NEW RANGE OF K VALUES AND START AGAIN?'
          WAIT' RESTART'

 START:FOR I:=1 STEP 1 UNTIL N DO
         BEGIN Q:=(AA(I)+BB(I))*(K+1)+S(I)'
            R:=K*AA(I)*BB(I)'
            T:=Q*Q-4*(K+1)*R'
            IF T LESS 0 THEN GOTO ALARM'
            C1:=(Q+SQRT(T))/(2*(K+1))'
            C2:=(Q-SQRT(T))/(2*(K+1))'
            IF C1/AA(I)LESS 1 THEN CA(I):=C1/AA(I)
            ELSE IF C2/AA(I)LESS 1 THEN CA(I):=C2/AA(I)
            ELSE GOTO ALARM
         END
         END OF CALCCA'

         REAL PROCEDURE SUMSQ(K)' REAL K'
         BEGIN INTEGER I' ARRAY DIFF(1:NO)'
            CALCCA(CA,I,NO)'
            LSQ(CA(I),DOBS(I),MM,CC,I,NO)'
            DELTA:=1/MM' DFREE:=-CC*DELTA'
            FOR I:=1 STEP 1 UNTIL NO DO
            DIFF(I):=CA(I)-(DOBS(I)/DELTA-DFREE/DELTA)'
            SUMSQ:=SIGMA(DIFF(I)**2,I,NO)
         END OF SUMSQ'

         REAL PROCEDURE MINX(A,B,EPS,X,FX,FVAL)'
         VALUE A,B,EPS' REAL A,B,EPS,X,FX,FVAL'
         BEGIN REAL SEP,FX1,FX2,AA,BB' INTEGER D' SWITCH S:=L,MOVEA'
        AA:=A' BB:=B'
        L:SEP:=(B-A)/3.0'
            X:=A+SEP'
            FX1:=FX/((X+1)**2)'
            X:=B-SEP'
            FX2:=FX/((X+1)**2)'
            IF FX2=FX1 THEN
            BEGIN D:=0'
               B:=B-SEP'
               GOTO MOVEA
            END'
            D:=1'
            IF FX2 GR FX1 THEN B:=B-SEP
            ELSE A:=A+SEP'
      MOVEA:IF SEP GREQ EPS THEN GOTO L'
            MINX:=X::=IF D NOTEQ 0 THEN A+SEP
                                 ELSE(A+B)/2.0'
            FVAL:=FX'
            IF (X-AA) LESSEQ 2*EPS THEN
            BEGIN PUNCH(3)' PRINT££L?NO ACCEPTABLE MINIMUM.
DECREASE LOWER LIMIT FOR K AND START AGAIN?'
            WAIT'RESTART
            END ELSE
            IF(BB-X) LESSEQ 2*EPS THEN
            BEGIN PUNCH(3)' PRINT££L?NO ACCEPTABLE MINIMUM.
INCREASE UPPER LIMIT FOR K AND START AGAIN?'
            WAIT'RESTART
            END
            END OF MINX'

         PROCEDURE GRAPH'
         BEGIN INTEGER M,N'
            M:=-10*ENTIER(DFREE/10)'
            N:=10*ENTIER(-(DELTA+DFREE)/10)'
            SETORIGIN(200,800,10,1)'
            AXES(0.1,10,10,0,(M-N)/10,0)'
            PLOTTER(10,1)'
            FOR I:=0 STEP 10 UNTIL M-N DO
            BEGIN MOVEPEN(-0.05,I)'
               PRINT DIGITS(3),I+N
            END'
            MOVEPEN(0,-(DFREE+N))'
            DRAWLINE(1,-(DELTA+DFREE+N))'
            FOR P:=1 STEP -0.5 UNTIL -0.05 DO
            BEGIN MOVEPEN((P-0.03),-2)'
               PRINT ALIGNED(1,1),P
            END'
            MOVEPEN(0.2,-10)'
            PLOTTER(15,1)'
            RR:=1' OUTSTRING(REF,RR)'
            MOVEPEN(0.48,-5)'
            PRINT PLOTTER(15,1),£C/A?'
            MOVEPEN(-0.1,(M-N)/2)'
            PRINT PLOTTER(15,3),£-DOBS?'
            FOR I:=NO STEP -1 UNTIL 1 DO
            BEGIN MOVEPEN(CA(I),-(DOBS(I)+N))'
               CENCHARACTER(2)
            END'
         MOVEPEN(0,M-N+50)'
      END OF GRAPH'

      BOOLEAN PROCEDURE N2(N)' VALUE N' INTEGER N'
      BEGIN INTEGER COL' SWITCH S:=L1,L2,FIN'
         COL:=+8191'
         ELLIOTT(7,0,0,0,0,3,COL)'
         ELLIOTT(0,5,N,0,4,2,L1)'
         ELLIOTT(4,0,L2,0,0,0,0)'
      L1:N2:=TRUE' GOTO FIN'
      L2:N2:=FALSE'
   FIN:END OF N2'

      FOR I:=1 STEP 1 UNTIL NO DO
      READ AA(I),BB(I),S(I),DOBS(I)'
      READER(2)' READ UPPER,LOWER,ACCY'
      K:=MINX(LOWER,UPPER,ACCY,K,SUMSQ(K),FVAL)'
      CALCCA(CA,I,NO)'
      LSQ(CA(I),DOBS(I),MM,CC,I,NO)'
      DELTA:=1/MM' DFREE:=-CC*DELTA'
      PUNCH(3)' PRINT ££L??' RR:=1' OUTSTRING(REF,RR)'
      PRINT ££L2?K=?,SAMELINE,FREEPOINT(5),K,££L?DELTA=?,
      DELTA,££L?DFREE=?,DFREE,££L3?ESTIMATE OF VARIANCE:?,
      FVAL/(NO-2),££L?STD.DEVIATION:?,SQRT(FVAL/(NO-2))'
      PUNCH(1)' PRINT££L?COMPLEXICON II£L3??'
      RR:=1' OUTSTRING(REF,RR)'
      PRINT ££L3S21?NUMBERS OF MOLES£L?
SAMPLE       A              B              S             C/A       DELTA OBS?'
      FOR I:=1 STEP 1 UNTIL NO DO
      PRINT ££S8??,DIGITS(2),I,SAMELINE,££S5??,SCALED(5),
      AA(I),££S4??,BB(I),££S4??,S(I),££S4??,
      CA(I),££S4??,ALIGNED(3,2),DOBS(I)'
      PRINT ££L2?ESTIMATED RANGE OF K£L?UPPER VALUE:?,
      FREEPOINT(4),SAMELINE,UPPER,££L?LOWER VALUE:?,
      LOWER,££L?ACCY:£S7??,ACCY,££L3S10?RESULTS£L2?K=?,
      FREEPOINT(5),K,££L?DELTA=?,DELTA,£C/S.£L?DFREE=?,DFREE,
      £C/S.£L3?ESTIMATE OF VARIANCE:?,FVAL/(NO-2),
      ££L?STANDARD DEVIATION:£S2??,SQRT(FVAL/(NO-2))'
      WAIT'
      IF N2(1)THEN GRAPH
      END OF INNER BLOCK'
      WAIT' RESTART
END OF COMPLEXICON II
END OF PLOTTER PACKAGE'
```